Interactive Molecules and Atomic Clusters: Reactions and Sensing Applications

A thesis submitted by

Chirantan Gayen

Roll No 166122102

To

Indian Institute of Technology Guwahati

For the award of the degree of

Doctor of Philosophy

Department of Chemistry

Indian Institute of Technology Guwahati

Guwahati- 781039 India

Statement

This thesis entitled "**Interactive Molecules and Atomic Clusters: Reactions and Sensing Applications**" is a work of research and investigation carried out by me under the supervision of Prof. Anumita Paul, FRSC, Professor, Department of Chemistry, Indian Institute of Technology Guwahati. This thesis has been submitted by me to the Department of Chemistry, Indian Institute of Technology Guwahati for the award of the degree of Doctor of Philosophy. I further declare that this work has not been submitted anywhere else for any degree, diploma, associateship or membership etc. of any Institute or University to the best of my knowledge.

Chirantan Gayen
Department of Chemistry,
IIT Guwahati,
Guwahati-781039, Assam, India
Date:
Place: Guwahati, Assam

Certificate

It is certified that the thesis entitled "**Interactive Molecules and Atomic Clusters: Reactions and Sensing Applications**" being submitted to the Indian Institute of Technology Guwahati by Chirantan Gayen (Roll. No. 166122102) for the award of the degree of Doctor of Philosophy in Chemistry, is a bonafide record of research work carried out by he. The information and data reported by he are solely the results of his original findings. He has meticulously carried out the investigations and followed the guidelines of the laboratory. This work has not been submitted elsewhere for any degree or diploma.

Anumita Paul
Thesis Supervisor
Professor, FRSC
Department of Chemistry,
IIT Guwahati,
Guwahati-781039, Assam, India.
Date:
Place: Guwahati, Assam

Dedicated to my

Grandfather, Grandmother,

Parents, Maa, Didi, Manu

and all Family Members

Acknowledgements

I would like to express my special thank of gratitude to my supervisor Prof. Anumita Paul for her continuous support, motivation and encouragement throughout my work. It is undoubted that without her valuable guidance, it won't possible to script my PhD. It's a great opportunity to work under her guidance and I am pretty much lucky to have such an enthusiastic and inspiring advisor in my life. Thank you very much Madam. God Bless you.

I am extremely thankful to Srestha Basu for her continuous support, valuable suggestions throughout my works.

I am extremely thankful to my doctoral committee members for their valuable suggestions and advice regarding research works.

I would also like to thank my lab members for their help and providing a friendly atmosphere in the lab.

I would like to thank Department of Chemistry, Center for Nanotechnology, Central Instrument Facilities (CIF) of IITG for providing research facilities.

I am highly grateful to all of my friends and well wishers.

Last but not least, a heartfelt gratitude goes to my parents and family members for their support and love.

Table of contents

Chapter 1

Introduction

Metal nanoclusters (NCs) are a fascinating and versatile class of nanomaterials endowed with unique chemical and optical properties. Their use has been indicated in a wide range of applications owing to their photoluminescence in visible region, large stokes shifted emission, high photo stability and chemical stability, and low cytotoxicity.[1] Notably, luminescent NCs, have been extensively used as chemical catalysts[2], sensors[3], therapeutic agents and as integral components of decisive electronic devices[4]. As regard to the case of chemical sensors, metal NCs have superseded their nanoparticle analogues, due to the difference in the optical behaviour of the two. Nanoparticle based sensors rely on UV-Vis absorption techniques whereas NCs based sensors depend on luminescence technique. In this regard, luminescence based detection methods offer greater degree of precision compared to colorimetric techniques owing to the background free nature of the former. Although NCs have been extensively used for detection of biologically and environmentally relevant molecules, key issues like specificity, interference of chemically allied molecules and poor detection limit remains to be addressed. A possible way to address the above mentioned limitations could be overcome through the concept of functionalization of NCs with molecules which is envisioned to introduce specific binding sites to the sensor system and rule out the possible interference of molecules with allied structures.

An interesting area that holds the key to further development in the field of nanoscale science and technology is envisioned to stem from chemical reactions of atomic clusters. In this regard, chemical reactions provide facile opportunities for tailoring the physical and chemical properties of atoms and molecules. This is chiefly attributed to the polarizability of atoms and molecules. However, nanoscale particles, for example nanoclusters, comprising of magic number of metal atoms lack intrinsic polarizability and hence direct chemical reactions of the constituent metal atoms is rather difficult. In this regard, the ligands stabilizing the metal nanoclusters readily provide avenues for such reaction based changes in properties of the nanocluster entities.

Nanoclusters (NCs)

Nanocluster are composed of a few atoms of a particular metal, typically in the range of ~ 2 nm in size, as a consequence of which metal NCs are unable to support surface plasmon resonance, unlike their nanoparticle analogues. As a result, their energy levels are discretized which confers the NCs with intrinsic luminescence.[5] Materials can be classified into three different regimes based on their size, namely bulk, nanoparticles and nanocluster or atomic cluster. Nanocluster make a bridging link between bulk and atomic cluster.[6]

Historical background of Nanocluster (NCs)

The journey of nanocluster started from 1950-1960. In this period nanoclusters were made within molecular beams at reduced localized temperature formed as a result of supersonic expansion of the molecular beam. With this technique it was possible to create few atom nanoclusters for few elements of the periodic table. Interestingly, a new class of carbon nanoclusters, Buckminsterfullerene (c_{60}) has been suggested to a stable nanocluster which have occurred during the creation of universe. Since 1980, extensive research has been carried out on nanocluster of superconductors and transition metals.[7]

Stability and Synthesis of nanocluster:

Stability of nanocluster largely depends on no of atoms present in the cluster, number of valance electrons and on the encapsulating scaffolds. In 1990 Heer and his co-worker made an atomic beam of clusters by using supersonic expansion of an atomic cluster source in presence of an inert gas.[8] Heer's team and Brack et al. discovered atomic nanoclusters which are stable and magic clusters.[9] Certain thiolated clusters such as $Au_{25}(SR)_{18}$, $Au_{38}(SR)_{24}$, $Au_{102}(SR)_{44}$ also show magic cluster stability.[10]

The synthesis of metal nanocluster with high quality is desirable from technological point of view. Some key experimental considerations towards achieving superior quality metal nano-clusters are 1) Strong interaction between metal and ligand. 2) Proper reducing condition for better quantum yield. In light of these factors, different approaches have been adopted to synthesize metal nano-cluster in a controllable manner. Some of these are discussed here.

Thiol: Thiol containing small molecules have been used firstly to synthesized gold nano-cluster(Au NCs) via chemical reduction of $NaBH_4$ owing strong Ag-S interaction.[10] Glutathione stabilized Au NCs have been synthesized with definite chemical formula by reducing Au^{+3} in presence of glutathione.[11] Many thiol containing molecules such as phenylethylthilate[12], tiopronin[13] and D- penicillamine[14] have been used as a template to prepare monolayer protected Au NCs.

DNA, proteins and peptides: DNA is a good template for synthesizing fluorescent metal nano-cluster. Firstly non-toxicity with good bio-compatibly and secondly functional roles for molecular recognition of DNA makes it advantageous for preparation of metal nano-cluster. Liu group prepared blue fluorescent poly cytosine DNA stabilized Au NCs at low pH and poly-adenine stabilized AuNCs at neutral pH.[15]

Peptide and proteins are also used as a stabilizer for synthesizing metal nano-cluster. Larger peptides and complicated proteins with high binding sides construct metal nano-cluster which act as a multifunctional nanoprobe.[16] Ying et al. report a simple one-pot, green synthetic route for preparation of BSA stabilized Au NCs, as depicted in the scheme below.[17]

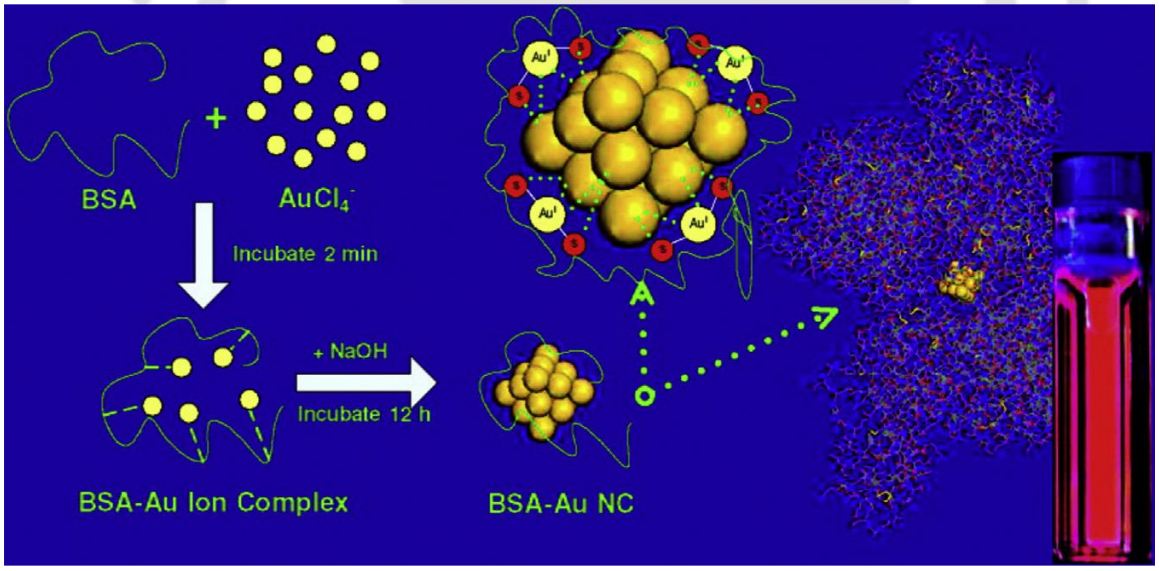

Fig 1: Schematic representation of BSA stabilized AnNCs. Reprinted with permission from reference 17. Copyright *J. Am. Chem. Soc.*, **2009**, *131*, 888-889. American Chemical Society.

Dendrimers: Dendrimers made of repeating branched units having specific molecular weight and small cavities, are used as ~~a~~ template for synthesis of metal nanoclusters. Poly-amidoamine (PAMAM) dendrimer is with different generations have been used as a stabilizer. Different kind of metal nano-cluster can be synthesized by PAMAM with different emission peak. Zhang

et al. made a class of Au NCs with different emission maxima ranging from UV-IR from mixture of gold salt, PAMAM and $NaBH_4$.[18]

Properties of nanocluster:

Optical properties:

Optical properties of nanoclusters are governed by band gap and electronic structure. The energy levels are discretised and the energy difference between highest occupied molecular orbitals (HOMO) and lowest unoccupied molecular orbitals (LUMO) is higher than the thermal energy (K_BT). So thermal energy is inadequate to excite the molecules from HOMO to LUMO. As a result of this phenomena nanocluster shows luminescence behaviour. On the other hand, in nanomaterials, the HOMO–LUMO gap is comparatively small with respect to thermal energy (K_BT). As a consequence of this plasman absorption dominates over luminescence in nanomaterials.

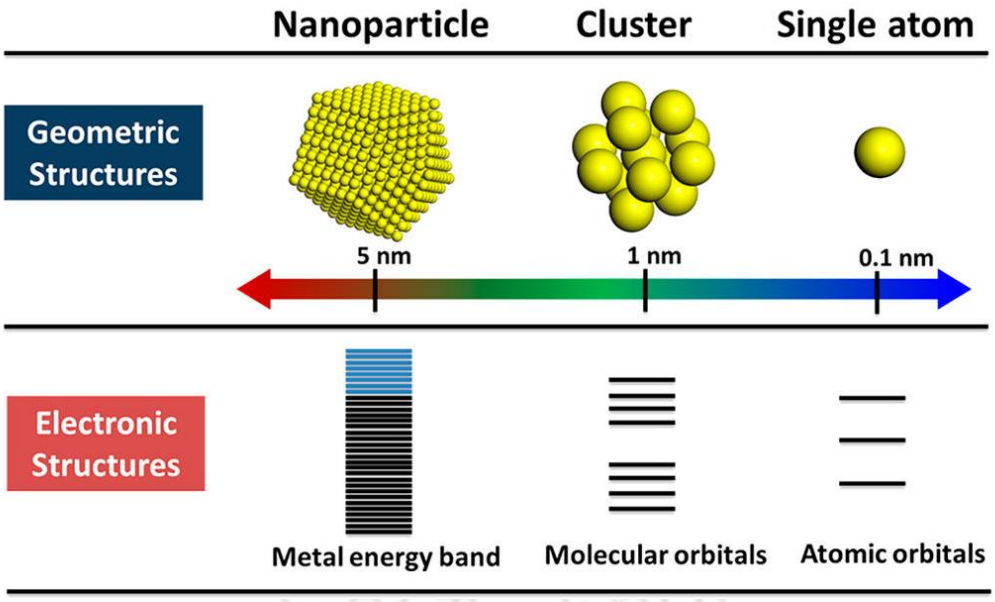

Fig 2: In metal nano-clusters the energy levels are discretised, yielding electronic transition from HOMO to LUMO upon interaction of matter with light, whereas bulk metal have continuous energy bands, thus failing to exhibit electronic transitions.

Goodson's group has observed a low quantum –yield visible luminescent in Au_{25} cluster in addition to the NIR luminescent.[19] They have showed electronic states and transition responsible for the dual emitting emission of gold nanocluster.

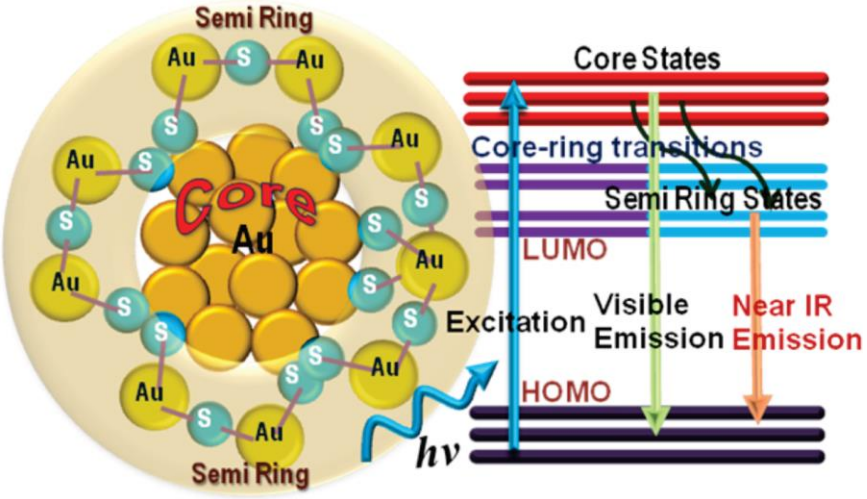

Fig 3: Schematic representation of electronic state and transition responsible for dual emitting gold nanocluster. Reprinted with permission from reference 19. Copyright *J. Phys. Chem. C* **2010**, *114*, 22417–22423. American Chemical Society.

Magnetic properties:

Magnetic moment of atom in cluster is greater than the magnetic moment of atom in bulk materials because most of the atoms are surface atom. This enhancement in magnetic moment is attributed due to large interatomic separation, lower dimensionality and lower coordination of atoms. As per result Vanadium(V) and Rhodium(Rh) are paramagnetic in bulk but become ferromagnetic in nanoclusters.

Reactivity of Nanocluster:

Metal nano-clusters have unique reactivity. Driven by large surface to volume ratio and low coordination of surface atoms. Bulk gold atom is chemically inert but upon reduction in size to nanometre range, it becomes highly reactive. In periodic table chlorine has highest electron affinity among all elements. Nano-clusters with high electron affinity are also called as super halide.

Applications of nanoclusters:

Sensing and bio-imaging:

Metal nanoclusters have been extensively used as ~~a~~ fluorescence probes for detection of heavy inorganic metal ion such as Hg^{+2}, Cd^{+2}, Pb^{+2} and biomolecules in biological systems and environment. Metal nano-clusters are attracting our attention because they have high bio-

compatibility, high photo-stability, target-specificity and high sensitivity. Importantly, unlike quantum dots, metal nano-clusters are non-toxic in nature.

Heavy metal ions: Heavy metal ions such as Hg^{+2}, Cu^{+}, Cd^{+2}, Pd^{+2} bind to the biological system like proteins, enzymes, nucleic acids, vital organs and tissues. Due to their high toxicity and bioaccumulation these hazardous metal ions alter biological functions and ultimately causes serious diseases. So to protect our health and environment some effective strategies must be taken to sense and detect these heavy metal ions. Au NCs have been utilized to detect Hg^{+2} by taking consideration of $5d^{10}$- $5d^{10}$ interaction between Hg^{+2} and Au^{+} which alter the electronic structure of Au NCs. Dong group developed a method to detect Hg^{+2} using DNA-duplex stabilized Au NCs.[20] Yu group has developed a strategy to detect the Hg^{+2} by using folic acid caped Au NCs based on quenching of FA- Au NCs by Hg^{+2}.[21]

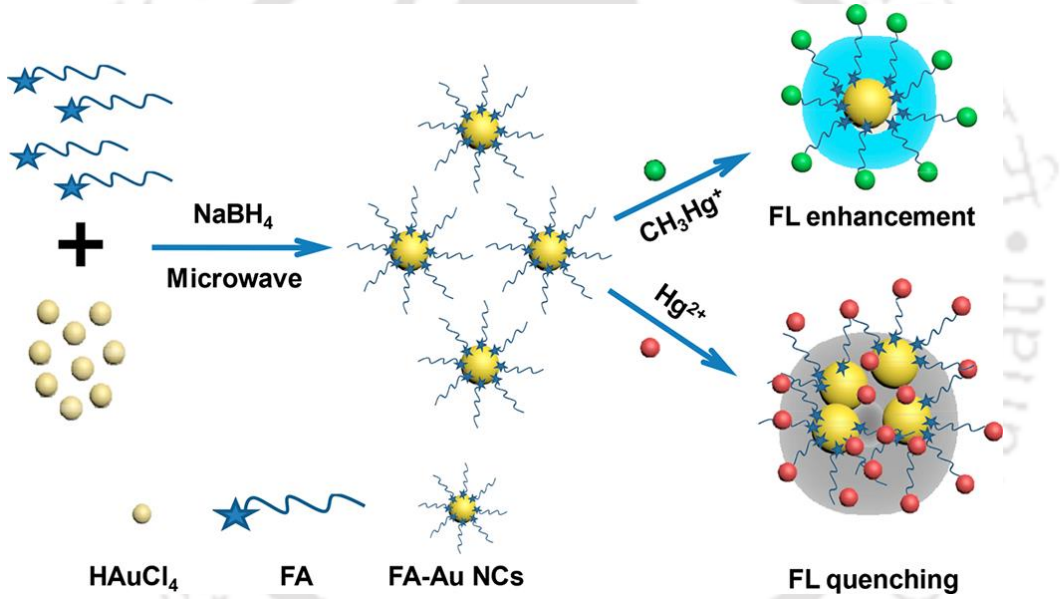

Fig 4: Schematic Diagram of the Preparation Strategy for detection of Hg^{+2} by using FA-Au NCs. Reprinted from Reference 21. Copyright *Anal. Chem.* **2018**, *90*, 6945−6951. American Chemical Society.

Copper is essential element for all plants and animals because it is involved in a variety of physiologic process and is present in many metallo-enzymes by combining with protein. But sometimes, higher levels of Cu^{+2} lead to cellular toxicity and damages cells and disrupts biological functions.[22] Chang and co-workers have developed a simple 'turn-off' method for detection of Cu^{+2} using water-soluble DNA/Ag NCs.[23] Dong group has developed a sensor for detection of Cu^{+2} based on fluorescent PMAA protected Ag NCs.[24]

Biological imaging and labelling:

Au NCs is an attractive fluorescent nanomaterials, as it possess ultrasmall size, good biocompatibility, photo stability, good water solubility and shows large stoke shift which make them promising as fluorescent probes for bio-imaging and bio labelling studies.[25,26] Huang group systemically summarize and design various kind of long lived emissive probes for bio imaging and sensing.[27] Lin group proposed a route of preparing Au NCs by using photo-sensitized, size-controlled Ag NCs as a template and they used this Au NCs as a fluorescent probe for cellular making in CAL-27 cancer cell and MC3T3-E1 normal cells respectively.[28] Gu and co-workers synthesized a BSA stabilized Au NCs as a fluorescent probe for tumor imaging and therapy.[29] They conjugated BSA stabilized Au NCs with methionine(Met) and MPA, to yield a near infrared fluorescent probe, Au-Met-MPA. Further, they investigated the targeted internalization of this fluorescent Au-Met-MPA by L02 normal human cell and MCF-7 tumor cells. Later Wang group synthesized the self-assembly of the gold nanoclusters with carborane amino derivatives (GNCs-CB) for the precise bioimaging of cancer cells and targeted delivery of this carborane compound to the tumors.[30]

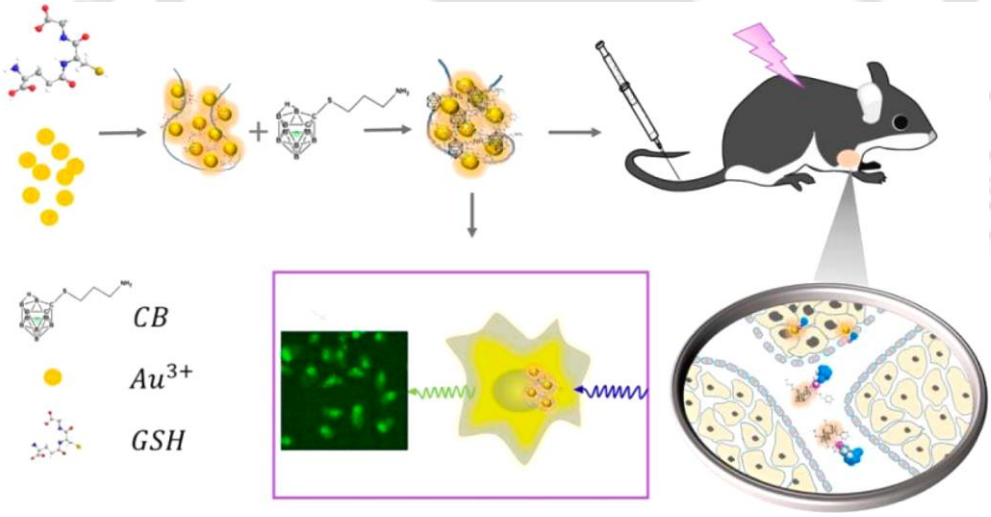

Fig 5: Schematic representation of the Bioimaging Process for Cancer Cells by Using Self-Assembled GNCs-CB 30. Copyright *Biomacromolecules* **2017**, *18*, 1466−1472. American Chemical Society.

Overview of the Thesis:

In the current thesis, chemical reactions of atomic clusters of gold has been pursued with chemical species, leading to changes in the optical properties of the former. Further, chemical interactions based identification of molecules, with precision up to "a few particle level" could be achieved using gold nanoclusters. This thesis is divided into 6 chapters whose contents are briefly listed below.

Chapter 1: In this chapter, literature survey, introduction and brief idea about AuNCs has been discussed.

Chapter 2: This chapter describes chromaticity index based discrimination of biothiols using chemically interactive dual emitting nanoprobe down to few particles level.

Chapter 3: This chapter describes crystallization induced emission enhancement of gold nanoclusters and luminescence intensity quenching in presence of sulphide ions of His Au NCs as the basis for intercellular logic operations.

Chapter 4: This chapter describes visible light excitation induced luminescence from gold nanocluster upon interaction with Zn^{+2} for daylight sensing and cellular imaging.

Chapter 5: This chapter describe tailoring the luminescence of atomic cluster via ligand exchange reaction mediated post synthetic modification.

Chapter 6: This chapter provides concluding remarks and discusses the various futuristic prospects of the current thesis.

References:

1. Zhang, L.; Wang, E. *Nano Today* **2014,** *9*, 132-157.
2. Li, G.; Jin, R. *Acc.Chem. Res.* **2013,** *46*, 1749-1758.
3. Jia, X.; Li, J.; Han, L.; Ren, J.; Yang, X.; Wang, E. *ACS Nano* **2012**, *6*, 3311-3317.
4. Sailapu, S. K.; Sahoo, A. K.; Ghosh, S. S.; Chattopadhyay, A. *Small* **2014**, *10*, 4067-4071.
5. Zheng, J.; Zhang, C.; Dickson, R. M. *Phys. Rev. Lett.* **2004**, *93*, 077402.
6. Zheng, J.; Nicovich, R. P.; Dickson, R. M.; Highly Fluorescent Noble-Metal Qantum Dots. *Phys. Chem. Rev. Lett. C.* **2007**, *58*, 409-431.
7. Jena, P.; Castleman, A. W. Jr.; Nanoclusters. ISBN 9780444534408.

8. Brack, M.; The Physics of Simple Metal Clusters: Self-consistent jellium model and semiclassical approaches. *Rev. Mod. Phys.* **1993**, *65*, 677.
9. Wilcoxon, J. P.; Abrams, B. L.; Synthesis, Structure and Properties of Metal Nanoclusters. *Chem.Soc. Rev.* **2006**, *35*, 1162-1194.
10. Negishi, Y.; Nobusada, K.; Tsukuda, T.; Glutathione- Protected Gold Clusters Revisited: Bridging the Gap between Gold(1)- Thiolate Complexes and Thiolate-Protected Gold Nanocrystals. *J. Am. Chem. Soc.* **2005**, *127*, 5261-5270.
11. Sanchez-Casyillo, A.; Nognez, C.; Garzon, I. Z.; On the origin of the optical Activity Displayed by Chiral-Ligand Protected Metallic Nanoclusters. *J.Am. Chem. Soc.* **2010**, *132*, 1504-1505.
12. Lee, D.; Donkers R. L.; Wang, G.; Harper, A. S.; Murray, R. W.; Electrochemistry and Optical Absorbance and Luminescence of Moecule-like Au_{38} Nanoparticals. *J. Am. Chem.* Soc. **2004**, *126*, 6193-6199.
13. Huang, T.; Murray, R. W.; Visible Luminescence of Water-Soluble Monolayer-Protected Gold Clusters. *J. Phys. Chem. B.* **2001**, *105*, 12498-12502.
14. Shang, L.; Dorlich, R. M.; Brandholt, S.; Schneider, R.; Trouillet, V.; Bruns, M.; Gerthsen, D.; Nienhaus, G. U.; Facile Preparation of Water-Soluble Fluorescent Gold Nano-Clusters for Cellular Imaging Applications. *Nanoscale.* **2011**, *3*, 2009-2014.
15. Kennedy, T. A.C.; Maclean, J. L.; Liu, J.; Blue Emitting Gold Nanoclusters Templated by Poly-Cytosine DNA at Low pH and Poly-Adenine DNA at Neutral pH. *Chem. Commun*. **2012**, *48*, 6845-6857.
16. Petty, J. T.; Story, S. P.; Hsiang, J. C.; Dickson, R. M.; DNA- Templated Molecular Silver Fluorophores. *J. Phys.Chem. Lett.* **2013**, *4*, 1148-1155.
17. Xie, J.; Zheng, Y.; Ying, J. Y.; Protein- Directed synthesis of Highly Fluorescent Gold Nanoclusters. *J. Am. Chem. Soc.* **2009**, *131*, 888-889.
18. Zheng, J.; Zhang, C.; Dickson, R. M.; Highly Fluorescent Water Soluble, Size-Tunable Gold Quantum Dots. *Phys. Rev. Lett.* **2014**, *93*, 077402.
19. Devadas, M. S.; Kim, J.; Sinn, E.; Lee, D.; Goodson, T. Unique Ultrafast Visible Luminescence in Monolayer-Protected Au25 Clusters. *J. Phys. Chem. C.* **2010**, *114*, 22417–22423.
20. Deng, L.; Zhow, Z.; Li, J.; Li, T.; Dong, S.; Fluorescent Silver Nanoclusters in Hybridized DNA Duplexes for the Turn- On Detection of Hg^{+2} ions. *Chem. Commun.* **2011**, *47*, 11065-11067.

21. Yang, J. Y.; Yang, T.; Wang, X. Y.; Chen, M. L.; Yu, Y. L.; Wang, J. H.; Mercury Speciation with Fluorescent Gold Nanocluster as a Probe. *Anal. Chem.* **2018**, *90*, 6945−6951.
22. Chen, L. Y.; Wang, C. W.; Yuan, Z.; Chang, H. T. Fluorescent Gold Nanoclusters: Recent Advances in Sensing and Imaging. *Anal. Chem.* **2015**, *87*, 216−229.
23. Lan, G. –Y.; Huang, C. –C.; Chang, H. –T.; Silver Nanoclusters as Fluorescent Probes for Selective and Sensitive Detection of Copper ions. *Chem. Commun.* **2010**, *46*, 1257-1259.
24. Shang, L.; Dong, S.; Silver Nanocluster-based Fluorescent Sensors for Sensitive Detection of Cu(II). *J. Mater. Chem.* **2008**, *18*, 4636-4640.
25. Stark, W. J.; Nanoparticles in Biological Systems. *Angew. Chem. Int. Ed.* **2011**, *50*, 1242 – 1258.
26. Kaur, N.; Aditya, R. N.; Singh, A.; Kuo, T. R. Biomedical Applications for Gold Nanoclusters: Recent Developments and Future Perspectives. *Nanoscale Res Let* **2018**, *13*, 302.
27. Zhang, K. Y.; Yu, Q.; Wei, H.; Liu, S.; Zhao, Q.; Huang, W. Long-Lived Emissive Probes for Time-Resolved Photoluminescence Bioimaging and Biosensing. *Chem. Rev.* **2018**, *118*, 1770−1839.
28. Wang, C.; Wang, Y.; Xu, L.; Shi, X.; Li, X.; Xu, X.; Sun, H.; Yang, B.; Lin, Q. A Galvanic Replacement Route to Prepare Strongly Fluorescent and Highly Stable Gold Nanodots for Cellular Imaging. *Small* **2013**, *9*, 413–420.
29. Chen, H.; Li, B.; Ren, X.; Li, S.; Ma, Y.; Cui, S.; Gu, Y. Multifunctional near-infrared-emitting nano-conjugates based on gold clustersfor tumor imaging and therapy. *Biomaterials* **2012**, *33*, 8461-8476.
30. Wang, J.; Chen, L.; Ye, J.; Li, Z.; Jiang, H.; Yan, H.; Stogniy, M. Y.; Sivaev, I. B.; Bregadze, V. I.; Wang, X. Carborane Derivative Conjugated with Gold Nanoclusters for Targeted Cancer Cell Imaging. *Biomacromolecules* **2017**, *18*, 1466−1472.

Chapter 2

Single particle level chromaticity index based discrimination of biothiols using chemically interactive dual emitting nanoprobe

Herein we introduce a unique approach for discrimination between two important biothiols (BTs) – cysteine (Cys) and glutathione (Glu), based on changes in chromaticity coordinates of a dual emitting single particle nanoprobe. A novel dual channel emission nanocomposite was developed by zinc-mediated conjugation of green emitting fluorescein with red emitting gold nanoclusters (Au NCs). Cys and Glu having different interactions with Zn-FL-Au NCs, were found to have different effects on the overall luminescence of the fluorescein-cluster conjugate (Zn-FL-Au NCs) which eventually led to observation of different chromaticity indices of the latter upon interaction with these two BTs. For example, upon addition of Cys to a dispersion of Zn-FL-Au NCs having chromaticity coordinates (0.38, 0.49), the luminescence peak due to Au NCs was found to have been selectively quenched, as a consequence of which the chromaticity coordinates of Zn-FL-Au NCs changed to (0.33, 0.52). On the other hand, upon interaction with Glu the intensity of the luminescence peak due to Au clusters as well as fluorescein enhanced to a certain extent, however, keeping the chromaticity coordinates almost similar to that of Zn-FL-Au NCs (0.38, 0.47). Allied results were obtained from super resolution microscopic analysis where luminescence of a single particle of Zn-FL-Au NCs was used to probe the differential interaction with the aforementioned biothiols leading to different degree of changes in the CIE coordinates of the former. Also, the specificity of the nanoprobe towards cysteine was confirmed by monitoring the interactions of Zn-FL-Au NCs with other interfering chemical compounds. Moreover, the optical properties of Zn-FL-Au NCs were found to be retained following incubation in human blood serum, which further supports the use of this nanoprobe for discrimination of BTs in practical systems.

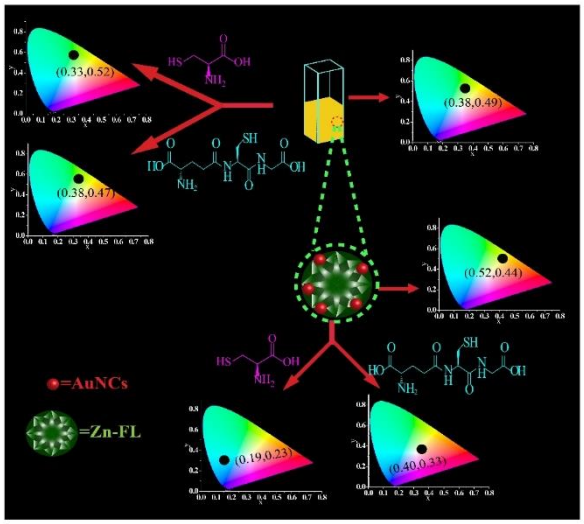

Gayen, C.; Basu, S.; Pan, U. N.; Paul, A. *ACS Omega* **2018**, *3*, 17220−17226.

Experimental Section

Materials and methods:

Tetrachloroauric acid ($HAuCl_4$), fluorescein and 11- mercaptoundecanoic acid were procured from Sigma Aldrich. Zinc acetate dihydrate and sodium hydroxide were purchased from Merck. Milli-Q water was used for all experiments. All the chemicals were used as received without further purification.

Synthesis of gold nanoclusters (Au NCs):

Gold nanoclusters were synthesized following slight modification of an earlier report.[1] Briefly, 0.4 mL $HAuCl_4$ (10 mM) was added to 10 mL water. Separately, ~5 mg of 11-mercaptoundecanoic acid (MUA) was dissolved in 1 mL water using 0.2 mL sodium hydroxide (1 M). 1 mL of this solution was added to the gold solution mentioned above. The resultant solution was stirred for 4 h at room temperature. This led to formation of a red luminescent dispersion ($\lambda_{emission}$ = 610 nm) upon excitation at 280 nm.

Synthesis of zinc-fluoresceinate:

1.5 mg fluorescein was added to 4 mL water. This led to partial dissolution of fluorescein. 2 mL of fluorescein solution was taken and added with ~ 150 mg of zinc acetate dihydrate. The resultant solution was stirred for a while and finally added with 0.2 mL NaOH (1 M). This led to formation of a yellow dispersion. The resultant dispersion was centrifuged at a speed of 10,000 rpm for 5 min. The pellet obtained was further washed with water and the cycle was repeated further. The supernatant was discarded and the pellet following redispersion in water was used for further experiments.

Synthesis of composite comprising of zinc fluoresceinate and Au NCs (Zn-FL-Au NCs) -

The pellet of zinc fluoresceinate as obtained above was dissolved in 1 mL water and added to 5 mL of Au NCs. The dispersion was stirred for 15 min followed by centrifugation at a speed of 10,000 rpm for 5 min. The supernatant was discarded and the pellet was washed with water. This cycle was repeated four times to ensure complete removal of the starting materials. Finally, the pellet was redispersed in water and used for further experiments.

Interaction of Zn-Fl-Au NCs with cysteine and glutathione-

The obtained pellet of Zn-FL-Au NCs (as mentioned above) was dissolved in 1 mL water. 0.2 mL of this dispersion was added to 0.8 mL water to make a 1 mL dispersion of the

composite. Further, 0.2 mL of the diluted dispersion (from 1 mL above) was added to 2 mL of phosphate buffer (pH = 7.04). The aforementioned dispersion was added with 0.05 mL of Cys and Glu to study the differential interaction of Zn-Fl-Au NCs with Cys and Glu.

Details of confocal laser scanning microscopic (CLSM) analysis:

Confocal measurements of all samples were carried out using Carl Zeiss LSM-880 confocal laser scanning microscope. All the samples were excited at 355nm using a maximum laser power of 30 mW. All analysis was done using GaAsP and Airyscan detector. Images were captured at a frame size of 64 × 64 μm^2. The resultant data were analysed by ZEN black software. The spectra of Zn-FL-Au NCs were acquired using lambda scan function of the CLSM.

Results and Discussions

Addition of mercaptoundecanoic acid (MUA) to a solution of $HAuCl_4$ led to the formation of colourless solution which upon excitation at 280 nm was luminescent with an emission maxima at ~610 nm (Fig. 2.1 A) suggesting the formation of Au nanoclusters (Au NCs). Transmission electron microscopic (TEM) analysis confirmed the presence of particles less than 2 nm which affirmed the formation of Au NCs (Fig. 2.1 B). These red emitting Au NCs were conjugated with green emitting fluorescein (FL) by coordination with zinc ions.

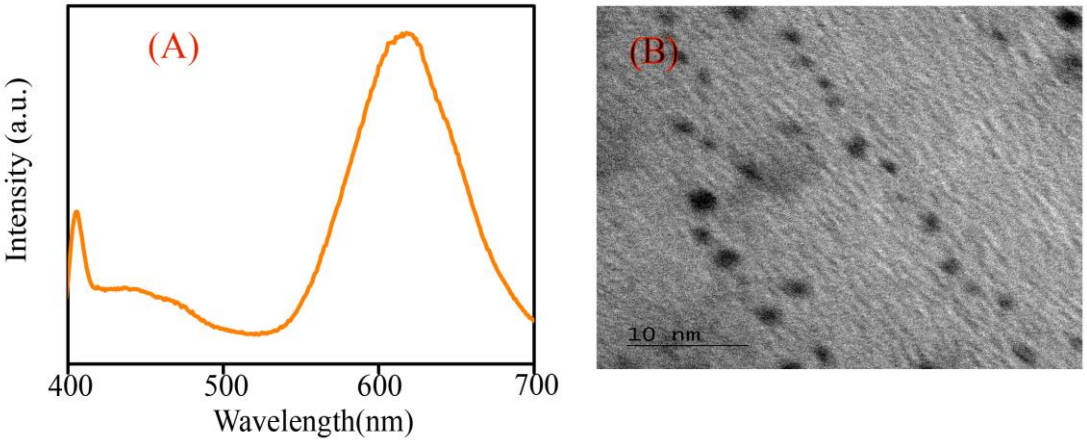

Fig. 2.1 (A): Photoluminescence spectra and (B) TEM image of Au NCs.

Addition of zinc acetate dihydrate solution to fluorescein (FL) led to enhancement in fluorescence of FL (Fig. 2.2). Electrospray ionization mass spectrometric (ESI-MS) analysis revealed the formation of a 1:1 complex possibly bonded through Zn^{2+} ion to the carboxylate

group of FL at pH = 8 (Fig. 2.3). Powder X-Ray diffraction (XRD) characterization of Zn-FL indicated generation of new peaks unmatched with that of the precursors, thereby indicating possible incorporation of zinc ion in the lattice of FL (Fig. 2.4). The powder XRD of FL shows sharp peaks at 2θ = 10.62, 11.93, 13.42, 16.60 and so on which matched well with those reported for fluoresceine sodium in the literature [2]. Upon addition of Zn(II) to FL the powder XRD changes dramatically and features broad peaks at 2θ = 8.53 and 12.98. The appearance of peak at lower scattering angles suggests crystalline phases formed with large lattice parameters. From the XRD peak width of Zn-Fl the average particle size of Zn-FL was estimated to be 7 nm. However further detailed crystallographic analysis would involve further refinements of the XRD data and maybe considered out of the scope of the current study.'

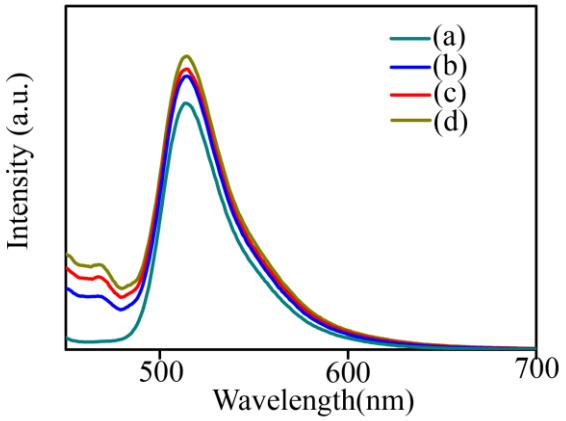

Fig. 2.2: Photoluminescence spectra of (a) FL and FL added with (b) 100 µL of zinc-acetate dihydrate (c) 200 µL of zinc-acetate dihydrate and (d) 300 µL of ~152mM zinc-acetate dihydrate.

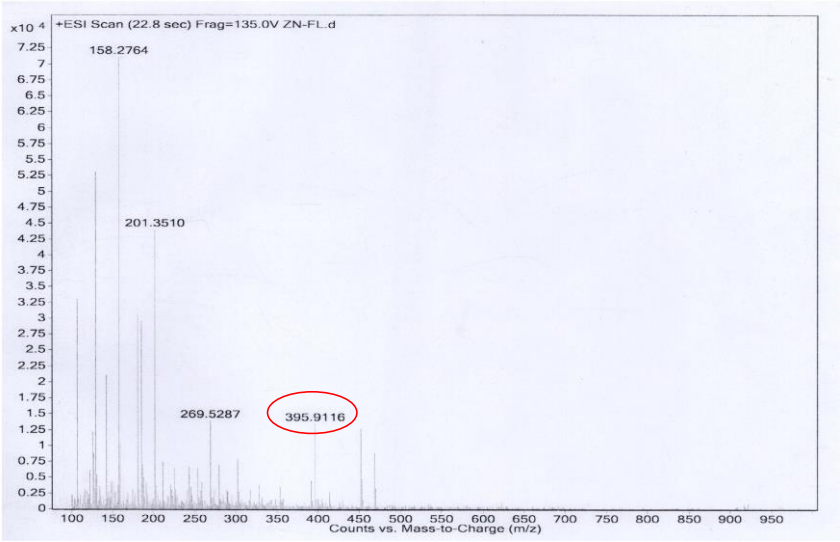

Fig. 2.3: ESI Mass Spectrum of Zn-FL. The peak marked red corresponds to the species Zn-FL

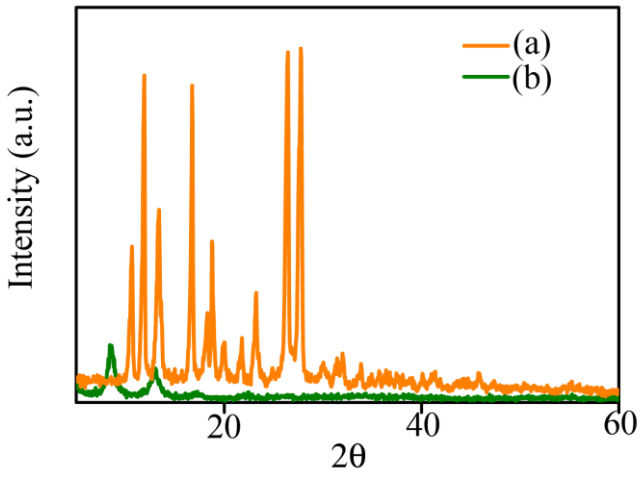

Fig. 2.4: Powder X ray Diffraction of (a) FL and (b) Zn-FL.

On the other hand, given the feasibility of coordination of zinc ions with the carboxylate groups of MUA attached to the surface of Au NCs, conjugation of FL with Au NCs via zinc ions seemed a facile strategy for formation of Zn-FL-Au NCs. It was interesting to observe that upon addition of increasing amount of zinc ions to Au NCs solution, the luminescence intensity of Au NCs underwent gradual enhancement indicating aggregation of Au NCs in presence of zinc ions via possible coordination (Fig. 2.5).[3,4]

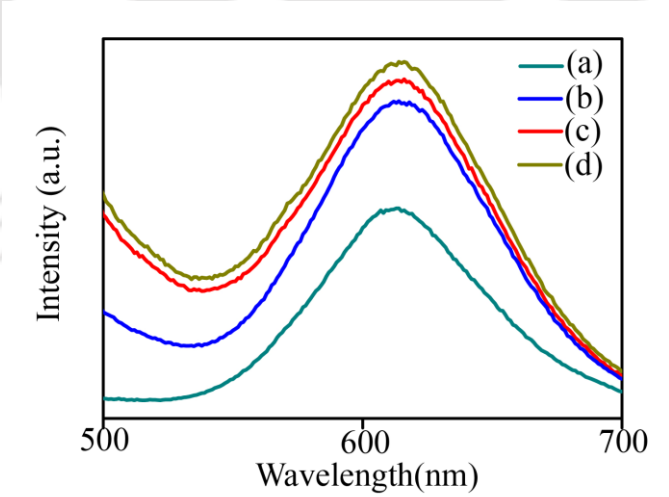

Fig. 2.5: Photoluminescence spectra of (a) Au NCs and Au NCs added with (b) 100 µL of zinc-acetate dihydrate (c) 200 µL of zinc-acetate dihydrate and (d) 300 µL of ~152mM zinc-acetate dihydrate.

Intriguingly, addition Au NCs to Zn-FL resulted in formation of a composite (Zn-FL-Au NCs) with two distinct absorbance maxima at ~400 nm and ~498 nm, attributed to absorbance due to Au NCs and FL respectively (Fig. 2.6 A-C).

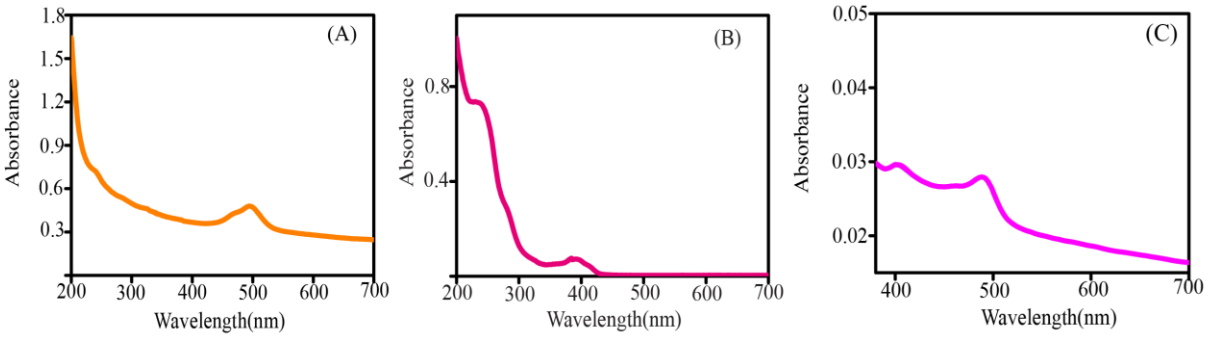

Fig. 2.6: UV-Visible spectra of (A) Zn-FL (B) Au NCs and (C) Zn-FL-Au NCs.

Moreover, as the absorbance peaks were observed to be present following repeated centrifugation and redispersion of the composite, it implied possible attachment of Au NCs to FL via zinc ions. In an allied vein, upon 355 nm excitation, the luminescence spectrum of Zn-FL-Au NCs showed the presence of emission maxima at ~520 nm and ~610 nm attributed to emission of FL and Au NCs respectively (Fig.2.7 A-C).

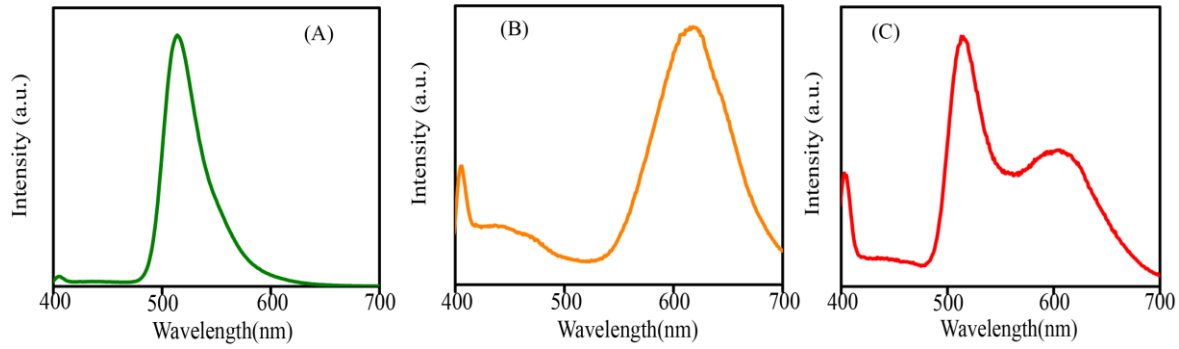

Fig.2.7: Photoluminescence spectra of (A) Zn-FL (B) Au NCs and (C) Zn-FL-Au NCs.

Moreover, the XRD profile of Zn-FL was significantly altered upon formation of Zn-FL-Au NCs, thereby indicating structural alteration of Zn-FL owing to interaction with Au NCs (Fig 2.8 A). Scanning transmission electron microscopic analysis (STEM) analysis revealed the formation of featureless Zn-FL-Au NCs moieties. Further, elemental mapping analysis was performed which confirmed the localization of Au NCs onto the surface of Zn-FL (Fig. 2.8 B-F). In order to quantitate the amount of zinc and gold ions present in the composite, inductively coupled plasma atomic emission spectrometric (ICP-AES) analysis was performed. It was found that 178 ppm of zinc and 17.7 ppm of gold (in 5.5 mL of HNO_3) was present in Zn-FL-Au NCs.

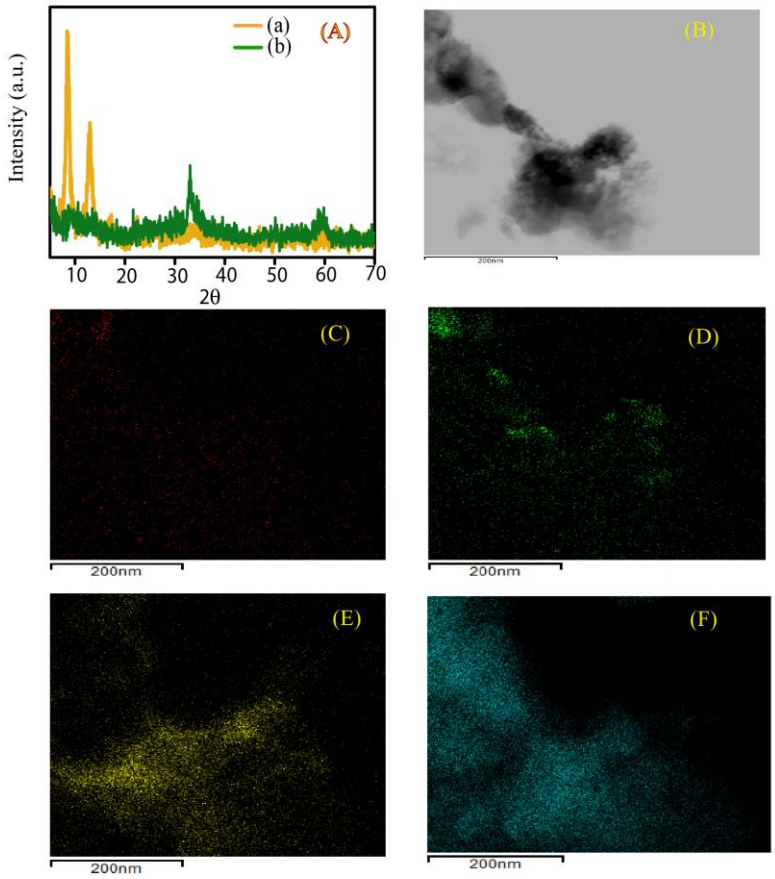

Fig. 2.8: (A) Powder XRD of (a) Zn-FL and (b) Zn-FL-Au NCs (B) STEM image of Zn-FL-Au NCs, Elemental Mapping of (C) Au (D) Zn (E) carbon and (F) oxygen Zn-FL-Au NCs in (B) substantiating the simultaneous localization of the aforementioned elements in Zn FL Au NCs.

The as prepared composite was further used for single particle level discrimination of BTs by confocal laser scanning microscope (CLSM). Typically, a dilute solution of the composite, drop cast on a microscope slide, was analysed under CLSM and a single particle was identified. In order to substantiate the single emitting nature of the particle, fluorescence intermittency (commonly known as blinking) profile of the single particle was acquired (Fig. 2.9 A).

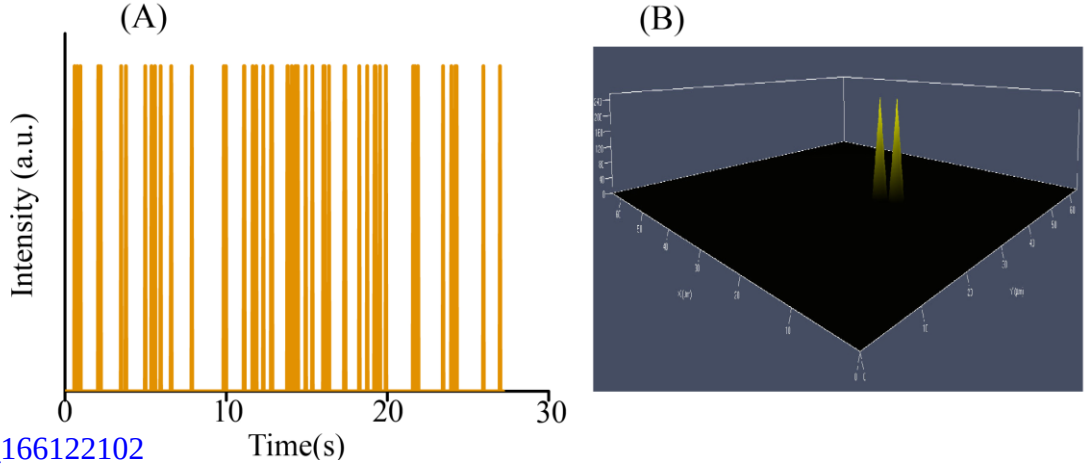

Fig. 2.9: (A) Blinking profile of a single particle of Zn-FL-Au NCs (λ_{exc}=355nm) and (B) Spatial intensity distribution fitted with a point spread function (PSF) to locate the position of single particle emitters of Zn-FL-Au NCs.

It was interesting to observe that the blinking profile comprised of square wave "off" periods and the photo bleaching occurred by sudden drop to background level instead of gradual decrease in luminescence intensity, thereby indicating the single emitting nature of the particle. Further, in order to localize the positions of the single particles of the composite, the photon spatial distribution was measured and fitted with a point spread function (PSF) (Fig. 2.9 B). Given the low density and high purity of emitters used in analysis, each isolated PSF corresponded to the image of a single emitter. Thereafter, the centre of the obtained PSF was determined using PSF fitting algorithms, which resolved the position of the single emitters. To this end, luminescence spectrum of such a typical single particle was acquired (Fig. 2.10 A-B) which featured two distinct emission peaks at ~520 nm and ~610 nm (λ_{exc} = 355 nm) owing to emission of FL and Au NCs respectively from the single particle. The chromaticity coordinates calculated from the spectrum acquired on such a single particle of Zn-FL-Au NCs was determined to be (0.52, 0.44) (Fig. 2.10 C). Similarly, a typical single particle (Fig. 2.11 A-B) of the composite treated with cysteine was also analysed under CLSM. Interestingly, the fluorescence spectrum acquired on such a particle exhibited a single emission peak at ~510 nm owing to emission of FL. However, the spectrum was nearly devoid of the emission of Au NCs, thereby suggesting possible quenching of the cluster emission in presence of Cys. This led to significant alteration of the chromaticity coordinates of Zn-FL-Au NCs to (0.19, 0.23) upon interaction with Cys (Fig. 2.10 D-F). On the other hand, super resolution microscopic analysis revealed that a typical single particle of Zn-FL-Au NCs (Fig. 2.11 C-D) treated with Glu exhibited two distinct emission peaks at ~520 nm and ~ 610 nm (λ_{exc} = 355 nm) and the chromaticity coordinates of the emitter calculated from the spectrum therein was found to be (0.40, 0.33) (Fig. 2.10 G-I).

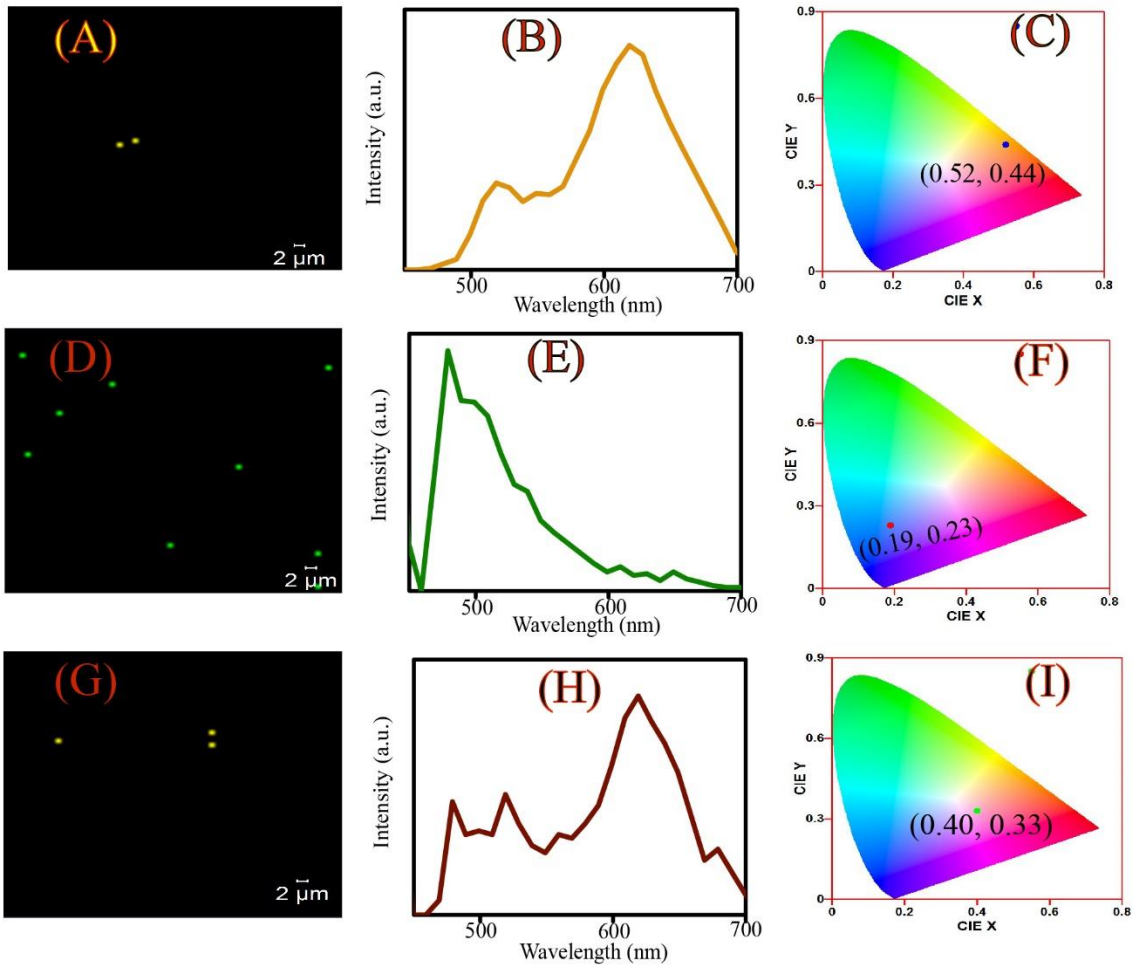

Fig. 2.10: (A) CLSM images of single particles of Zn-FL-Au NCs. (B) PL spectrum acquired on a single particle shown in (A) and (C) corresponding chromaticity coordinates. (D) CLSM images of single particles of Zn-FL-Au NCs treated with Cys. (E) PL spectrum acquired on a single particle shown in (D) and (F) corresponding chromaticity coordinates. (G) CLSM images of single particles of Zn-FL-Au NCs treated with Glu. (H) PL spectrum acquired on a single particle shown in (G) and (I) corresponding chromaticity coordinates.

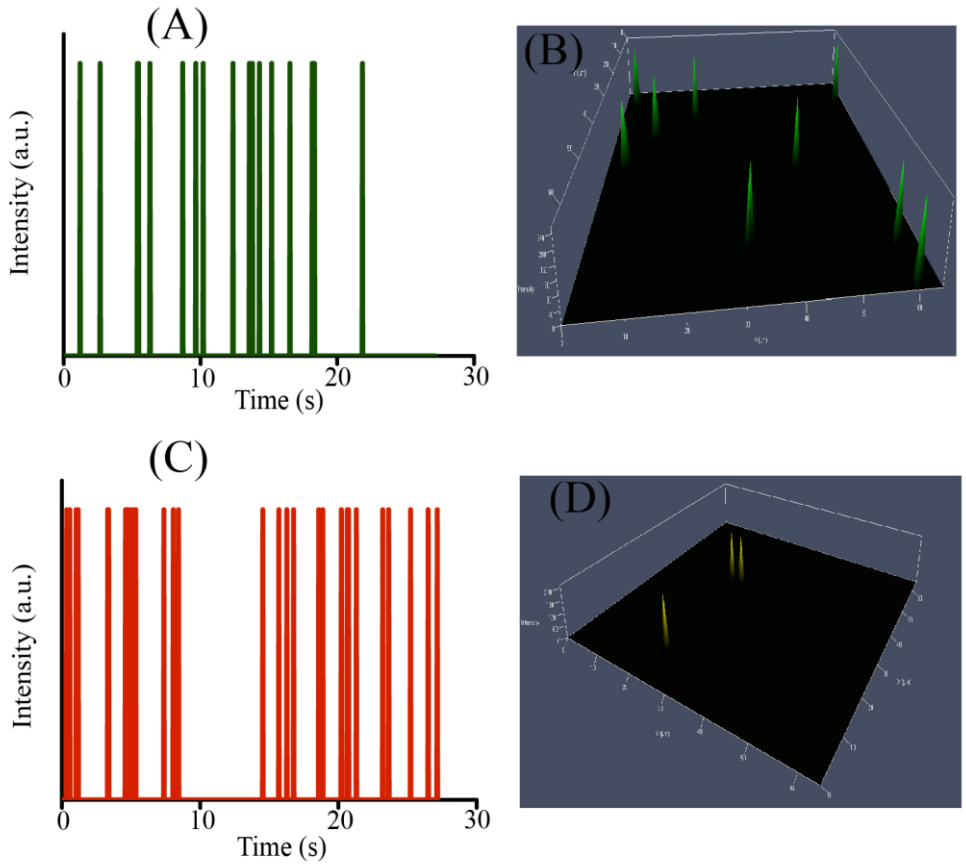

Fig. 2.11: (A) Blinking profile of Zn-FL-Au NCs treated with cysteine (λ_{exc}=355nm) and (B) PSF fitted spatial intensity distribution of Zn-FL-Au NCs treated with cysteine and (C) Blinking profile of Zn-FL-Au NCs treated with glutathione (D) PSF fitted spatial intensity distribution of Zn-FL-Au NCs treated with glutathione.

Allied results were obtained when bulk phase discrimination of Cys and Glu was pursued in presence of Zn-FL-Au NCs. The luminescent dispersion of Zn-FL-Au NCs exhibited two discernible peaks at ~ 520 nm and ~610 nm owing to emission from FL and Au NCs components respectively (λ_{exc} = 355 nm) (Fig. 2.12 A). It is to be mentioned here that the emission profile of the composite in the solution phase differed slightly from the solid phase (containing same proportion of Au NCs and FL) where the luminescence due to Au NCs was observed to be relatively much lower in solution phase as compared to solid state. This could be attributed to the well-known "restricted intramolecular motion" enhanced fluorescence of Au NCs peak in solid state of Zn-FL-Au NCs. It was interesting to observe, that while the luminescence due to Au NCs was effectively quenched upon addition of (50 µL of ~165 mM) Cys to the dispersion containing Zn-FL-Au NCs (Fig. 2.12 B), addition of (50 µL of ~165 mM) of Glu to Zn-FL-Au NCs dispersion led to enhanced luminescence of Au NCs and to an extent enhanced luminescence of FL as well (Fig. 2.12 C).

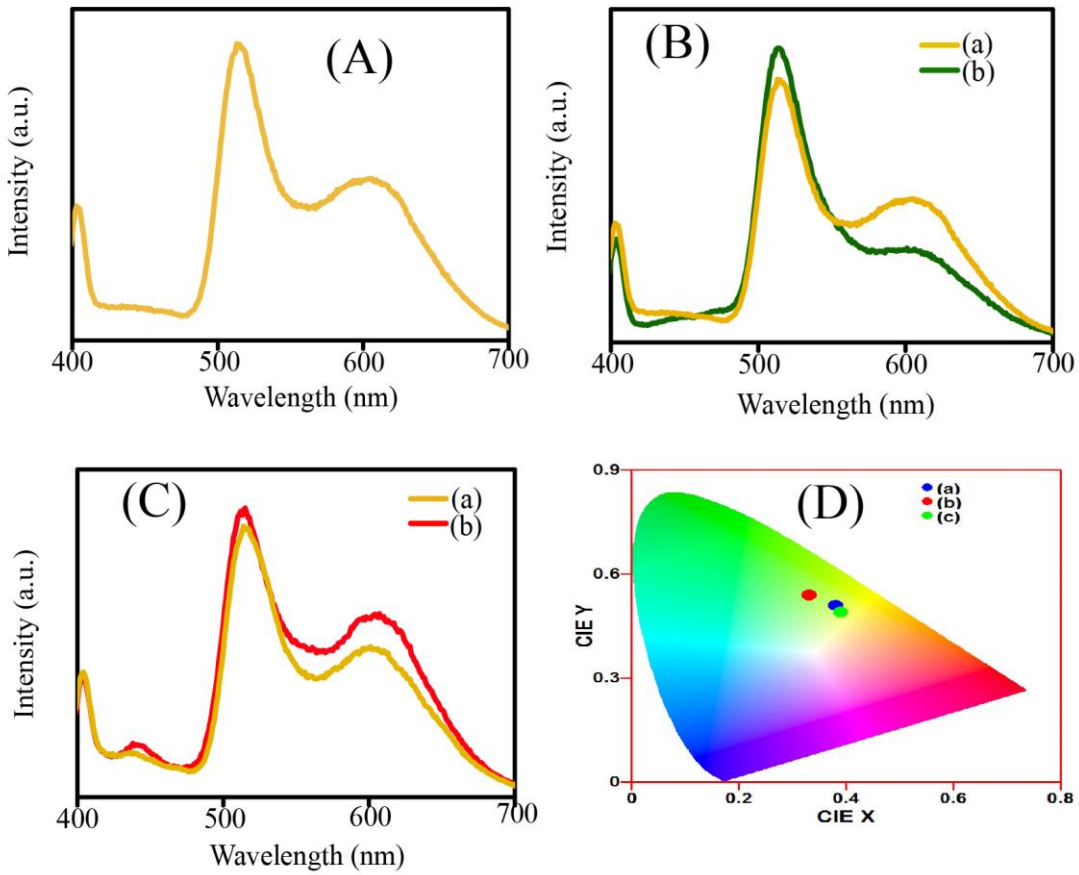

Fig. 2.12: (A) PL spectra of a dispersion of Zn-Fl-Au NCs (B) PL spectra of (a) Zn-Fl-Au NCs and (b) Zn-Fl-Au NCs treated with 50 µL of Cys (~165 mM). (C) PL spectra of (a) Zn-Fl-Au NCs and (b) Zn-Fl-Au NCs treated with 50 µL of Glu (~165 mM). (D) Chromaticity coordinates of (a) Zn-Fl-Au NCs and that following addition of (b) Cys and (c) Glu.

As a result, for the solution phase, the calculated chromaticity coordinates of Zn-FL-Au NCs was found to be (0.38, 0.49), which upon addition of Cys changed to (0.33, 0.52), (owing to significant quenching of the luminescence due to Au NCs), while on the other hand upon addition of Glu, the chromaticity coordinates changed to (0.38, 0.47) (owing to simultaneous enhancement in emission due to FL and Au NCs) (Fig. 2.12D). Discernible discrimination between the two thiols could be achieved in concentration as low as 530 µM in solution phase (Fig. 2.13). However, it should be mentioned here that at a single (or a few particle level) in principle discrimination at even lower concentrations (of the order of a few molecules) should be achieved which is rather unprecedented in current literature.

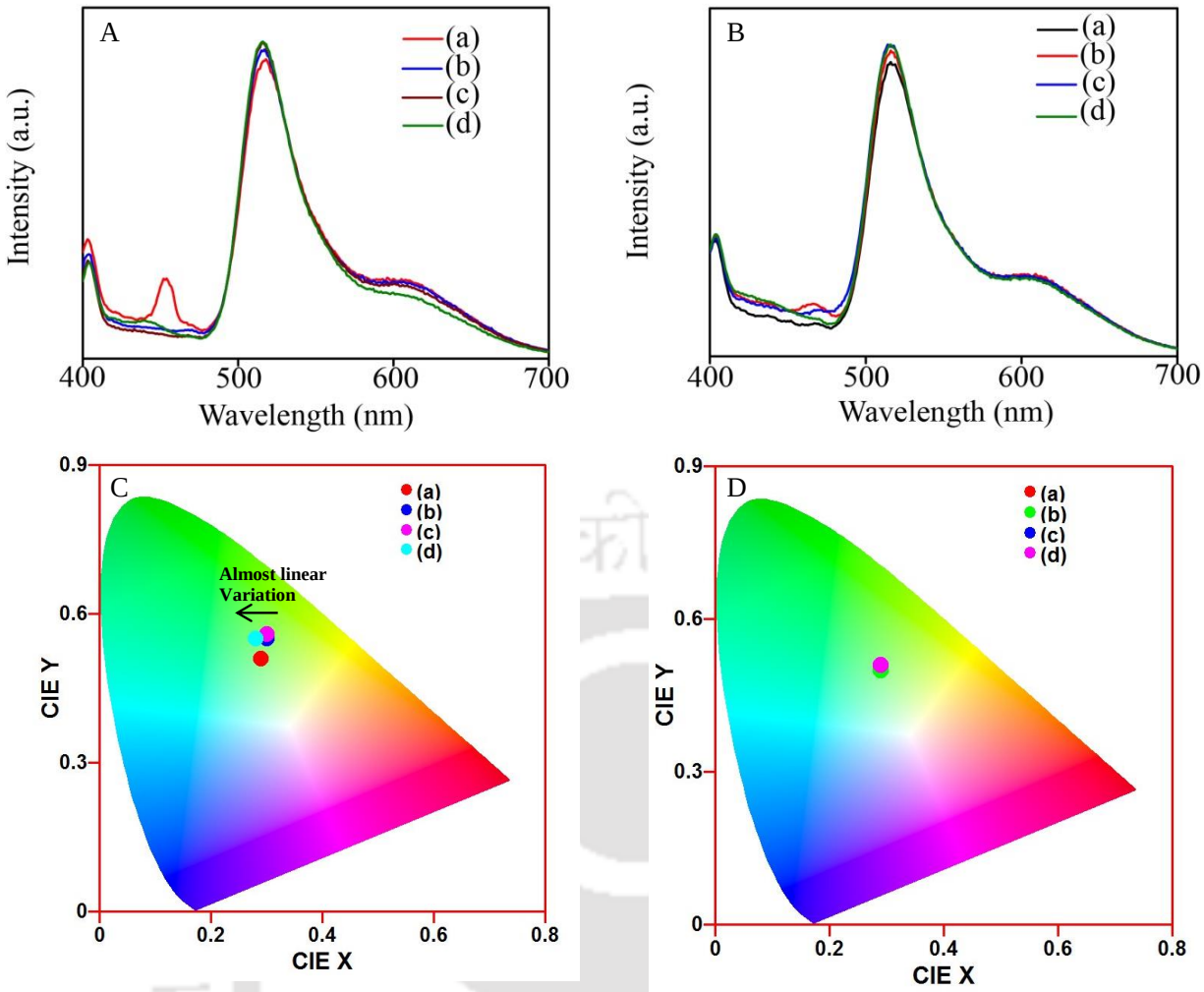

Fig. 2.13 (A): Luminescence spectrum of (a) Zn-FL-Au NCs and that following addition of (b) 0.53 mM (c) 1.057 mM and (d) 1.58 mM of Cys. (B) Luminescence spectrum of (a) Zn-FL-Au NCs and that following addition of (b) 0.53 mM (c) 1.057 mM and (d) 1.58 mM of Glu. (C) Chroamticity coordiates obatined based on plot (A). (D) Chroamticity coordiates obatined based on plot (B).

The practical utility of a chemical sensor is mainly determined by two factors - stability and specificity. Thus, to substantiate the stability of Zn-FL-Au NCs, the same was incubated in human blood serum for 20 h. Interestingly, although the luminescence intensity of Zn-FL-Au NCs was attenuated to a slight extent, the relative intensity of the emission due to FL and Au NCs in Zn-FL-Au NCs was found to remain unaltered (Fig. 2.14 A). It is to be mentioned here that owing to the presence of proteins and other biomolecules in blood serum, an emission peak was observed at ~425 nm.[5] On the other hand, the specificity of Zn-FL-Au NCs towards Cys was verified in presence of several interfering biomolecules (histidine, glycine, glutamic acid, aspartic acid, glucose and lactose), cations (sodium ions) and anions (chloride ions). Further, to demonstrate the discrimination of Cys and Glu using Zn-FL-Au NCs in human

blood serum, Cys and Glu were added to a Zn-FL-Au NCs in blood serum and the corresponding effects on luminescence of Zn-FL-Au NCs were recorded. It was interesting to observe that the CIE coordinates of Zn-FL-Au NCs varied to a negligible extent upon interaction with these chemical species (Fig. 2.14B).

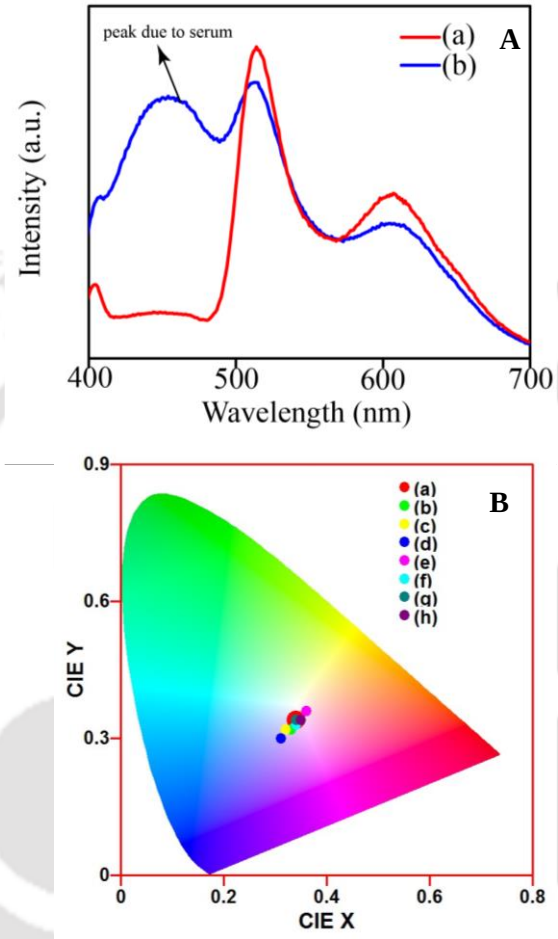

Fig. 2.14 (A): Luminescence spectrum of (a) Zn-FL-Au NCs and (b)that following incubation in human blood serum for 20 h. (B) CIE coordinates of (a) Zn-FL-Au NCs and that following interaction with (b) Glucose, (c) lactose, (d) histidine, (e) glycine, (f) aspartic acid (g) glutamic acid and (h) NaCl.

Interestingly, similar results as that obtained in buffer medium could be observed in serum as well (Fig. 2.15 A-B). However, a little variation was observed with regard to the intensity of the peak of Zn-FL-Au NCs at ~ 510 nm, which in buffer medium got increased upon addition of Cys, however, in serum got decreased upon addition of Cys. Also, we could demonstrate that other amino acids, metal ions and carbohydrates (control samples) had no discernible effect on the chromaticity coordinates of Zn-FL-Au NCs (Fig. 2.16) in blood serum.

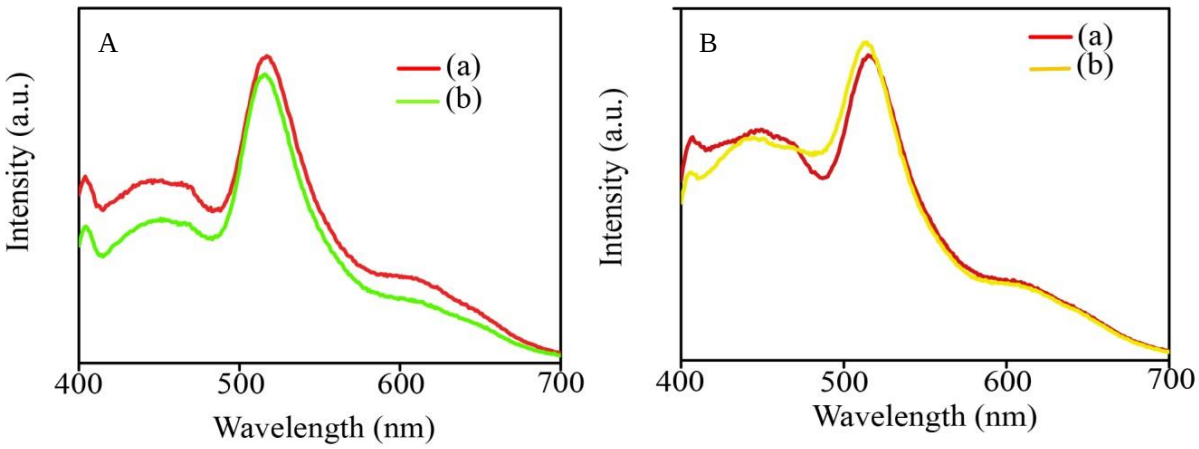

Fig. 2.15: (A) Luminescence spectrum of (a) Zn-FL-Au NCs and that following addition of (b) 2.6 mM Cys in human blood serum. (B) Luminescence spectrum of (a) Zn-FL-Au NCs and that following addition of (b) 2.6 mM Glu in human blood serum.

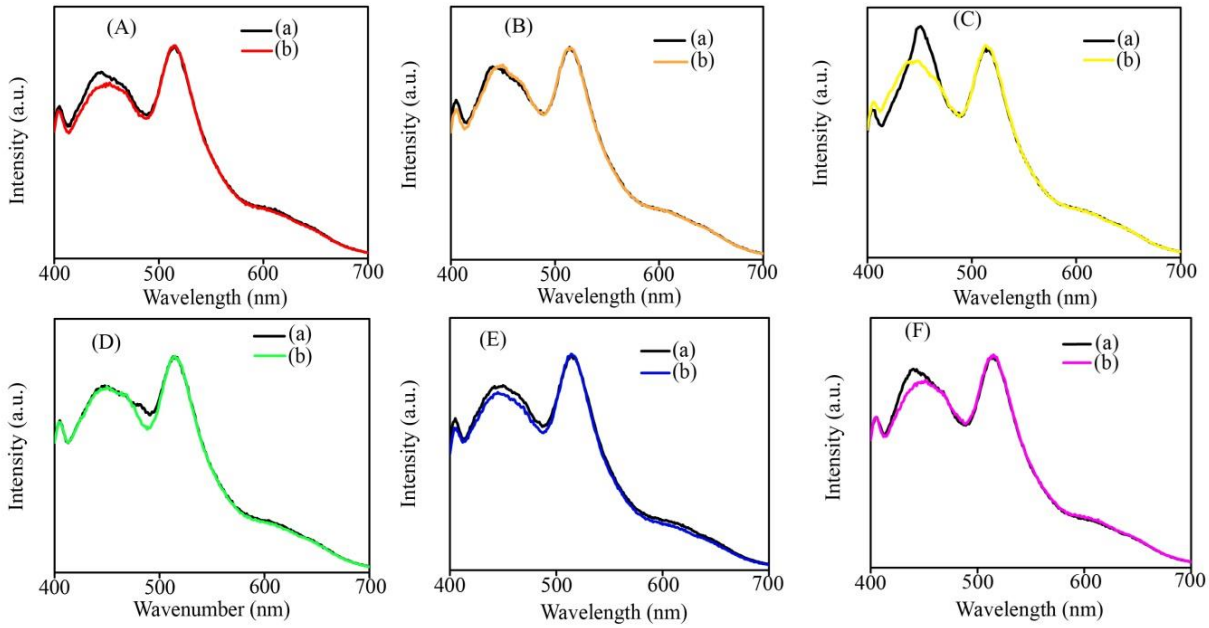

Fig. 2.16: (A) Luminescence spectrum of (a) Zn-FL-Au NCs and that following addition of 2.6 mM (b) aspartic acid. (B) Luminescence spectrum of (a) Zn-FL-Au NCs and that following addition of 2.6 mM (b) glutamic acid. (C) Luminescence spectrum of (a) Zn-FL-Au NCs and that following addition of 2.6 mM (b) glucose. (D) Luminescence spectrum of (a) Zn-FL-Au NCs and that following addition of 2.6 mM (b) glycine. (E) Luminescence spectrum of (a) Zn-FL-Au NCs and that following addition of 2.6 mM (b) histidine. (F) Luminescence spectrum of (a) Zn-FL-Au NCs and that following addition of 2.6 mM of (b) NaCl. All these experiments were performed in human blood serum.

In order to justify the critical role of dual emitting nanoprobe for discrimination of BTs, effect of Cys and Glu on luminescence of FL (with added zinc ions) and Au NCs, as separate entities, was studied. Interestingly, addition of Cys and Glu had negligible effect on the luminescence of FL (Fig. 2.17 A). On the other hand, both Glu and Cys were observed to quench the luminescence of Au NCs by an insignificant amount albeit to a much similar extent (Fig. 2.17 B). Thus, as individual entities, neither FL nor Au NCs could enable discrimination of Cys and Glu. However, upon conjugation of the two (FL and Au NCs) by zinc ions, facile discrimination of Glu and Cys was possible.

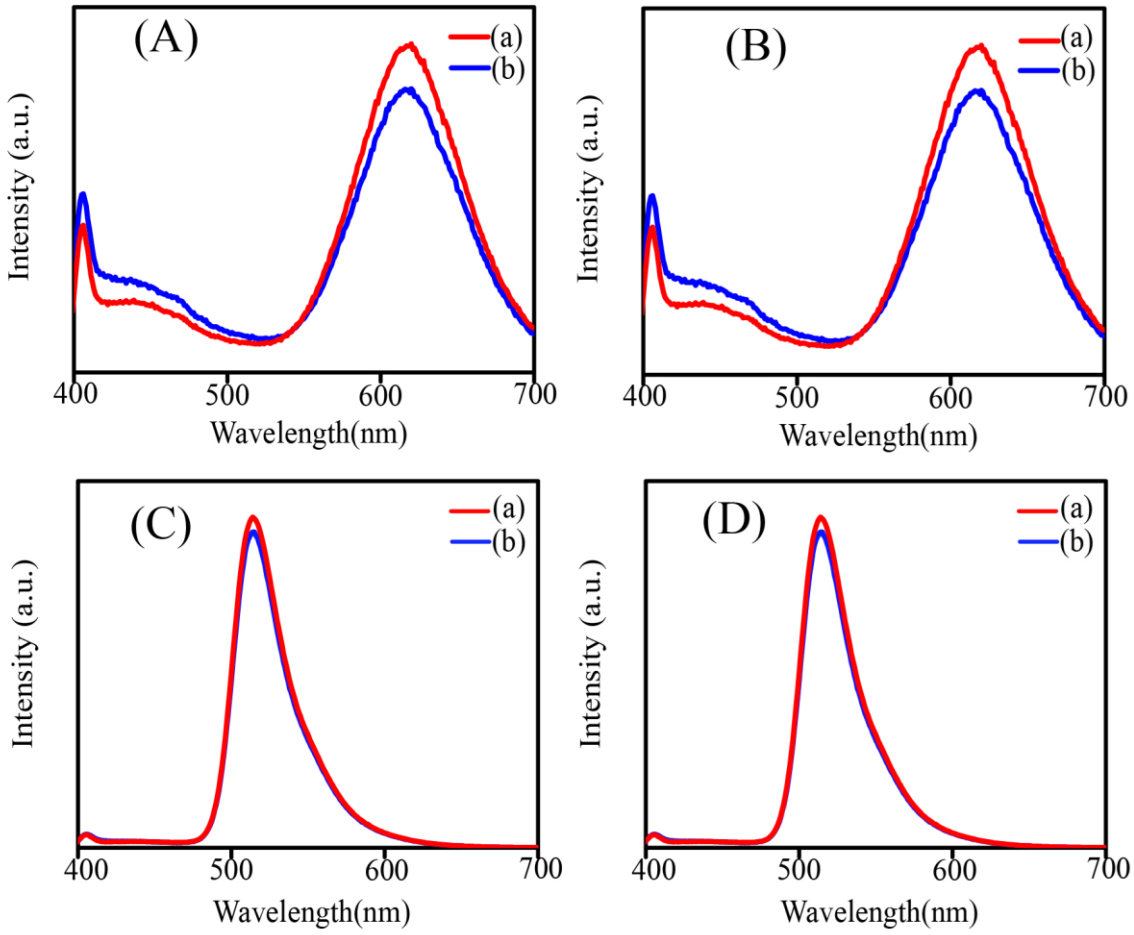

Fig. 2.17: (A) Photoluminescence (PL) spectra of (a) Au NCs added with (b) 50 µL cysteine(~165 mM), (B) PL spectra of (a) Au NCs added with (b) 50 µL glutathione(~165 mM), (C) PL spectra of (a) Zn-FL added with (b) 50 µL cysteine(~165 mM), and (D) PL spectra of (a) Zn-FL added with (b) 50 µL glutathione(~165 mM).

It is worth mentioning here that although the emission maxima of Zn-FL-Au NCs remains same upon interaction with Glu and Cys, the relative intensity of the two emission peaks of Zn-FL-Au NCs at 520 nm (owing to emission from FL) and 610 nm (owing to

emission from Au NCs, changes significantly upon interaction with Cys. Precisely, upon interaction between Zn-FL-Au NCs and Cys, the intensity of the emission peak at 610 nm is quenched and the intensity of the emission peak at 520 nm in enhanced, which significantly alters the chromaticity coordinates of emission from Zn-FL-Au NCs – the overall emission of Zn-FL-Au NCs being shifted to green region as compared to the emission of original Zn-FL-Au NCs. However, upon interaction between Zn-FL-Au NCs and Glu, the intensity of the peak at 520 nm remains unaltered and the intensity of the peak at 610 nm is increased, albeit to a small extent. Thus, there is significantly different effect of Cys and Glu on the chromaticity coordinates of Zn-FL-Au NCs. Thus, the method introduced herein, portends to form a facile basis of distinction between biothiols using chromaticity coordinates of emission of a fluorophore. Further, in future, sensing devices may be constructed using this principle which would be coupled with electronic devices capable of computing chromaticity coordinates and further be used for accurate distinction of chemically allied compounds.

Though deciphering the detailed mechanism controlling the differential interaction of Cys and Glu with Zn-FL-Au NCs, requires further analysis and is beyond the scope of the current study, a plausible mechanism of discrimination of BTs is proposed herein. Zinc ions conjugating the FL component with Au NCs, may bind with Cys, thereby displacing the Au NCs present in Zn-FL-Au NCs. In this regard, it may be mentioned here that binding of Cys with zinc ions is a well-known and facile complexation reaction. Also, as mentioned above, the luminescence Au NCs enhances upon addition of zinc ions, possibly due to aggregation leading to restricted intramolecular (RIM) of the ligands stabilizing the clusters[2,3] (Fig. 2.5). Thus upon being detached from zinc ions the Au NCs get segregated and consequently their luminescence is reduced. On the other hand, Glu, owing to its larger size as compared to Cys, imposes significant steric crowding upon interaction with zinc ions. Therefore, the nature of interaction of Glu with Zn-FL-Au NCs might be more of non-covalent interactions rather than strong chemical interaction. This might have eventually led to further association of Au NCs and FL, possibly through hydrogen bonding, thereby enhancing both their luminescence. It may be mentioned here that hydrogen bonding in Glu moieties is known to be favourable. To further establish the proposed mechanism, further experiments were performed where cystine which is an oxidized dimer of cysteine, was added to Zn-FL-Au NCs and the corresponding effect on luminescence was recorded. The choice of cystine (shown below) for control experiment was made, as it serves both purpose of lacking a thiol group and having approximately twice the size of cysteine. Interestingly owing to the absence of free thiol group,

no discernible change in luminescence and chromaticity coordinates of Zn-FL-Au NCs could be observed upon interaction with cystine (Fig. 2.18).

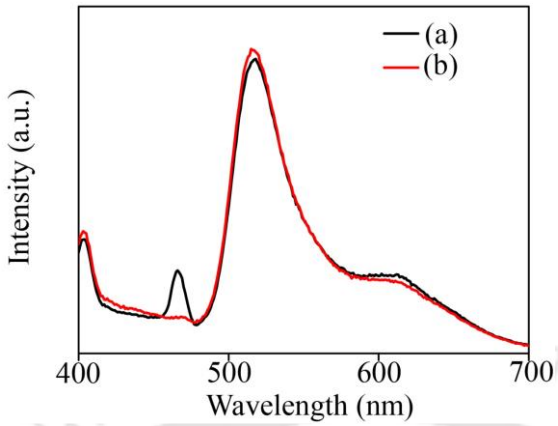

Fig. 2.18: Luminescence spectrum of (a) Zn-FL-Au NCs and that following addition of (b) 2.6 mM cystine (an oxidized dimer of cysteine).

This clearly highlights the pivotal role of thiol group in attachment to zinc ions in discrimination of Cys and Glu using Zn-FL-Au NCs. On the other hand, the larger size of cystine, might have limited the ability of the same to displace Au NCs from Zn-FL-Au NCs, akin to Glu, which further caused no change in luminescence of Zn-FL-Au NCs. Thus, different mode of interaction of Zn-FL-Au NCs with Cys and Glu offered a facile route to chromaticity index based discrimination of BTs at a single particle level. A plausible schematic illustration of the mechanism responsible for discrimination of BTs is depicted herein (Scheme 1).

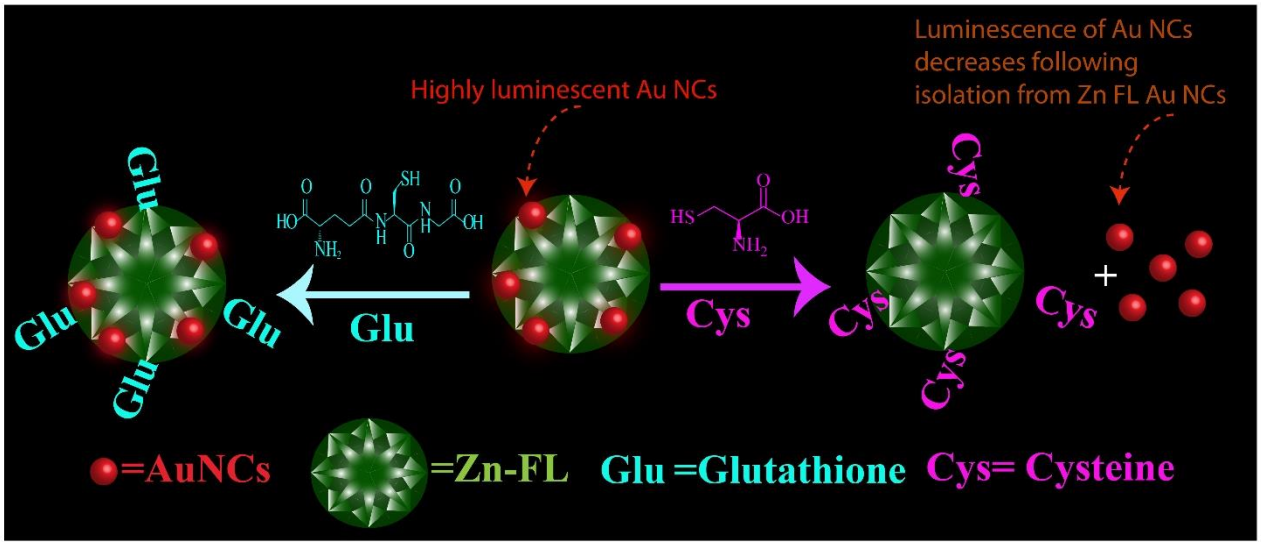

Scheme 1: Schematic illustration of a plausible mechanism responsible for discrimination between Cys and Glu upon interaction with Zn-FL-Au NCs.

Conclusion

In a nutshell, we report an unprecedented strategy for discrimination of BTs (Cys and Glu) at a single particle level using a dual emitting nanoprobe based changes in chromaticity coordinates of the sensor. The dual emitting nanoprobe was fabricated by zinc mediated conjugation of red emitting Au NCs and green emitting FL. The luminescence of Au NCs in the composite was selectively quenched upon interaction with Cys, thereby altering the chromaticity coordinates of Zn-FL-Au NCs. On the other hand, the luminescence of Au NCs and FL was enhanced, albeit to a small extent upon interaction with Glu. Thus, the chromaticity coordinates of Zn-FL-Au NCs was affected to a lesser degree upon interaction with Glu as compared to interaction with Cys. Further, the discrimination between the aforementioned BTs has been achieved on the basis of differential chemical interaction of Zn-FL-Au NCs with Cys and Glu, which is envisioned to pave the ground for the advent of facile routes for distinction between chemically allied compounds.

References

1. Sun, J.; Zhang, J.; Jin, Y., 11-Mercaptoundecanoic acid directed one-pot synthesis of water-soluble fluorescent gold nanoclusters and their use as probes for sensitive and selective detection of Cr3+ and Cr6+. *J. Mater. Chem. C* **2013**, *1*, 138-143.
2. Yahiaa, I. S.; Faraga, A. A. M.; Yakuphanoglub, F.; Farooq, W.A. Temperature dependence of electronic parameters of organic Schottky diode based on fluorescein sodium salt. *Synthetic Metals* **2011**, *161*, 881–887.
3. Basu, S.; Paul, A.; Chattopadhyay, A., Zinc-Coordinated Hierarchical Organization of Ligand-Stabilized Gold Nanoclusters for Chiral Recognition and Separation. *Chem. Eur. J* **2017**, *23*, 9137-9143.
4. Basu, S.; Paul, A.; Chattopadhyay, A., Zinc mediated crystalline assembly of gold nanoclusters for expedient hydrogen storage and sensing. *J. Mater. Chem. A* **2016**, *4*, 1218-1223.
5. Khandelia, R.; Bhandari, S.; Pan, U. D.; Ghosh, S. S.; Chattopadhyay, A.; Gold Nanocluster Embedded Albumin Nanoparticles for Two-Photon Imaging of Cancer Cells Accompanying Drug Delivery. *Small*, **2015**, *11*, 4075-4081.

Chapter 3

Crystallization induced emission enhancement of nanoclusters and one step conversion of "nanoclusters to nanoparticles" as the basis for intracellular logic operations

Herein we report the unprecedented construction of intracellular logic operations using luminescent histidine stabilized gold nanoclusters (His Au NCs). The luminescence intensity of His Au NCs was found to be significantly enhanced following interaction with zinc ions, owing to "Crystallization induced emission enhancement". Further, the luminescence intensity of His Au NCs was found to be effectively quenched in presence of sulphide ions, owing to transformation of emissive His Au NCs to non-emissive gold nanoparticles. Thus the collective and individual effects of zinc ions and sulphide ions causing significant variation in the luminescence intensity of His Au NCs, were used as input parameters for construction of intracellular logic operations such as Tri state buffer, "on-off" switch and INHIBIT gate within mammalian cells.

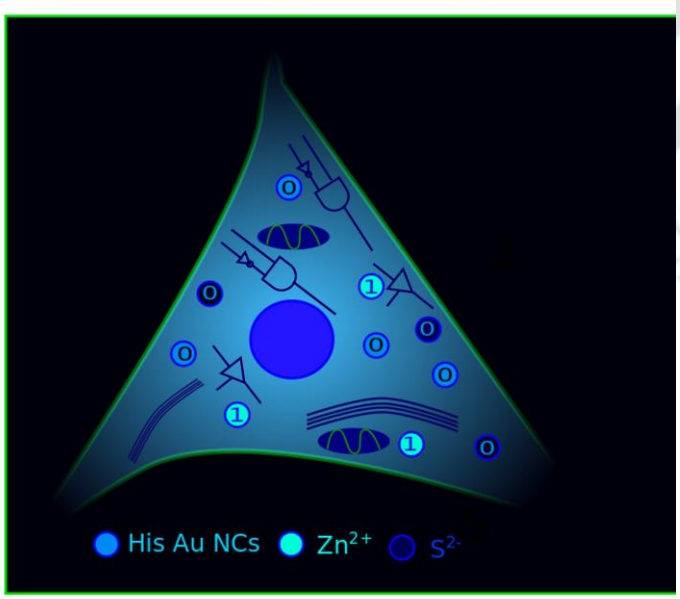

Gayen, C.; Goswami, U.; Gogoi, K.; Basu, S.; Paul, A. *ChemPhysChem* **2019**, *20*, 953 –958.

Experimental Section

Chemicals:

Histidine (Fluka), tetrachloro auric acid (Sigma Aldrich), zinc acetate dihydrate (Merck), sodium sulphide (Merck) were used as purchased without further purifications.

Synthesis of His Au NCs:

Histidine stabilized Au NCs were prepared following a reported protocol.[1] Briefly, ~ 47 mg of histidine was added to 3 mL water under stirring condition. The resultant solution was further treated with 1 mL HAuCl4 (10 mM) and stirred for ~ 1 hr. This resulted in formation of a luminescent dispersion exhibiting emission maximum around 468 nm, upon excitation at 370 nm.

Treatment of His Au NCs with zinc acetate dihydrate:

Typically, 800 µL dispersion of His Au NCs was diluted with 200 µL of water. Further, 500 µL of this dispersion was diluted with 1.5 mL of water. The resultant dispersion was added with varying volumes of 750 µg/mL of Zn-acetate-dihydrate and thereafter the luminescence spectra of His Au NCs were recorded.

Treatment of zinc ion added His Au NCs with sulphide ions:

The aforementioned dispersion of zinc ion added His Au NCs, was added with varying volumes of 750 µg/mL of Na_2S and thereafter the luminescence spectra of His Au NCs were recorded.

Cell culture:

To check the viability of cervical cancer (HeLa cells), following the treatment with dispersion of His Au NCs, zinc ions and Na2S, MTT (3-(4,5-dimethylthiazolyl-2)-2,5-diphenyltetrazolium bromide) based assay was carried out. For this 96 well plates were seeded with 15× 103 cells/well and were allowed to grow for 24 h. First to find out the optimal doses, treatments with varied concentrations of His Au NCs (0.8 mL as synthesised His Au NCs diluted to 1mL), zinc ions (750 µg/mL) and Na_2S (750 µg/mL) were given for 24 h in triplicates individually. Following this the non-toxic dose of His Au NCs was chosen and added along with varied concentration of zinc ions and Na_2S respectively. The assay was carried out based

on the formazon formation which with DMSO gives purple colour having absorbance at 550 nm and is calculated using the following formula.

$$\%\ of\ cell\ viability = \frac{(A_{550} - A_{655})_{sample}}{(A_{550} - A_{655})_{control}} \times 100$$

Confocal Laser Scanning microscopic imaging:

Confocal laser microscopic imaging was carried out with Zeiss LSM 880 microscope for which 15× 103 cells were used for entire sets and were allowed to grow in a coverslip in 35 mm culture plates. The cells were incubated in CO2 incubator for 24 h and after attaining desired morphology and confluency treatments were given. For the present work four sets were required which consists of treatments with His Au NCs and various combinations like His Au NCs+ zinc ions, His Au NCs+ Na_2S, His Au NCs+ zinc ions+ Na_2S and control i.e. without any treatment. The cells treated with only His Au NCs were incubated for 3 h. For the next two sets first His Au NCs were added and incubated for 1 h after which the plates were replenished with fresh media followed by addition of zinc ions and Na_2S for 2 h respectively. Similarly, for the last set treatment with His Au NCs were given for 1 h and after replacing with fresh media zinc ions were added and incubated for 1h followed by incubation with Na_2S for 1h. For bio imaging, following incubation first the cells were washed with PBS and then fixed with 4% formaldehyde (10 min at 37°C). The coverslips were gently taken out from the plates and were placed upside down on a glass slide with sides sealed. The samples were analysed under CSLM with λex = 405 nm and λem = 475 nm

Calculation of mean intensity inside HeLa cells:

Image J software has been used to calculate the mean luminescent intensity of HeLa cells from quantitative image analysis of CLSM images of four different sets of HeLa cells incubated with (i) His AuNCs ,(ii) His Au NCs and zinc ions (iii) His Au NCs and sulphide ion, (iv) His Au NCs, zinc ions and sulphide ion. For each set of data, 25 different cells have been considered to calculate corrected total cell fluorescence (CTCF) value. For the calculation, each cell has been selected and background intensities were subtracted from the area integrated luminescence intensity of each cell area. The mean luminescence intensity was then obtained by dividing the CTCF by cell area under consideration.

Results and Discussions

The UV-vis absorbance spectrum of a dispersion containing His Au NCs was devoid of any discernible peak at ~ 520 nm, thereby negating the formation of surface Plasmon active gold nanoparticles (Fig. 3.1 A). Further, as synthesised His Au NCs, upon excitation at 370 nm, featured an emission maximum at 468 nm, (Fig. 3.1 B). Transmission electron microscopic (TEM) analysis of the dispersion containing His Au NCs revealed the formation of particles with size around 2 nm (Fig. 3.2).

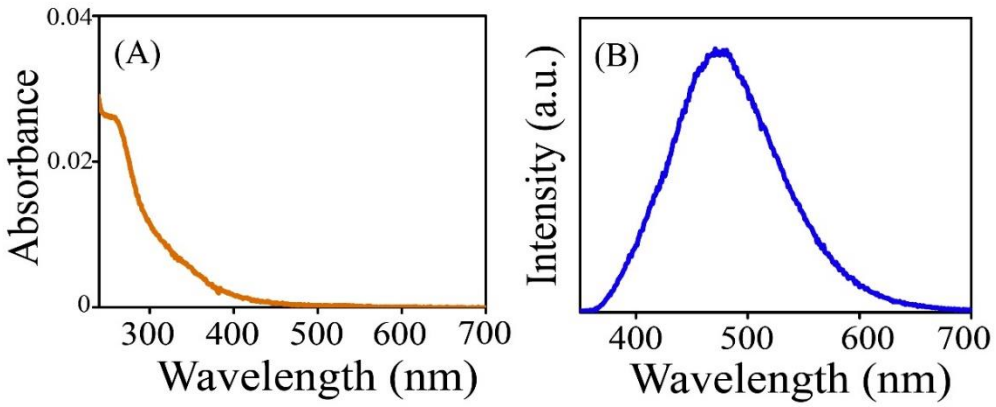

Fig. 3.1 (A) UV-vis absorbance spectrum of His Au NCs. (B) Luminescence emission spectrum of His Au NCs.

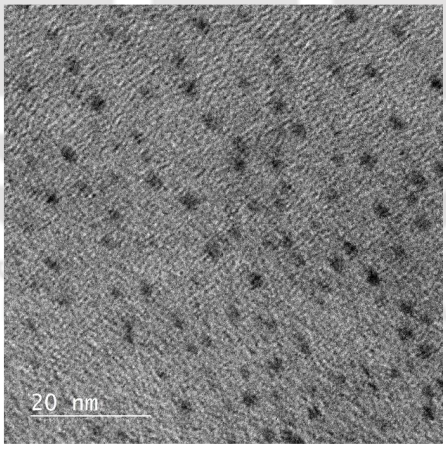

Fig. 3.2 Transmission electron microscopic image of as synthesized His Au NCs

Interestingly, sequential addition of a solution of zinc acetate dihydrate to an aqueous dispersion of His Au NCs, led to enhancement in luminescence intensity of His Au NCs (Fig. 3.3 A). Moreover, a significant bathochromic shift of ~ 17 nm was observed in the emission spectrum of His Au NCs upon addition of zinc ions (Fig. 3.3 B). This indicated possible

chemical interaction between His Au NCs and zinc ions, leading to alteration of the energy states of the former. On the other hand, treatment of His Au NCs with a solution of sulphide ions led to considerable decrease in luminescence intensity of His Au NCs (Fig. 3.3 C). In an allied vein consecutive addition of zinc ions followed by sulphide ions to an aqueous dispersion of His Au NCs led to enhancement and quenching respectively (Fig. 3.3 D) of the luminescence of His Au NCs. The digital photographs of all of these solutions (under UV excitation of 365 nm) are provided in supporting information (Fig.3.4).

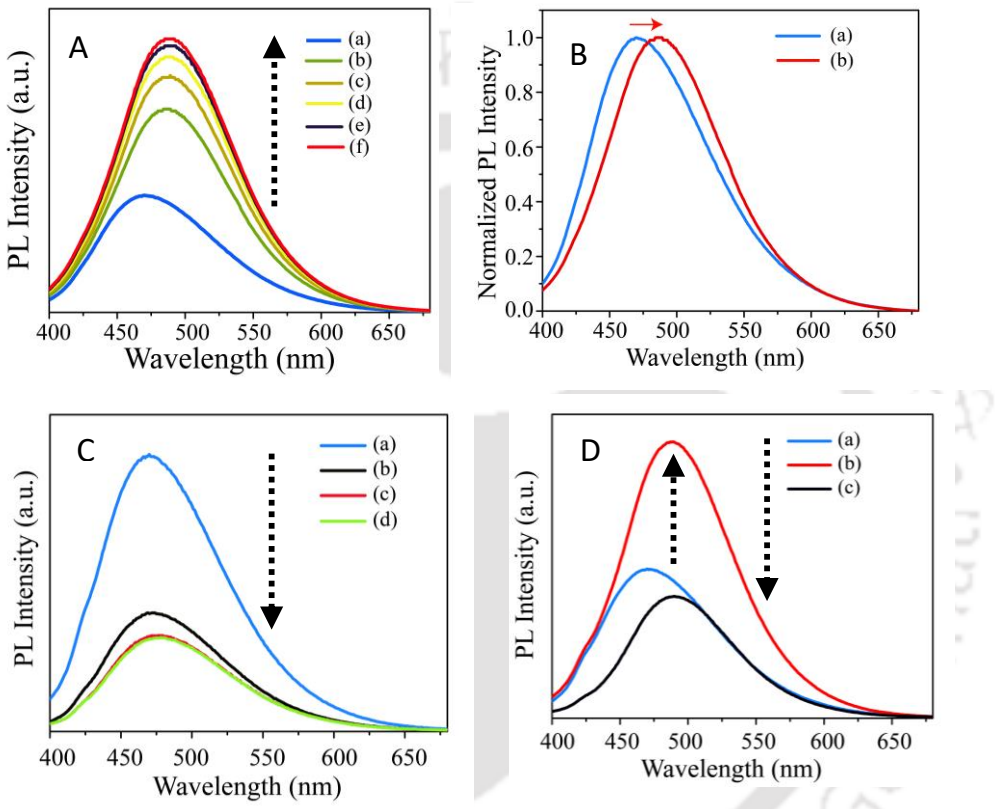

Fig. 3.3: (A) Emission spectrum of (a) His Au NCs and that following addition of (b) 40 µL, (c) 80 µL, (d) 120 µL, (e) 160 µL and (f) 200 µL of Zn-acetate dihydrate (750 µg mL-1). (B) Normalized luminescence emission spectra of His Au NCs (a) before and (b) after addition of zinc ions. The excitation wavelength was set at 370 nm. (C) Emission spectrum of (a) His Au NCs and that following addition of (b) 40 µL, (c) 80 µL, (d) 120 µL of Na2S (750 µg mL-1). (D) Emission spectrum of (a) His Au NCs and that following addition of (b) 40 µL of zinc acetate dihydrate (750 µg mL-1) and (c) 40 µL of Na2S (750 µg mL-1). The excitation wavelength was set at 370 nm.

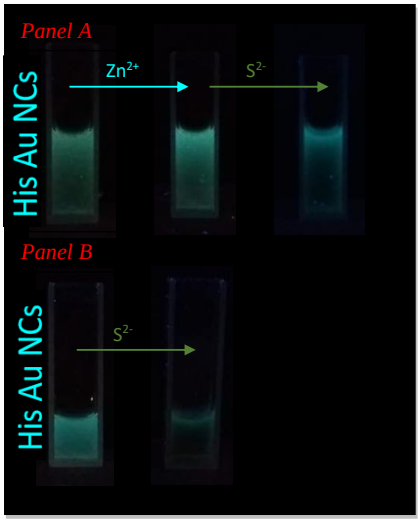

Fig. 3.4 Panel A: Digital photographs of luminescent His Au NCs upon addition of (a) zinc ions followed by (b) sulphide ions. Panel B: Digital photographs of luminescent His Au NCs upon addition of sulphide ions. The excitation wavelength was set at 365 nm.

In typical examples, increase in luminescence intensity of metal nanoclusters upon addition of metal ions; have generally been attributed to "aggregation induced emission enhancement" of NCs.[2] However, in our case, TEM analysis revealed the aggregation of ultra-small His Au NCs (Fig. 3.5 A1-A3) into crystalline particles (Fig. 3.5 B1-B3) upon interaction with zinc ions, and hence, the enhancement in luminescence intensity of His Au NCs upon addition of zinc ions has been attributed to "crystallization induced emission enhancement". Further high resolution TEM analysis revealed the presence of lattice fringes with spacing of 7.4 ± 0.1 Å. Molecular modelling analysis using Avogadro software (Fig. 3.6) showed that this distance corresponds to Zn-His-Au repeat unit in a three dimensional crystalline arrangement of His Au NCs via Zn ions. The linkage between His Au NCs and zinc ions is proposed to have occurred through coordination between zinc ions and imine nitrogen of histidine molecules stabilizing the Au NCs. It is worth mentioning here that such coordination between metal ions and functional groups (carboxylate groups and imine nitrogen) of ligands stabilizing metal nanoclusters has been demonstrated to be facile.[3,4] "It is interesting to note that in the solid crystal of Di-(L-Histidino)- Zn(II) complexes [DOI: 10.1021/jp003167n, Acta Cryst. (1963). 16,r651] two molecules of histidine chelate through the amino group and N2 imidazole nitrogen leading to tetrahedral geometry around the Zn(II) ion and yielding a monoclinic crystal with lattice parameters a = 16.4 A, b = 14.7 A, c = 11 A and β = 129.6^{o} and each unit cell holding two Zn(II) centres. On the other hand, histidine stabilized gold nanoclusters when exposed to Zn (II) a chelate structure of His with Zn (II) is unlikely due to the strong Au NCs-amino group interactions. Thus a smaller lattice spacing in the TEM images of Fig. 3.5 is due to mono dentate binding of Zn to the His Au NCs, as supported by

computational structure of Fig. 3.6. On the other hand, the decrease in luminescence intensity of His Au NCs upon interaction with sulphide ions, has been attributed to the formation of Au nanoparticles (NPs) as evinced from TEM analysis (Fig. 3.5 C1-C2). Further, selected area electron diffraction (SAED) analysis pattern of a typical particle formed out of reaction between His Au NCs and sulphide ions, (Fig. 3.5 C3) matched with those (Au NPs) reported in the literature.

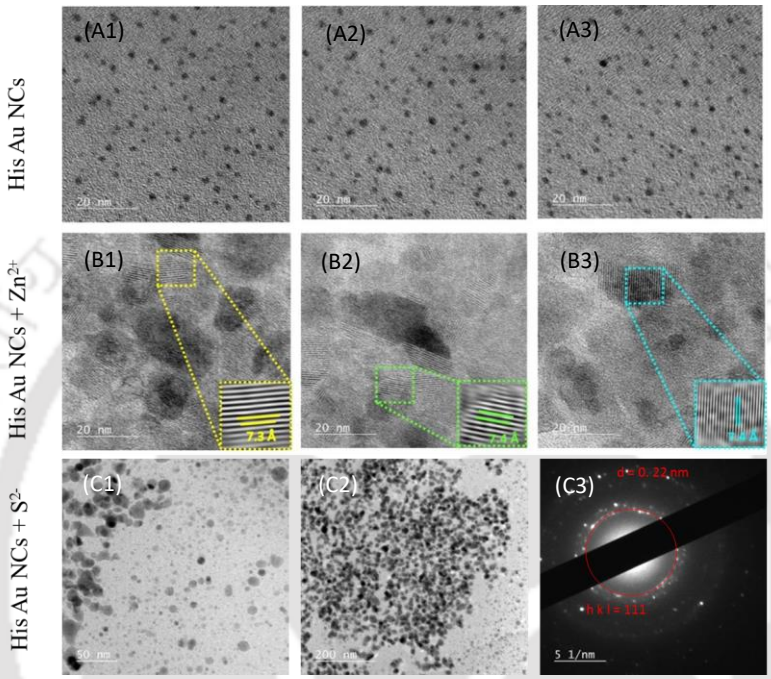

Fig. 3.5: Transmission electron microscopic (TEM) images of (A1-A3) His Au NCs acquired over various regions on the TEM grid. (B1-B3) TEM and High resolution TEM images of crystalline particles formed out of reaction between His Au NCs and zinc ions. (C1-C2) TEM images of the product formed upon addition of sulphide ions to His Au NCs and (C3) selected area electron diffraction (SAED) pattern acquired on a typical particle shown in C1 and C2.

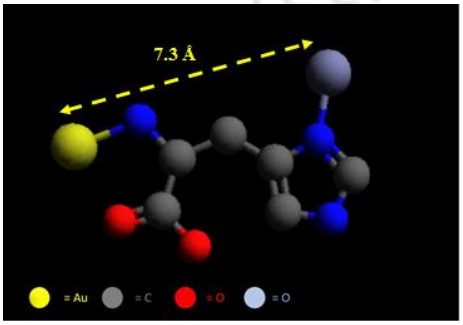

Fig. 3.6: Computationally optimised distance between His Au NCs and zinc ion

The luminescence variation of His Au NCs (in solution phase) upon interaction with zinc ions and sulphide ions (both sequentially and individually) were found to be closely concordant with that at cellular level as well. For this, primarily MTT based cell viability assay was performed to ensure that no significant killing of cells occurred upon treatment with the aforementioned analytes (Zn^{2+} and S^{2-}) in the concentration range at which cell imaging was performed. (Fig. 3.7). On treating the cells with highest concentration of Au NCs (5 µL of diluted His Au NCs; details of dilution as mentioned in experimental section) around 84% cells remained viable. Therefore, to find out the optimal doses, varied concentrations (as mentioned in Figure legend of Fig. 3.7) of Zn^{2+} (750 µg/mL) and S^{2-} (750 µg/mL) with fixed amount of Au NCs (5µL) were used for treating cells. Viability of 89.04% and 96.48 % of cells were obtained with 33.33 µg/ mL and 16.66 µg/ mL of Zn^{2+} and S^{2-} along with fixed concentration of Au NCs respectively (Fig. 3.7). After obtaining the optimal doses, treatment with fixed concentration of Au NCs and Zn^{2+} (33.33 µg/mL) with varied concentration of S^{2-} was done, where with highest concentration of S^{2-} (83.33 µg/mL), 68.79 % of cells were viable (Fig. 3.8). It was found that with 16.66 µg/mL of S^{2-} 93.28 % cells remains viable, and thus this amount was used for imaging studies. In a nutshell, with fixed concentration of His Au NCs, 33.33 µg/mL of Zn^{2+} and 16.66 µg/mL of S^{2-} , cell imaging and eventual construction of intracellular logic operations has been demonstrated

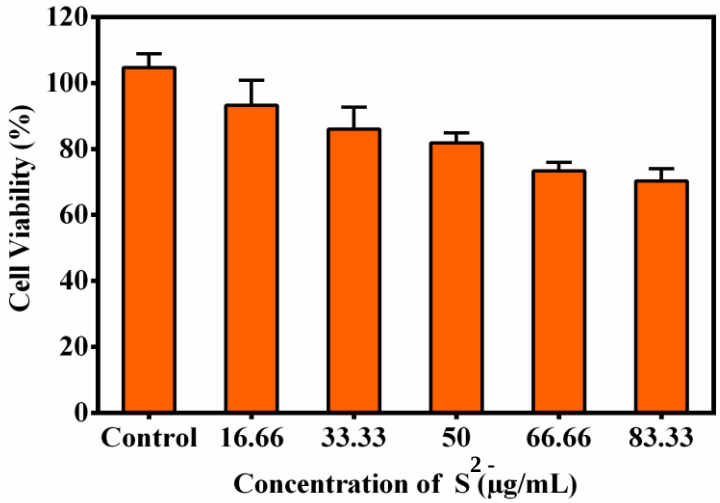

Fig. 3.7: MTT based cell viability assay of HeLa cells treated with the mentioned samples at a concentrations mentioned in Fig. legends. The assay was performed following 24 hours of incubation of the HeLa cells with respective samples.

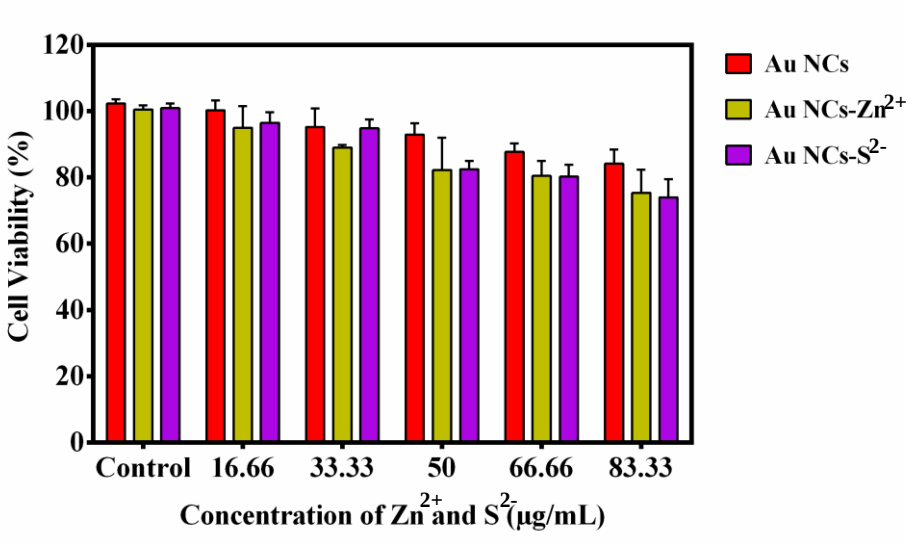

Fig. 3.8: MTT based cell viability assay of HeLa cells treated with the sulphide ions at concentrations mentioned in Fig. legends. The assay was performed following 24 hours of incubation of the HeLa cells with respective samples.

Further, Fig. 3.9 A1-A3 shows the confocal laser scanning microscopic (CLSM) image of HeLa cells treated with His Au NCs. Depth projection analysis was further performed to confirm the internalization of His Au NCs within HeLa cells (Fig. 3.10 A). The mean luminescence intensity of HeLa cells treated with His Au NCs was calculated using established procedures, as described in the experimental section. However, upon treatment of HeLa cells with zinc ions following incubation with His Au NCs, the mean luminescence intensity was found to be enhanced to a substantial extent (Fig. 3.9 B1-B3). The corresponding depth projection analysis has been shown in Fig. 3.10 B. This is attributed to the phenomenon of crystallization induced emission enhancement of His Au NCs upon complexation with zinc ions, as observed in solution phase. Further, upon treatment of HeLa cells with sulphide ions, formerly treated with His Au NCs and zinc ions, the mean luminescence intensity was observed to have gone down significantly (Fig. 3.9 C1-C3). This, akin to solution phase results, has been attributed to formation of Au NPs, which are known to be non-luminescent. In an allied vein, treatment of HeLa cells treated with sulphide ions following treatment with His Au NCs (Fig. 3.9 D1-D3) showed decrease in mean luminescence intensity of His Au NCs. The depth projection analysis has been shown in Fig. 3.10 C. It is worth mentioning here that the concentrations of the analytes used for TEM analysis, were similar to those used for luminescence studies. Thus, the observation of the TEM analysis could presumably be extended to explain the changes in luminescence of His Au NCs.

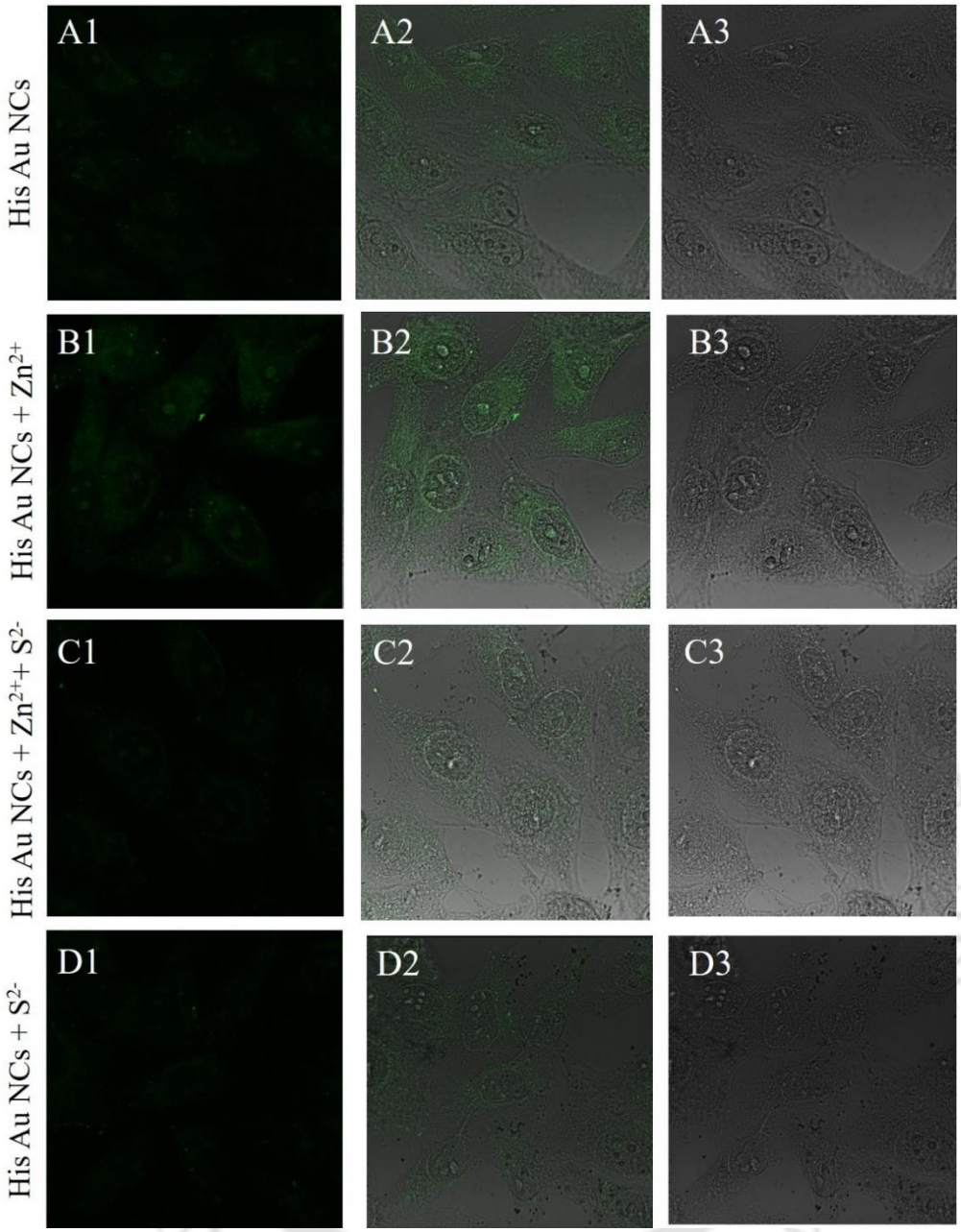

Fig. 3.9 CLSM images of HeLa cells treated (A1-A3) His Au NCs, (B1-B3) His Au NCs and zinc ions, (C1-C3) His Au NCs, zinc ions followed by sulphide ions and (D1-D3) His Au NCs and sulphide ions. Frame size for all images were 64 × 64 μm^2.

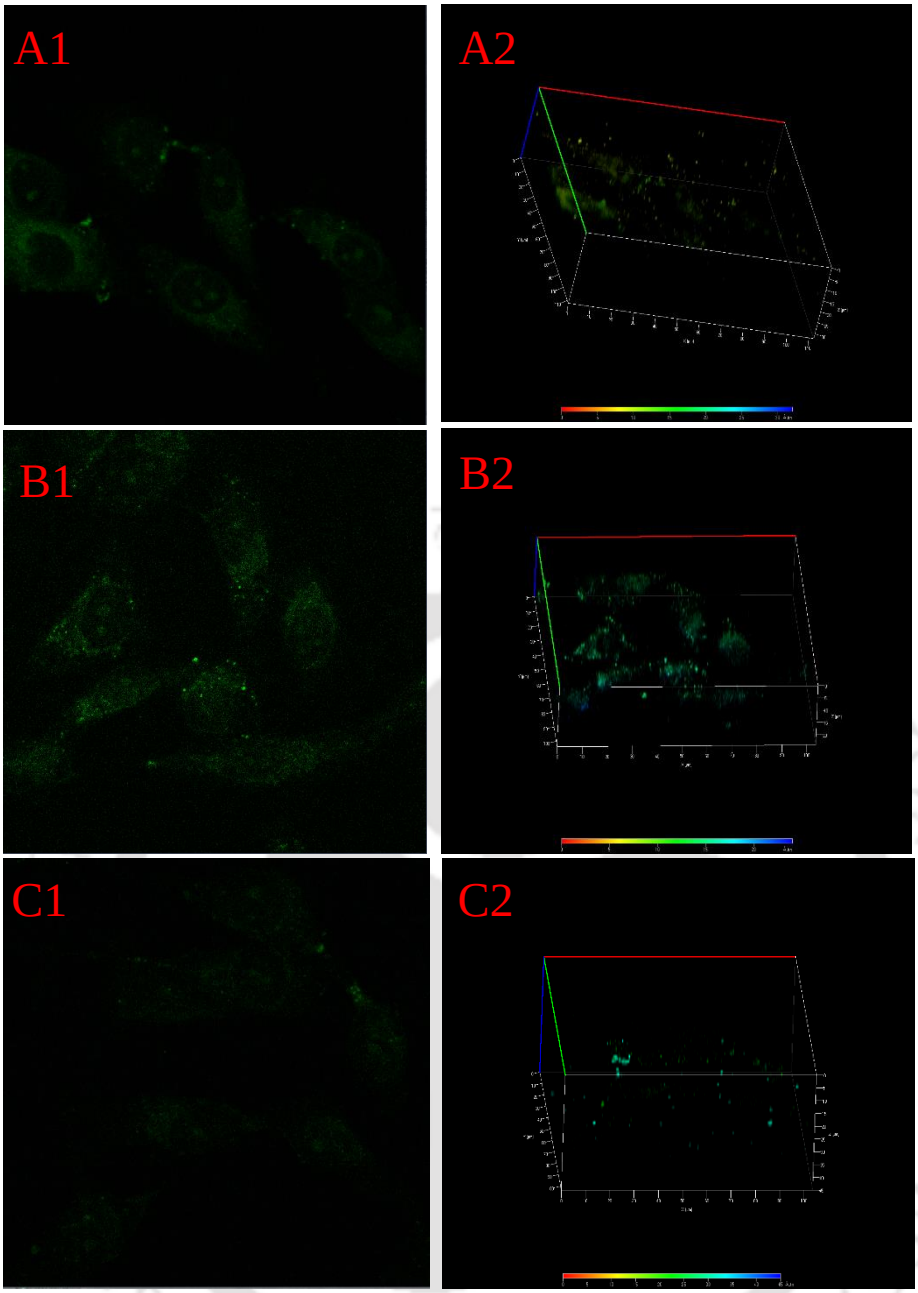

Fig. 3.10: CLSM images and corresponding depth projection analysis of HeLa cells treated with (A) His Au NCs (B) His Au NCs followed by zinc ions and (C) His Au NCs followed by sulphide ions.

The interesting trend of variation of luminescence intensities of His Au NCs upon interaction with zinc ions and sulphide ions within cellular environment provided an impetus for development of nanocluster based logic gate operating inside mammalian cells. Firstly, as mentioned above, significant enhancement in luminescence intensity of HeLa cells incubated with His Au NCs, was observed following post treatment with zinc ions. This provided an option for development of tri state buffer within single mammalian cell. Tri state buffers are ubiquitous in biological systems and are considered important in dealing with multiple signals.

In our case, the mean intensity of HeLa cells treated with His Au NCs was found to be 0.7 units (following normalization with respect to luminescence intensity of zinc ions added HeLa cells) upon laser excitation of 405 nm. This state has been considered to be 0. However, following addition of zinc ions, the mean intensity of HeLa cells pre-treated with His Au NCs was calculated to be 1 unit and the corresponding state was denoted as 1. This trend in luminescence change of His Au NCs suited a tri state buffer logic operation (Fig. 3.11). The truth table for the aforementioned logic operation has been represented in Table 1.

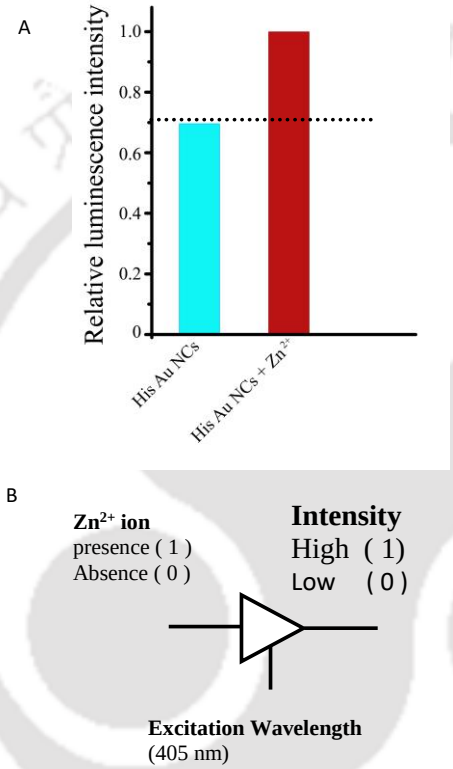

Fig. 3.11: (A) Mean luminescence intensity of His Au NCs and zinc ion added His Au NCs inside HeLa cells. (B) A tri state buffer where presence and absence of Zn^{2+} ions in Au NCs cluster is considered as the input signal. High intensity is considered as logic high level and low intensity is considered as logical low level where excitation wavelength of 405 nm is considered as the control input.

	Zn^{2+}	Output
Presence	1	1
Absence	0	0

Table 1: Truth table for tristate buffer where excitation wavelength of 370 nm is the control signal.

In the next step, a "one time on-off switch" effective inside cell could be constructed using the variation of luminescence of His Au NCs upon sequential interaction with zinc ions followed by sulphide ions. The initial state that is HeLa cells treated with as synthesised His Au NCs was considered to be 0. Further, addition of zinc ions to cells treated with His Au NCs resulted in notable enhancement of luminescence. This state was considered to be 1. Further, upon treatment with sulphide ions, the HeLa cells treated formerly with His Au NCs followed by zinc ions, exhibited significant decrease in luminescence, even lesser than the initial intensity of HeLa cells treated with His Au NCs. This state therefore denoted 0. This pattern of luminescence variation matched with that of luminescent molecular switch operating inside cells.

Finally, the collective and individual effects of zinc ions and sulphide ions on the luminescence of His Au NCs suited the construction of INHIBIT gate inside HeLa cells. In this particular logic operation, the output signal is 1 only when one particular is 1. Thus in order to construct an INHIBIT gate, the initial intensity of HeLa cells treated with His Au NCs was set to be 0. Further, addition of zinc ions to His Au NCs treated HeLa cells led to enhancement in luminescence intensity of the former and this state was considered to be 1. On the other hand, incubation of HeLa cells (formerly treated with His Au NCs) with sulphide ions (in absence of zinc ions) led to decrease in luminescence intensity of His Au NCs and therefore denoted a 0 state. Moreover, upon addition of both zinc ions and sulphide ions (sequentially) to His Au NCs added HeLa cells, owing to the higher effect of sulphide ions on the luminescence intensity of His Au NCs, an overall quenching of luminescence inside HeLa cells was observed. This set of observation enabled construction of an INHIBIT gate where the luminescence intensity of HeLa cells treated with His Au NCs could be considered to be in state 1, only when treated with zinc ions (Fig. 3.12 A-C). The truth table for the aforementioned logic operation has been represented in Table 2.

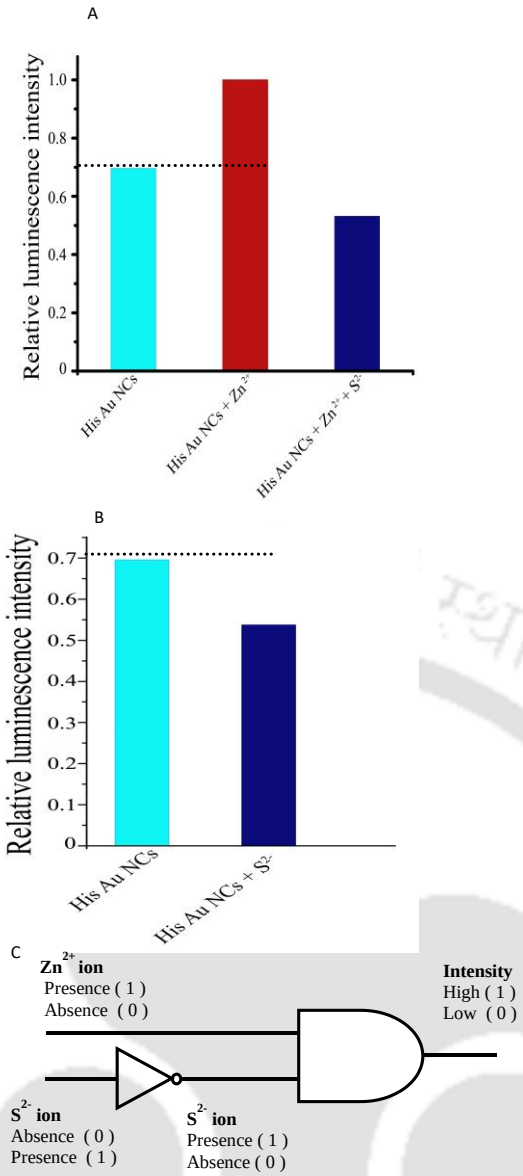

Fig. 3.12: (A) Mean luminescence intensity of His Au NCs, zinc ion added His Au NCs and zinc and sulphide ions treated His Au NCs, inside HeLa cells. (B) Mean luminescence intensity of His Au NCs and sulphide ion added His Au NCs inside HeLa cells. (C) The logical function implemented is ($\underline{S^{-2}}$. Zn^{+2}), where presence and absence of Zn^{2+} and S^{2-} are considered as input signals.

Zn^{2+}	S^{2-}	Output
0	1	0
1	0	1
1	1	0

Table 2: Truth table for INHIBIT gate observed in the system.

Conclusions

In a nutshell we report unprecedented construction of multilevel logic operation inside mammalian HeLa cells using luminescent gold nanocluster. Crystallization induced emission enhancement of histidine stabilized gold nanoclusters upon addition of zinc ions has enabled the construction of an intracellular tri state buffer. Further sulphide induced transformation of gold nanoclusters to gold nanoparticles led to loss of emission intensity of gold nanoclusters. This, in conjunction with the observation of crystallization induced enhancement of emission intensity of gold nanoclusters, facilitated the fabrication of a one-time 'on-off' switch as well as hierarchical logic operation like INHIBIT gate in a cellular environment.

References

1. Yang, X.; Shi, M.; Zhou, R.; Chen, X.; Chen, H. Blending of HAuCl4 and histidine in aqueous solution: a simple approach to the Au10 cluster. *Nanoscale*. **201**1, *3*, 2596-2601.
2. Goswami, N.; Yao, Q.; Luo, Z.; Li, Z.; Chen, T.; Xie, J. *J. Phys. Chem. Lett.* **2016**, *7*, 662-975.
3. Basu, S.; Paul, A.; Chattopadhyay, A. Zinc mediated crystalline assembly of gold nanoclusters for expedient hydrogen storage and sensing. *J. Mater. Chem. A.* **2016**, *4*, 1218-1223.
4. Basu, S.; Goswami, U.; Paul, A.; Chattopadhyay, A. Crystalline assembly of gold nanoclusters for mitochondria targeted cancer theranostics. *J. Mater. Chem. B.* **2018**, *6*, 1650.

Chapter 4

Visible light excitation induced luminescence from gold nanoclusters following surface ligand complexation with Zn^{2+} for day light sensing and cellular imaging

Herein we report complexation reaction mediated extended aggregation of gold nanoclusters exhibiting luminescence under visible light excitation. Complexation reaction between carboxylate groups of mercaptopropionic acid (3-MPA) and zinc ions induced aggregation of gold nanoclusters, which featured bright green luminescence upon excitation with visible light of wavelength 450 nm and beyond. This luminescence of aggregated Au NCs, easily discernable with bare eyes (under broad day light excitation), was used as a probe for luminescence based detection of molecules based on the pKa values of the latter. This aspect, has been an unfilled dream of scientists pursuing research on development of nanoscale sensors, since luminescence based detection techniques offer greater degree of accuracy and sensitivity compared to absorption based methods, and was thus far unexploited/untapped area by nanoscale materials. Moreover, facile imaging of mammalian cells was achieved using these aggregated clusters upon excitation with visible light. This study, demonstrates the utility of luminescent nanoclusters, akin to organic dyes, as materials active under visible light excitation. Thus, complexation reaction based tailoring of optical properties of nanoclusters served as an effective tool in pushing the absorption maxima of nanoclusters from UV to visible range, enabling luminescence of nanoclusters under broad day light excitation. Hence, the work embodied herein offers a unique route to widen the application potential of metal nanoclusters as sensors and bioimaging agents operating under visible light excitation.

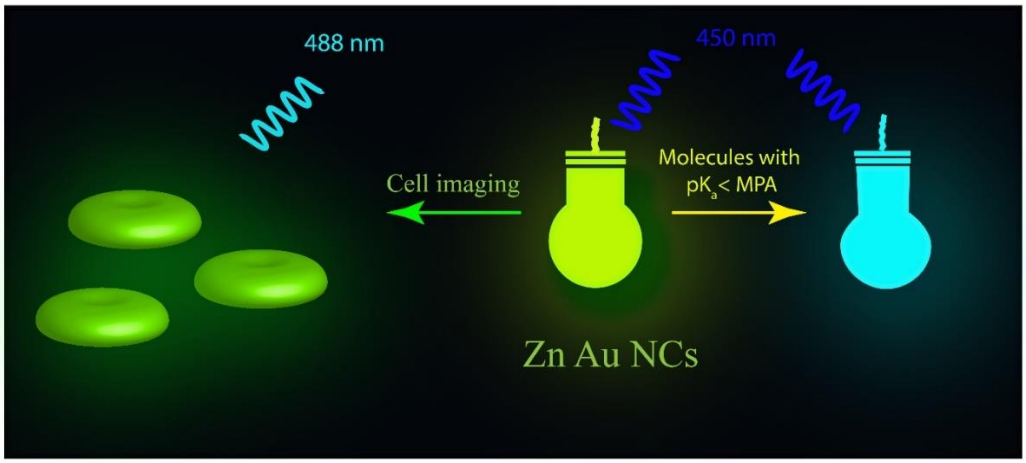

Gayen, C.; Basu, S.; Goswami, U.; Paul, A. *Langmuir* **2019**, *35*, 9037−9043.

Experimental Section

Materials:

Tetrachloroauric acid, mercaptopropionic acid and potassium bromide were procured from Sigma Aldrich. Zinc acetate dihydrate was purchased from MERCK. All experiments and synthesis were done using Milli Q water. All glasswares were thoroughly washed with aqua regia prior to experiments and synthesis.

Synthesis of gold nanoclusters:

Gold nanoclusters were synthesized by slightly modifying a procedure reported in our previous work. Briefly, to 10 mL water, 1 mL of HAuCl4 (10 mM) was added. To the resultant solution, 0.4 mL MPA (0.11 M) was added. This led to formation of a colorless dispersion exhibiting a weak luminescence at ~ 575 nm.

Complexation reaction between gold nanoclusters and zinc acetate dihydrate:

To the above formed dispersion of Au NCs, ~ 100 mg of zinc acetate dihydrate was added which resulted in formation of a dispersion exhibiting bright luminescence a ~ 575 nm.

MTT based cell viability assay:

To check the viability of mammalian cells on exposure with Au NCs and Zn Au NCs MTT (3-(4,5-dimethylthiazolyl-2)-2,5-diphenyltetrazolium bromide) assay was carried out. The assay was conducted following the treatment of Hela cells (1×104) with varying concentration of Au NCs for 24h. After the treatment period, MTT dye was added and incubated for 3h which resulted in purple color formazon formation and its absorbance was measured at 550 nm based on the following formula:

Confocal Laser Scanning Microscope (CLSM) studies:

The viable dose after MTT assay was selected and CLSM was conducted with Zeiss LSM 880 microscope. For imaging first the Hela cells (10×103) were grown in a coverslip and after attaining 70% confluency, treatment with both Au NCs and Zn Au NCs were given for 3 h (incubated in CO2 incubator 37°C) respectively. Following treatment, the media were removed and the cells were fixed with fixed 4% formaldehyde (10 min at 37°C). The coverslips were then gently lifted with tweezers and placed upside down in a glass slide with its side sealed. Under CSLM the samples were excited with visible wavelength i.e. λ_{ex} = 488 nm.

Instruments:

Luminescence (emission and excitation) spectra of all samples were acquired using Horiba Jobin Yvon Fluoromax-4 spectrofluorimeter. UV-vis spectra were recorded using PerkinElmer Lambda-25 spectrophotometer. Digital photographs were captured using smartphone (Lenovo vibes). FTIR spectra were acquired in PerkinElmer, Spectrum One spectrophotometer. KBr was used for preparation of pellets for FTIR analysis. Confocal laser scanning microscopic images were acquired using Zeiss LSM 880 confocal microscope.

Results and discussion

Addition of mercaptopropionic acid (MPA) to an aqueous solution of tetracholoroauric acid resulted in the formation of a colorless dispersion with no discernible peak in UV-visible absorption spectrum and exhibiting a weak luminescence at 575 nm upon excitation at 300 nm (Fig. 4.1 A-B). It is worth mentioning here that the formation of non-luminescent Au NCs upon reaction between HAuCl4 and MPA is not surprising and our result matches well with that reported by others.24 Transmission electron microscopic analysis of this dispersion affirmed the formation of nanoscale particles with sizes around 2 nm (Fig. 4.1 C). In order to confirm the oxidation state of Au in Au NCs, XPS analysis was performed. As evident from the XPS spectrum, two distinct peaks at 83.8 eV and 87.3 eV corresponding to Au (0) and Au (I) was observed. This suggested the presence of both Au (0) and Au (I) as constituents of Au NCs (Fig. 4.2).

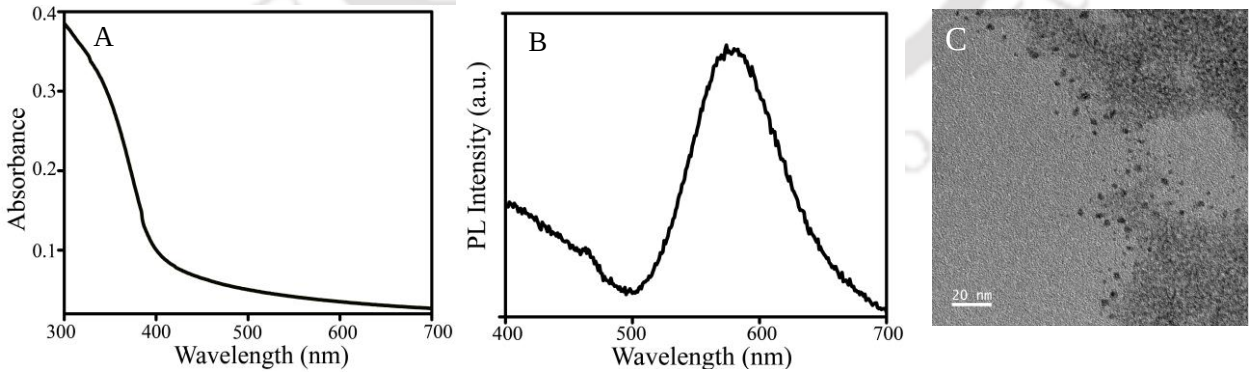

Fig. 4.1: (A) UV-vis absorbance spectrum of Au NCs. (B) Emission spectrum of Au NCs. The excitation wavelength was set at 300 nm. (C) TEM image of Au NCs.

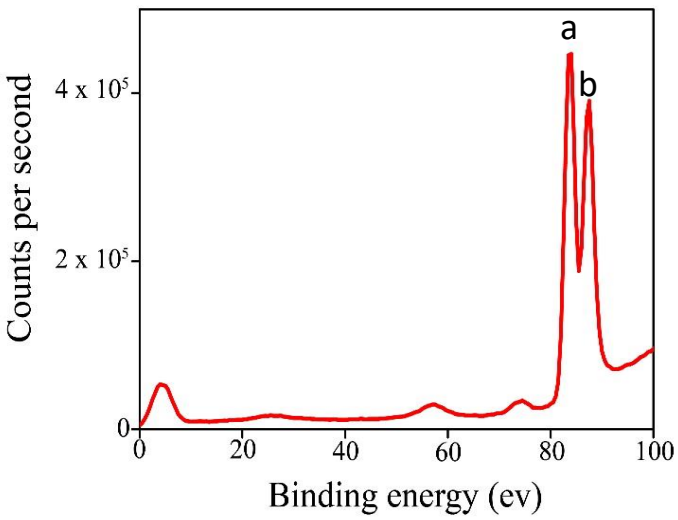

Fig. 4.2: XPS spectrum of Au NCs indicating the presence of Au (0) and Au (I) at (a) 83.8 and (b) 87.3 eV respectively.

Recent research from our laboratory reports the synthesis of gold nanoclusters (Au NCs) using MPA and an additional ligand (for example histidine, tryptophan, tyrosine, cysteine and mercaptobenzoic acid) as stabilizers.[1-5] These nanoclusters (NCs) have further been used for formation of crystalline assembly of clusters for various applications. The presence of additional ligands was found to be essential for complexation reaction mediated crystalline assembly of NCs. However, in a work allied to ours it has been shown that without the presence of these additional ligands aggregation of nanoclusters occurs which lack crystallinity and hence are devoid of distinct structural features.[6]

In the next step we were interested in pursuing assembly of these NCs. As mentioned above, the earlier reported NCs from our group were used for versatile applications ranging from energy storage,[1] chiral recognition and separation,[2] to organelle-targeted theranostics.[3] On the other hand, designing of extended assembly of nanoclusters with optical properties unobtainable in individual nanoclusters is an endeavor worth pursuing. In this regard, we wanted to achieve emission from assembly of NCs upon excitation in visible region of light. It is worth mentioning here that the as synthesized Au NCs were devoid of luminescence upon excitation in visible range. Thus the as synthesized Au NCs were mixed with zinc acetate dihydrate. This led to significant enhancement in luminescence intensity of the weakly luminescent NCs upon excitation at 300 nm (Fig. 4.3 A-B). No significant enhancement of luminescence intensity was observed of Au NCs upon excitation with visible light even immediately after addition of zinc ions to a dispersion of Au NCs (Fig. 4.3 C). However,

following incubation of zinc added Au NCs dispersion for around an hour at room temperature, the color of the dispersion changed from colorless to greenish-yellow (Fig. 4.3 D).

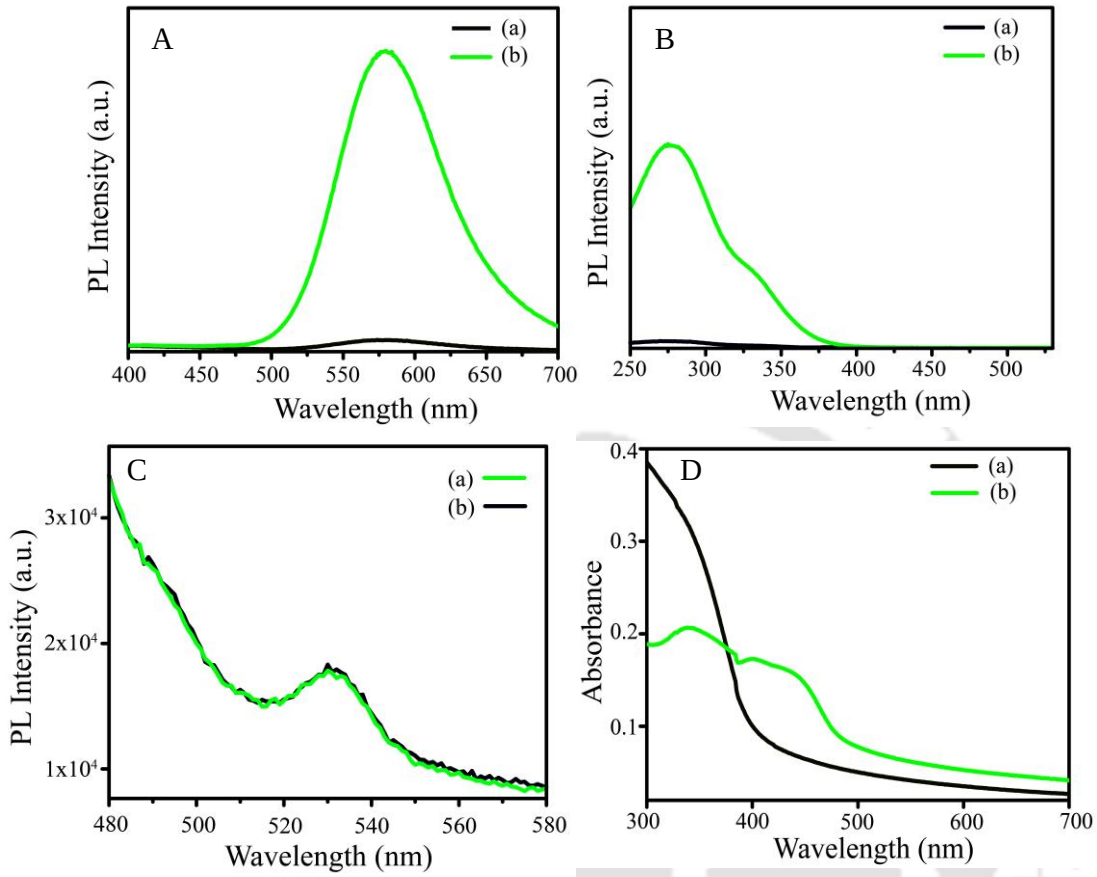

Fig. 4.3: (A) Emission spectrum of (a) Au NCs and (b) that following addition of zinc acetate dihydrate. The excitation wavelength was set at 300 nm. (B) Excitation spectrum of (a) Au NCs and (b) that following addition of zinc acetate dihydrate. The emission wavelength was set at 578 nm. (C) Emission spectrum of (a) Au NCs and (b) that following addition of zinc acetate dihydrate. The excitation wavelength was set at 450 nm. (D) UV-vis absorbance spectrum of (a) Au NCs and (b) that following addition of zinc acetate dehydrate

Upon excitation of this dispersion at 300 nm, a gradual growth of a peak centred around 470-485 nm was observed with time. This was supplemented with gradual decrease in the emission peak at 570 nm (Fig. 4.4 A). Similarly, the excitation spectra of the same dispersion (with emission wavelength set at ~ 568 nm) featured a decrease in intensity as well (Fig. 4.4 B). Upon excitation of this incubated yellow dispersion of zinc added Au NCs at 450 nm (visible light) an emission peak at 514 nm was observed (Fig. 4.4 C). On the other hand, upon

fixing emission at 514 nm and recording the excitation spectrum of this dispersion a broad excitation was observed ranging from 375 nm to 475 nm and beyond (Fig. 4.4 D).

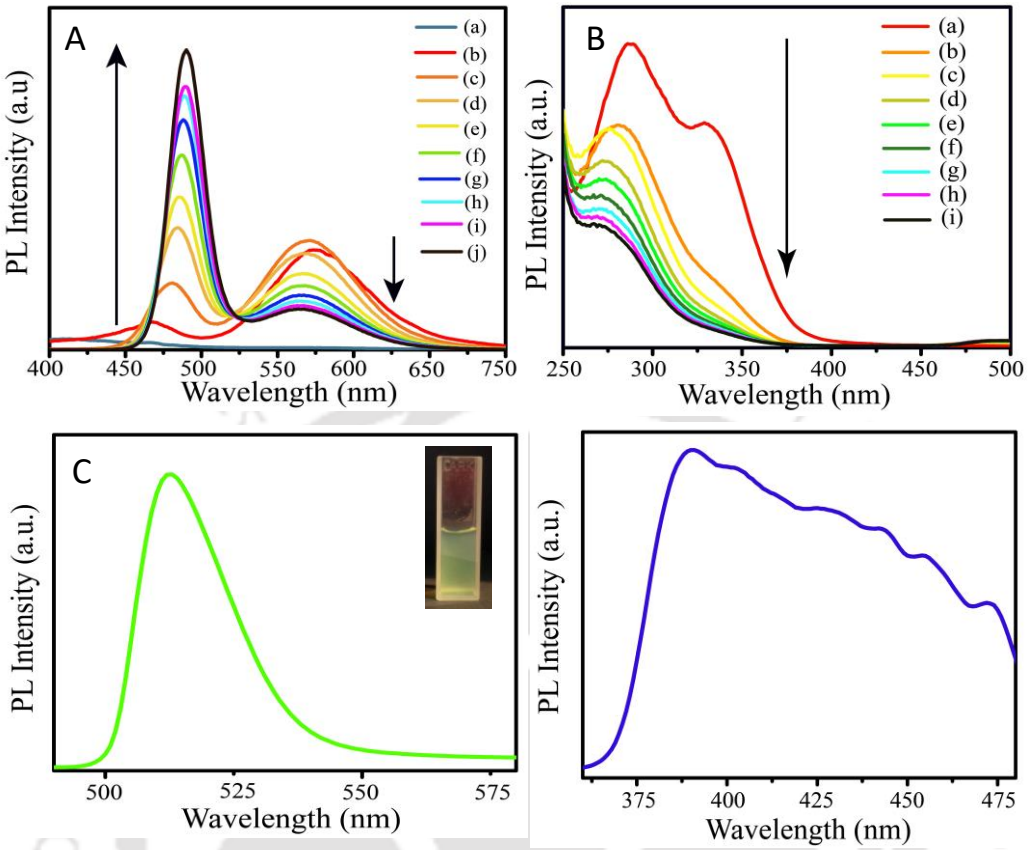

Fig. 4.4: (A) Emission spectrum of (a) Au NCs and that following addition of ~100 mg Zn-acetate dihydrate at (b) 0 min, (c) 3 min, (d) 6 min, (e) 9 min, (f) 12 min, (g) 15 min, (h) 18 min, (i) 21 min and (j) 24 min. The wavelength of excitation was set at 300 nm. (B) Excitation spectra of zinc added Au NCs at (a) 0 min, (b) 3 min, (c) 6 min, (d) 9 min, (e) 12 min, (f) 15 min, (g) 18 min, (h) 21 min and (i) 24 min. The wavelength of emission was set at ~ 568 nm. (C) Emission spectrum of zinc added Au NCs after ~100 h of reaction between Au NCs and zinc acetate dihydrate. The wavelength of excitation was set at 450 nm. The inset shows the digital photograph of a dispersion of Zn Au NCs captured in broad day light. (D) Corresponding excitation spectrum of Zn Au NCs. The wavelength of emission was set at 512 nm.

In order to understand the effect of zinc addition on the morphology of Au NCs, TEM analysis of the dispersion containing zinc added Au NCs was performed. As evident from TEM analysis (Fig. 4.5), upon interaction with zinc ions, Au NCs underwent aggregation into nanoparticles in the size range of 7-8 nm, consisting of nanoclusters. The emission

corresponding to 514 nm has possibly originated due to the formation of extended assembly of Au NCs mediated by Zn ions which has lowered the energy difference between the excited and ground state and have also pushed the absorption maxima to the visible regions. An evidence in support of this statement is further corroborated from life measurements of Zn Au NCs. Surprisingly, the emission lifetime (comprising of two components) corresponding to the peak maxima at 495 nm was found to be as high as 54 μs and 6 μs (Fig. 4.6). This is attributed to thermally activated delayed fluorescence (TADF). In typical cases of TADF, the photo excited electrons of the species undergo transition from singlet excited state to triplet state. However, owing to thermal activation the system reverts to the singlet excited state resulting in emission with same energy as that of normal fluorescence, but with a longer emission lifetime.[7]

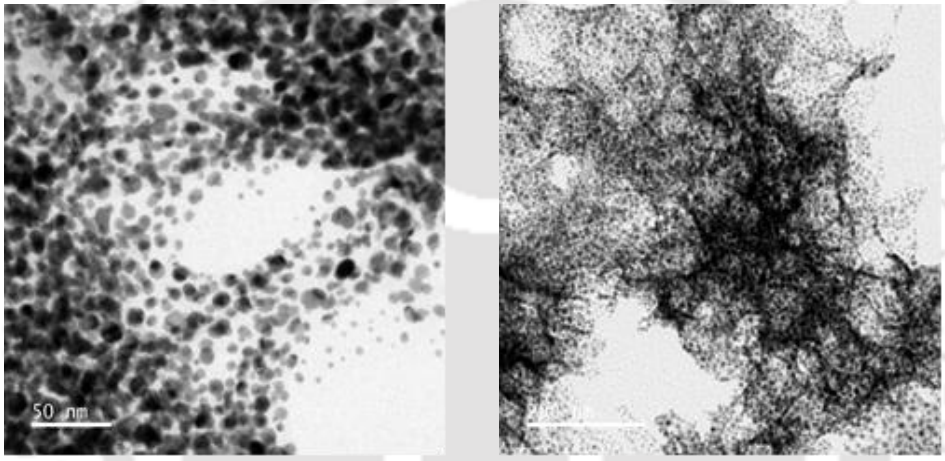

Fig 4.5: Representative TEM images of Zn Au NCs acquired on various positions of TEM grids.

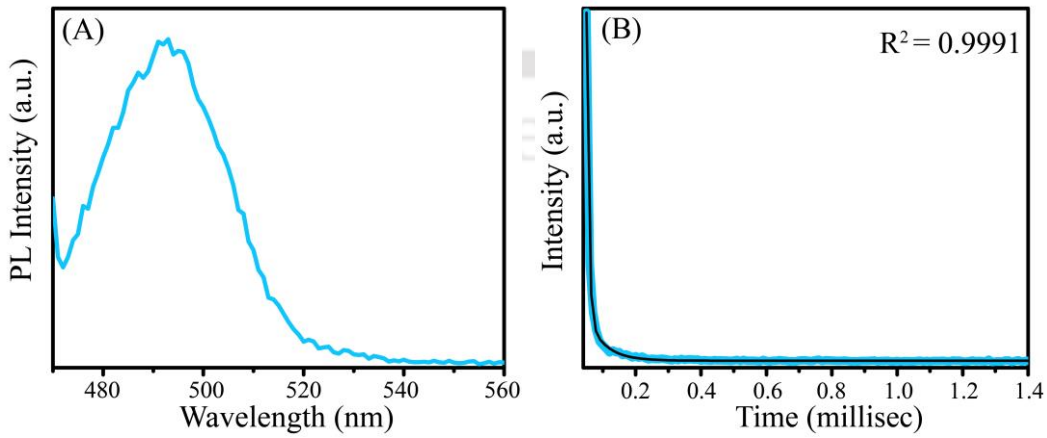

Fig. 4.6: Delayed fluorescence emission spectrum of (A) Zn Au NCs and (B) Time resolved delayed fluorescence decay curve of Zn Au NCs. The excitation wavelength was set at 450 nm.

This phenomenon of aggregation of Au NCs upon addition of zinc ions, as evident from Fourier transformed infrared (FTIR) analysis (Fig. 4.7), was further attributed to chemical coordination between carboxylate groups of MPA and zinc ions. In order to further affirm the aggregation of Au NCs upon interaction with zinc ions, time dependant UV-vis absorption spectra of zinc salt added Au NCs were acquired at various time intervals. As evident from Fig. 4.8, the UV-vis absorbance spectra of zinc added Au NCs featured the emergence of a new peak at ~ 430 nm with increase in time. As per literature reports, this observation of gradual emergence of unprecedented peaks in UV-visible absorption spectra of conjugated molecules has often been attributed to their aggregation.[8, 9] Thus, the gradual appearance of the new peak at 430 nm in the UV-vis absorption spectra of zinc added Au NCs has been attributed to the aggregation of Au NCs following complexation with zinc ions. Thus, zinc-coordinated assembly of Au NCs exhibiting bright photoluminescence upon visible light excitation was achieved. The non-luminescent/ weakly luminescent Au NCs, upon interaction with zinc ions, were transformed into luminescent aggregates. This observation may be attributed to aggregation induced emission. In absence of zinc ions, the ligands stabilizing the weakly luminescent Au NCs i.e. MPA were flexible to under intramolecular rotations and vibrations. As a consequence, the non-radiative decay pathway might have been promoted leading to vibrational and rotational relaxation. This led to lowering of luminescence of Au NCs. However, upon complexation with zinc ions, the MPA molecules stabilizing the Au NCs underwent restricted intramolecular rotation and vibration. This is commonly referred to as restricted intramolecular motions (RIM). [10] Owing to the structural rigidity imposed on the Au NCs following coordination with zinc ions, the non-radiative decay pathway might have got blocked and instead, the radiative decay pathway got promoted leading to enhancement in luminescence of Au NCs.

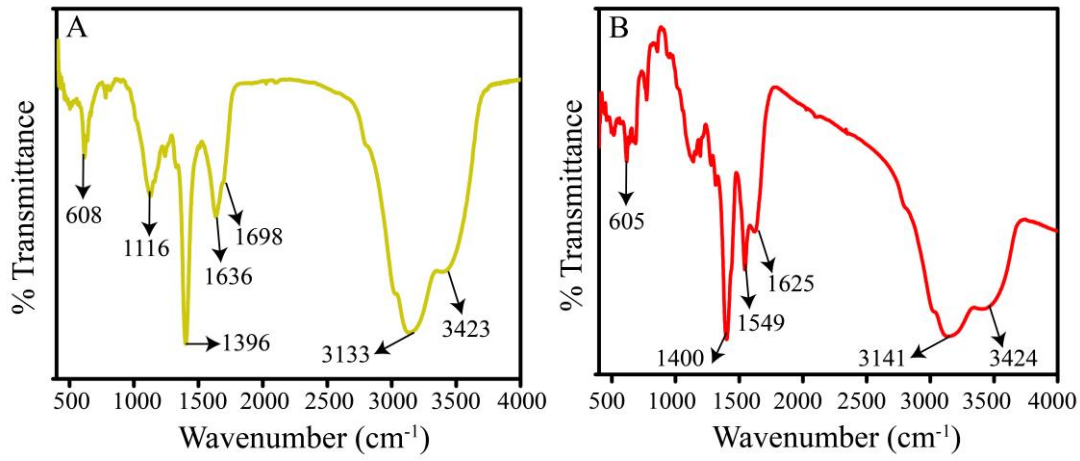

Fig. 4.7: FTIR spectrum of **(A)** Au NCs and **(B)** that following addition of zinc acetate dihydrate.

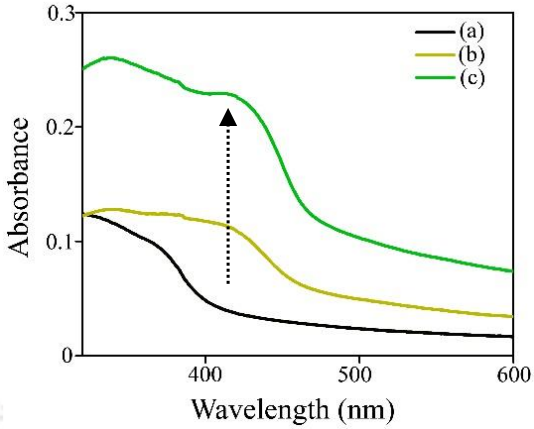

Fig. 4.8: UV-vis absorption spectra of Au NCs added with zinc ions acquired (a) prior to, (b) 60 min and (c) 70 min after addition of ~ 100 mg zinc acetate dihydrate.

Given the bright photoluminescence of Zn Au NCs upon visible light excitation, chemical sensing of analytes using Zn Au NCs as a "visible light sensor" was deemed possible. It is important to note here that based on previous results from our laboratory we could demonstrate the specific reactivity of ligands on the surface of the assembled particles constituting the clusters. It has been observed and reported that the coordinating groups, and orientation of surface ligands play an important role in deciding the nature of interactions with added molecules and thereby control the core properties (for example luminescence) of the assembly of clusters.[2] Using this principle, the nanoscale assembly endowed with luminescence under visible light excitation, designed herein, was used as a probe for sensing molecules interacting specifically with the MPA ligands present on the surface of Zn Au NCs. The pKa of MPA as reported in literature is 4.34. The pH of a typical dispersion of Zn Au NCs was recorded to be ranging from 5 - 5.9. Thus at this pH the surface MPA moieties were expected to exist in their deprotonated state, i.e. as carboxylate end groups. Under this condition any molecule with pKa less than that of MPA is supposed to act as proton donor to MPA. On the other hand, molecules with pKa higher than that of MPA would not interact with the latter via acid-base reaction. It is worth mentioning here that previous reports claim that the luminescence of nanoclusters primarily arise from ligand to metal charge transfer, i.e. the stabilizing ligands and the core metal clusters.[11] Now here the MPA molecules being deprotonated will allow facile ligand to metal charge transfer. On the other hand, if these MPA molecules are protonated such charge transfer may not be as facile as otherwise. The emission upon visible light excitation is believed to be a consequence of such a charge transfer owing to

long range interactions between the NCs mediated by Zn ions. Thus, with this knowledge, a system could be readily designed wherein molecules with pKa less than the pKa of the stabilizer MPA and molecules having pKa greater than that of MPA could be differentiated based on simple luminescence study (Fig. 4.9). The feasibility of development of such system was demonstrated using amino acids and peptides. As shown in Fig. 4.10 A1-A3, molecules bearing acidic side chains (amino acids: aspartic acid and glutamic acid and tripeptide glutathione) upon interaction with Zn Au NCs led to a phenomenal shift in the emission peak of the latter when excited with visible light, i.e. 450 nm. However as seen in Fig. 4.10 B1-B3, no such shift was observed upon interaction of molecules amino acids such as cysteine, cystine and tyrosine with MPA stabilizing the Zn Au NCs aggregates. This may be attributed to the fact that in case of aspartic acid and glutamic acid, the side chains being acidic and having pKa lesser than that of MPA, might have protonated the MPA molecules on the surface of Zn Au NCs, thereby inhibited the ligand to metal charge transfer thereby causing a significant change in wavelength of emission.

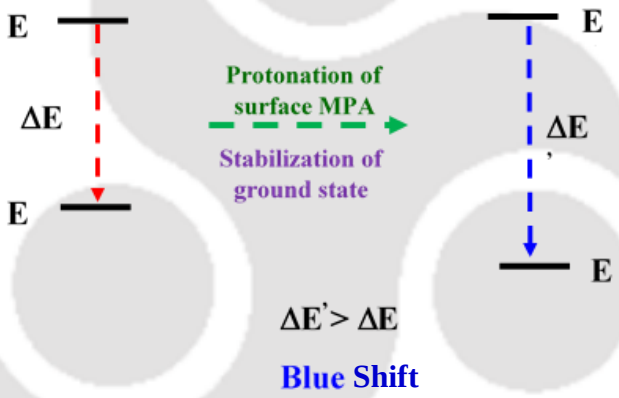

Fig 4.9: Schematic representation of protonation of the surface MPA ligands leading to stabilization of the ground state of gold cluster.

Similar is the case with glutathione which is again comprised of glutamic acid as one of the component amino acid. On the other hand, the side chains of other amino acids like cysteine, cystine and tyrosine are non-acidic and hence might have been non-instrumental in protonating the MPA molecules, as a consequence of which the emission of Zn Au NCs aggregates remained nearly unaltered. As proof of concept we have shown the additional examples (using other amino acids) of such selective interaction and their effect on luminescence of Zn Au NCs under visible light excitation in Fig. 4.11.

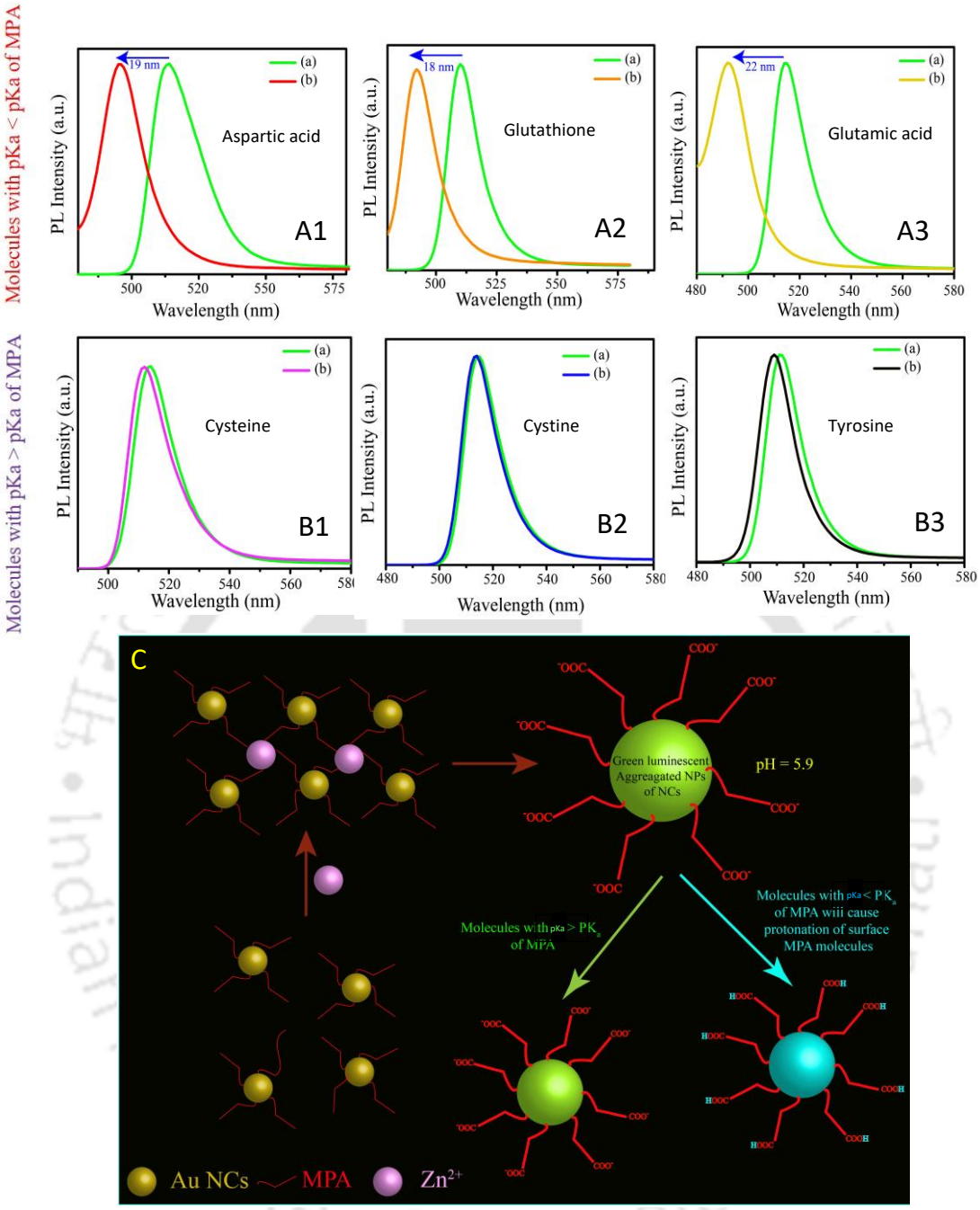

Fig. 4.10: (A1) Luminescence spectrum of (a) Zn Au NCs and that following addition of (b) 980 µM of aspartic acid. (A2) Luminescence spectrum of (a) Zn Au NCs and that following addition of (b) 980 µM of glutathione. (A3) Luminescence spectrum of (a) Zn Au NCs and that following addition of (b) 980 µM of glutamic acid. (B1) Luminescence spectrum of (a) Zn Au NCs and that following addition of (b) 980 µM of cysteine. (B2) Luminescence spectrum of (a) Zn Au NCs and that following addition of (b) 980 µM of cystine. (B3) Luminescence spectrum of (a) Zn Au NCs and that following addition of (b) 980 µM of tyrosine. (C)

Schematic illustration of the plausible mechanism responsible for change in luminescence of Zn Au NCs upon interaction with various molecules. Excitation wavelength was set at 450 nm.

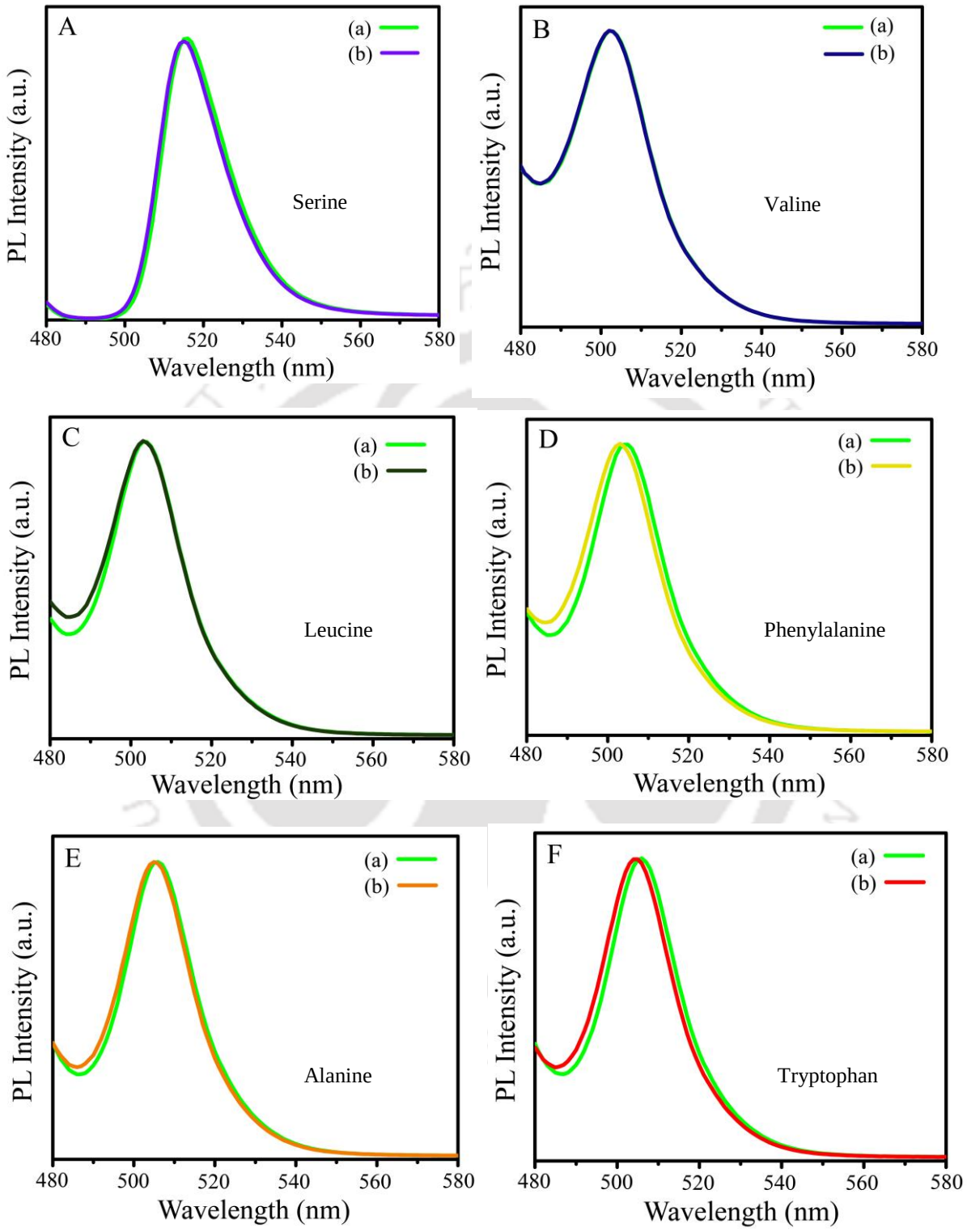

Fig. 4.11: (A) Luminescence spectrum of (a) Zn Au NCs and that following addition of (b) 980 µM of serine. **(B)** Luminescence spectrum of (a) Zn Au NCs and that following addition of (b) 980 µM of valine. **(C)** Luminescence spectrum of (a) Zn Au NCs and that following addition of (b) 980 µM of leucine. **(D)** Luminescence spectrum of (a) Zn Au NCs and that following

addition of (b) 980 µM of phenylalanine. **(E)** Luminescence spectrum of (a) Zn Au NCs and that following addition of (b) 980 µM of alanine. **(B3)** Luminescence spectrum of (a) Zn Au NCs and that following addition of (b) 980 µM of tryptophan. Excitation wavelength was set at 450 nm.

The trend of change in emission wavelength of Zn Au NCs upon interaction with the aforementioned analytes was also concordant with the change in excitation spectra of Zn Au NCs. As shown in Fig. 4.12 the excitation of Zn Au NCs in the visible range (acquired upon fixing emission at 512 nm) decreases drastically upon interaction with glutathione, glutamic acid and aspartic acid. However, upon interaction with cysteine, cystine and tyrosine, no discernible change in visible light excitation of Zn Au NCs was observed. Also, the effects of glutamic acid, aspartic acid, glutathione, tyrosine, cysteine and cystine on the UV vis absorbance of Zn Au NCs were studied. In concordance with the trend obtained in emission spectra of Zn Au NCs, the peak at ~ 430 nm in the UV-vis absorbance spectrum of Zn Au NCs disappeared upon addition of aspartic acid, glutamic acid and glutathione (Fig. 4.13 A-C). While upon addition of tyrosine, cysteine and cystine, no significant change was observed in the peak at 430 nm (Fig. 4.13 D-F).

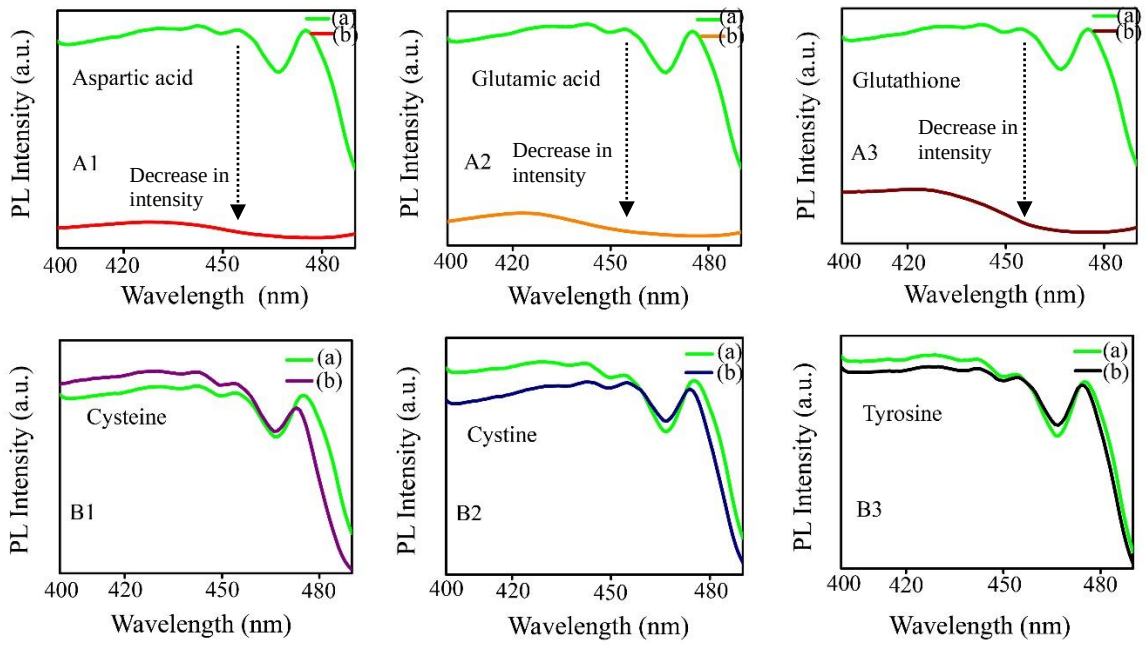

Fig. 4.12: (A1) Excitation spectrum of (a) Zn Au NCs and that following addition of (b) 1.21 mM of aspartic acid. (A2) Excitation spectrum of (a) Zn Au NCs and that following addition of (b) 1.21 mM of glutamic acid. (A3) Excitation spectrum of (a) Zn Au NCs and that following addition of (b) 1.21 mM of glutathione. (B1) Excitation spectrum of (a) Zn Au NCs and that

following addition of (b) 1.21 mM of cysteine. (B2) Excitation spectrum of (a) Zn Au NCs and that following addition of (b) 1.21 mM of cystine. (B3) Excitation spectrum of (a) Zn Au NCs and that following addition of (b) 1.21 mM of tyrosine. Emission wavelength was set at 512 nm.

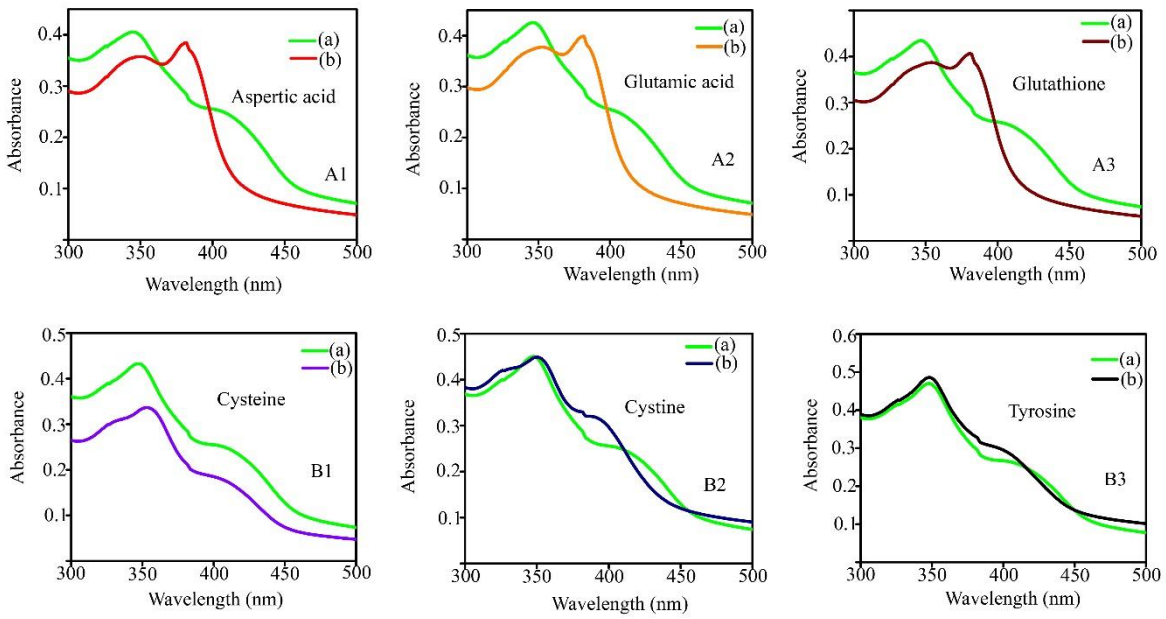

Fig. 4.13: (A1) UV-vis absorption spectrum of (a) Zn Au NCs and that following addition of (b) 1.16 mM of aspartic acid. (A2) UV-vis absorption spectrum of (a) Zn Au NCs and that following addition of (b) 1.16 mM of glutamic acid. (A3) UV-vis absorption of (a) Zn Au NCs and that following addition of (b) 1.16 mM of glutathione. (B1) UV-vis absorption spectrum of (a) Zn Au NCs and that following addition of (b) 1.16 mM of cysteine. (B2) UV-vis absorption spectrum of (a) Zn Au NCs and that following addition of (b) 1.16 mM of cystine. (B3) UV-vis absorption spectrum of (a) Zn Au NCs and that following addition of (b) 1.16 mM of tyrosine.

This further suggested that the change in emission wavelength of Zn Au NCs upon interaction with glutathione, aspartic acid and glutamic acid might have occurred due to ground state interaction between Zn Au NCs and the respective analytes as opposed to excited state phenomenon. However, no specific pattern in change of lifetime of Zn Au NCs was observed upon addition of the aforementioned analytes. Nevertheless, the values of lifetimes of Zn Au NCs prior to and following interaction with the analytes are given here in tabulated form in the supporting information (Table 1).

Sample	T_1		T_2		T_3	
	Lifetime (ns)	**Contribution (%)**	**Lifetime (ns)**	**Contribution (%)**	**Lifetime (ns)**	**Contribution (%)**
Zn Au NCs (sample A)	5.3	15.52	20.24	82.48	1.13	2.00
Zn Au NCs (sample B)	5.82	23.17	22.15	73.03	1.12	3.80
Zn Au NCs (sample C)	3.65	13.16	14.29	85.99	4.27	0.85
Zn Au NCs + Aspartic acid	2.16	21.18	14.07	75.13	2.98	3.69
Zn Au NCs + Glutamic acid	2.23	21.10	14.21	75.46	3.27	3.44
Zn Au NCs + Glutathione	2.78	9.28	19.12	89.86	1.87	0.86
Zn Au NCs + Cysteine	6.08	12.00	21.54	85.86	1.70	2.14
Zn Au NCs + Cystine	6.99	22.32	20.64	74.06	1.81	3.62
Zn Au NCs + Tyrosine	6.90	21.56	17.51	72.48	2.06	5.96

Table 1: Time resolved photoluminescence analysis of Zn Au NCs.

T_{avg} of Zn Au NCs (sample A) = $\frac{(15.32\times 5.3+82.48\times 20.24^2+2.00\times 1.13^2)}{(15.32\times 5.3+82.48\times 20.24+2.00\times 1.13)}$ = **19.52 ns**

T_{avg} of Zn Au NCs (sample B) = $\frac{(23.17\times 5.82^2+73.03\times 22.15^2+3.80\times 1.12^2)}{(23.17\times 5.82+73.03\times 22.15+3.80\times 1.12)}$ = **20.84 ns**

T_{avg} of Zn Au NCs (sample C) = $\frac{(13.16\times 3.65^2+85.99\times 14.29^2+0.85\times 4.27^2)}{(13.16\times 3.65+85.99\times 14.29+0.85\times 4.27)}$ = **14.17 ns**

T_{avg} of (Zn Au NCs + Aspartic acid) = $\frac{(21.18\times 2.16^2+75.13\times 14.07^2+3.69\times 2.98^2)}{(21.18\times 2.16+75.13\times 14.07+3.69\times 2.98)}$ = **13.47 ns**

T_{avg} of (Zn Au NCs + Glutamic acid) = $\frac{(21.10\times 2.23^2+75.46\times 14.21^2+3.44\times 3.27^2)}{(21.10\times 2.23+75.46\times 14.21+3.44\times 3.27)}$ = **13.60 ns**

T_{avg} of (Zn Au NCs + Glutathione) = $\frac{(9.28\times 2.78^2+89.86\times 19.12^2+0.86\times 1.87^2)}{(9.28\times 2.78+89.86\times 19.12+0.86\times 1.87)}$ = **18.86 ns**

T_{avg} of (Zn Au NCs + cysteine) = $\frac{(12.00\times 6.08^2+85.86\times 21.54^2+2.14\times 1.70^2)}{(12.00\times 6.08+85.86\times 21.54+2.14\times 1.70)}$ = **20.91 ns**

T_{avg} of (Zn Au NCs + cystine) = $\frac{(22.32\times 6.99^2+74.06\times 20.64^2+3.62\times 1.81^2)}{(22.32\times 6.99+74.06\times 20.64+3.62\times 1.81)}$ = **19.30 ns**

T_{avg} of (Zn Au NCs + tyrosine) = $\frac{(21.56\times 6.90^2+72.48\times 17.51^2+5.96\times 2.06^2)}{(21.56\times 6.90+72.48\times 17.51+5.96\times 2.06)}$ = **16.27 ns**

Another premise where significant advancements of luminescent materials, especially that of nanoscale particles, has been effective is that in bio imaging. As discussed in earlier sections, the domain of cellular imaging has significantly benefited from the emergence of luminescent nanoclusters. However, nanoclusters or their assembled systems, exhibiting luminescence under visible light excitation poises to be a better choice than the existing systems. To this end, the system of zinc-assisted aggregation of Au NCs was used as probes for imaging mammalian cells under visible light excitation. As evident from Fig. 4.14 (A1-A3) and (B1-B3) upon treatment of HeLa Cells with 66 μg/mL of Zn Au NCs and following incubation for around 3 hours, bright luminescence could be observed upon excitation at 488 nm.

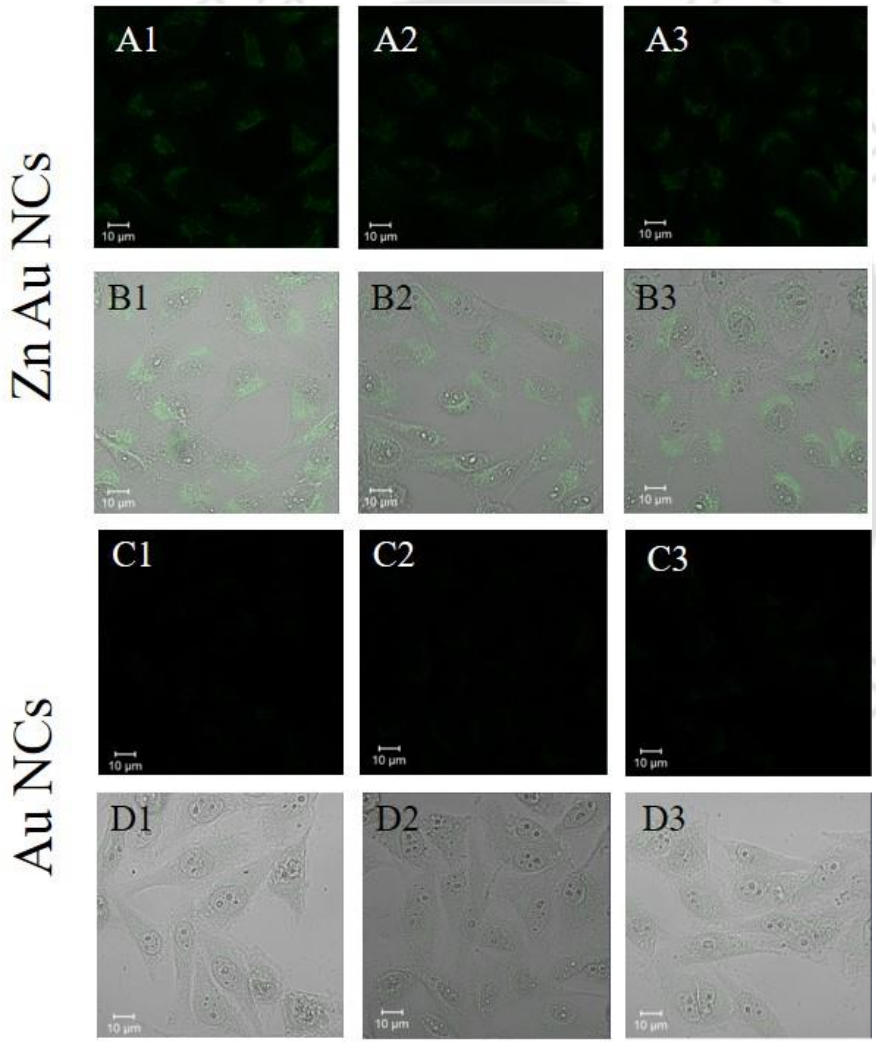

Fig. 4.14: (A1-A3) Representative CLSM images of HeLa cells treated with Zn Au NCs upon excitation at 488 nm. (B1-B3) Corresponding merged images of HeLa cells treated with Zn Au NCs shown in (A1-A3) acquired in CLSM mode and bright field mode. (C1-C3) Representative CLSM images of HeLa cells treated with only Au NCs upon excitation at 488

nm. (D1-D3) Corresponding merged images of HeLa cells treated with Zn Au NCs shown in (C1-C3) acquired in CLSM mode and bright field mode.

On the other hand, upon treatment of HeLa cells with Au NCs (without zinc ions), no significant (very weak) luminescence was observed within HeLa cells upon excitation at 488 nm. It is important to note here that as per MTT based cell viability assay (Fig. 4.15) at the concentrations of Zn Au NCs and Au NCs, at which cell imaging was performed, no significant killing of HeLa cells was observed. Further the internalization of Zn Au NCs within HeLa cells was confirmed through depth projection analysis (Fig. 4.16). The facile imaging of HeLa cells under visible light excitation using Zn Au NCs is an unprecedented application with regard to nanoscale particles. This is attributed to long-range order charge transfer between gold clusters via zinc ions coordinated to MPA stabilizing the clusters. To the best of our knowledge, so far no reports exist on nanoscale particle based cellular imaging under visible light excitation.

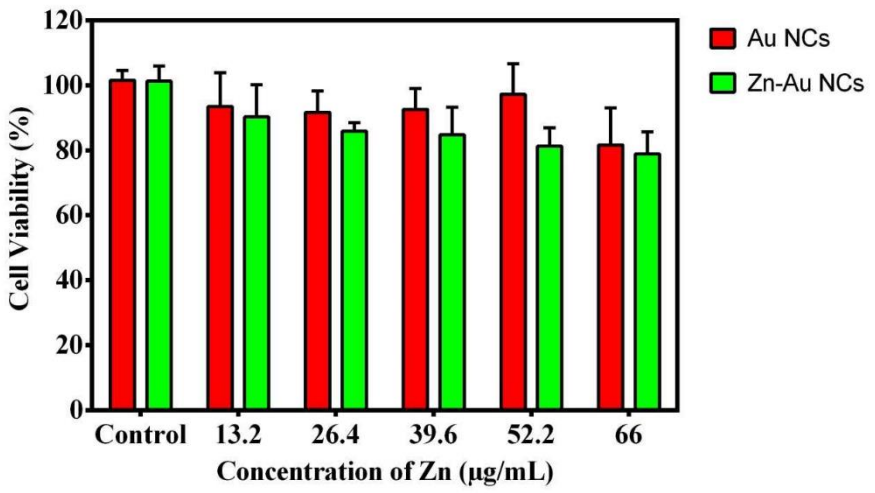

Fig. 4.15: MTT based cell viability assay of Au NCs (shown in red) and Zn Au NCs (shown in green).

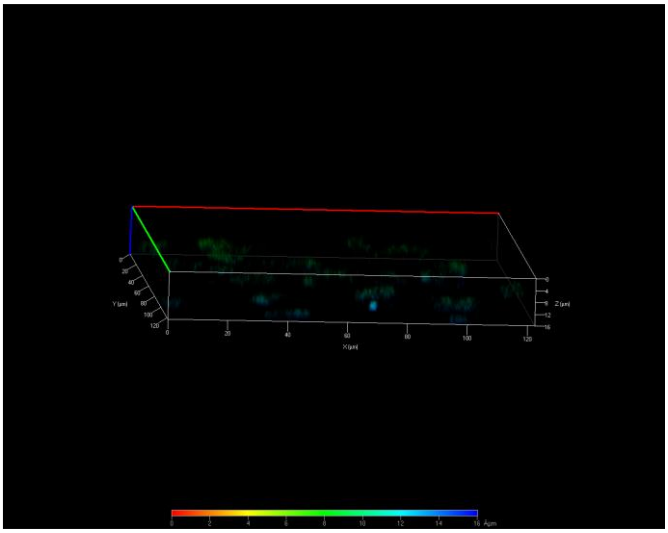

Fig. 4.16: Depth projection analysis performed on typical CLSM images of HeLa cells treated with Zn Au NCs.

Conclusions

In essence, we have demonstrated that zinc mediated complexation reaction based aggregates of Au NCs exhibit luminescence under visible light excitation. Further, the luminescence of aggregated Au NCs was used for mammalian cell imaging and as a probe for luminescence-based detection of molecules with varying pKa. Thus, as envisioned by Sakka et al.,[12] this is considered to be an important advancement in the field of nanoscale assembly of clusters as well as in the domain of development of sensors and bio imaging agents based on visible light excitation induced luminescence of these nanomaterials.

References

1. Basu, S.; Paul, A.; Chattopadhyay, A. Zinc mediated crystalline assembly of gold nanoclusters for expedient hydrogen storage and sensing. J. Mater. Chem. A. 2016, 4, 1218-1223.
2. Basu, S.; Paul, A.; Chattopadhyay, A. Zinc-Coordinated Hierarchical Organization of Ligand-Stabilized Gold Nanoclusters for Chiral Recognition and Separation. *Chem. Eur. J.* **2017**, *23*, 9137-9143.
3. Basu, S.; Goswami, U.; Paul, A.; Chattopadhyay, A. Crystalline assembly of gold nanoclusters for mitochondria targeted cancer theranostics. *J. Mater. Chem. B.* **2018**, *6*, 1650-1657.
4. Basu, S.; Bhandari, S.; Pan, U. N.; Paul, A.; Chattopadhyay, A. Crystalline nanoscale assembly of gold clusters for reversible storage and sensing of CO2 via modulation of photoluminescence intermittency. *J. Mater. Chem. C.* **2018**, *6*, 8205-8211.
5. Basu, S.; Chattopadhyay, A. Room Temperature Delayed Fluorescence of Gold Nanoclusters in Zinc Mediated Two-Dimensional Crystalline Assembly. *Langmuir* **2019**, DOI: 10.1021/acs.langmuir.9b00149
6. Kuppan, B.; Maitra, U.; Instant room temperature synthesis of self-assembled emission-tunable gold nanoclusters: million-fold emission enhancement and fluorimetric detection of Zn^{2+}. *Nanoscale* **2017**, *9*, 15494-15504.

7. Li, T.; Yang, D.; Zhai, L.; Wang, S.; Zhao, B.; Fu, N.; Wang, L.; Tao, Y.; Huang, W. Thermally Activated Delayed Fluorescence Organic Dots (TADF Odots) for Time-Resolved and Confocal Fluorescence Imaging in Living Cells and In Vivo. *Adv. Sci.* **2017**, *4*, 1600166.
8. Draper, E. R.; Greeves, B. J.; Barrow, M.; Schweins, R.; Zwijnenburg, M. A.; Adams, D. J. pH-Directed Aggregation to Control Photoconductivity in Self-Assembled Perylene Bisimides. *Chem* **2017,** *2*, 716–731.
9. Shi, R.; Chen, H.; Qi, Y.; Huang, W.; Yin, G.; Wang, R. From aggregation-induced to solution emission: a new strategy for designing ratiometric fluorescent probes and its application for in vivo HClO detection. *Analyst* **2019**, *144*, 1696.
10. Ren, Y.; Lam, J. W. Y.; Dong, Y.; Tang, B. Z. Wong, K. S. Enhanced Emission Efficiency and Excited State Lifetime Due to Restricted Intramolecular Motion in Silole Aggregates. *J. Phys. Chem. B* **2005**, *109*, 1135-1140.
11. Shaoo, A. K.; Banerjee, S.; Ghosh, S. S.; Chattopadhyay, A. Simultaneous RGB Emitting Au Nanoclusters in Chitosan Nanoparticles for Anticancer Gene Theranostics. *ACS Appl. Mater. Interfaces* **2014**, *6*, 712-724.
12. Sun, H. T.; Sakka, Y. Luminescent metal nanoclusters: controlled synthesis and functional applications. *Sci. Technol. Adv. Mater.* **2014**, *15*, 014205.

Chapter 5

Tailoring the luminescence of atomic clusters via Ligand Exchange Reaction Mediated post synthetic modification

The growing prominence of atomic nanoclusters in the fields of practical relevance has made modulation of their luminescent characteristics an important challenge for their futuristic applications. Herein we report chemical reaction assisted modulation of luminescence of histidine stabilized gold nanoclusters via ligand exchange reaction with cysteine. Upon addition of 3.8 mM cysteine, as evinced by X-ray photoelectron spectroscopy in conjunction with transmission electron microscopic analyses, histidine molecules were found to desorb from the surface of Au NCs leading to the latter's aggregation into macroscopic units. Consequently, the luminescence of His Au NCs underwent a large bathochromic shift from 475 nm to 500 nm with concomitant decrease in luminescence intensity. Thereafter, upon addition of 18 mM cysteine to a dispersion of His Au NCs, cysteine molecules by virtue of strong aurophilic interactions, were found to adsorb on to the surface of Au NCs leading to the disaggregation of the macroscopic structures. This was accompanied by restoration of luminescence features of the Au NCs to an emission maximum of 486 nm with partial recovery of luminescence intensity. Thus, the work embodied herein demonstrates post-synthetic chemical reactions of nanoclusters as an effective and viable tool for tailoring the photoluminescence of atomic clusters to meet the application demand.

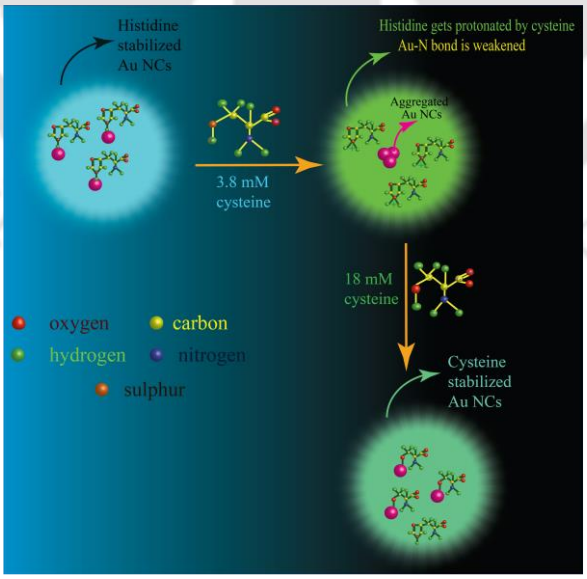

Gayen, C.; Basu, S.; Pan, U. N.; Paul, A. *ACS Omega* **2018**, *3*, 17220−17226.

Experimental Section

Materials:

$HAuCl_4$ (sigma Aldrich), Histidine (Fluka), cysteine (Sigma Aldrich) were used as received and were not purified further.

Instruments:

Luminescence spectra of all samples were acquired in Horiba Jobin Yvon Fluoromax-4. All UV-vis spectra were acquired in Perkin Elmer, Lambda 750 UV-visible spectrophotometer. TEM measurements were performed in JEOL JEM 2100F and JEOL JEM 2100. The accelerating voltage was set at 200 kV. XPS spectra were acquired using an AXIS Supra X-ray photoelectron spectrometer, Kratos Analytical (UK).

Synthesis of gold nanoclusters:

Gold nanoclusters were synthesized as per a previous report.[1] Briefly, 1 mL of 10 mM $HAuCl_4$ was added with 47 mg of histidine and the resultant mixture was stirred for 1 h. This resulted in the formation of a dispersion exhibiting bright luminescence with emission maximum at 475 nm when excited with 370 nm light.

Results and Discussion

The mixture of His and $HAuCl_4$ was found to be luminescent with emission maximum at ~ 475 nm upon excitation at 365 nm (Fig. 5.1 A-B). Moreover, the resultant mixture containing His and $HAuCl_4$ featured no significant peak in the UV-vis absorption spectrum (Fig. 5.1 C). These results possibly indicated the formation of His Au NCs. Further, TEM analysis of this mixture featured the presence of ultra-small nanoclusters in the size range of 2 nm (Fig. 5.2) with no significant crystallinity. This confirmed the successful synthesis of gold nanoclusters stabilized by histidine.

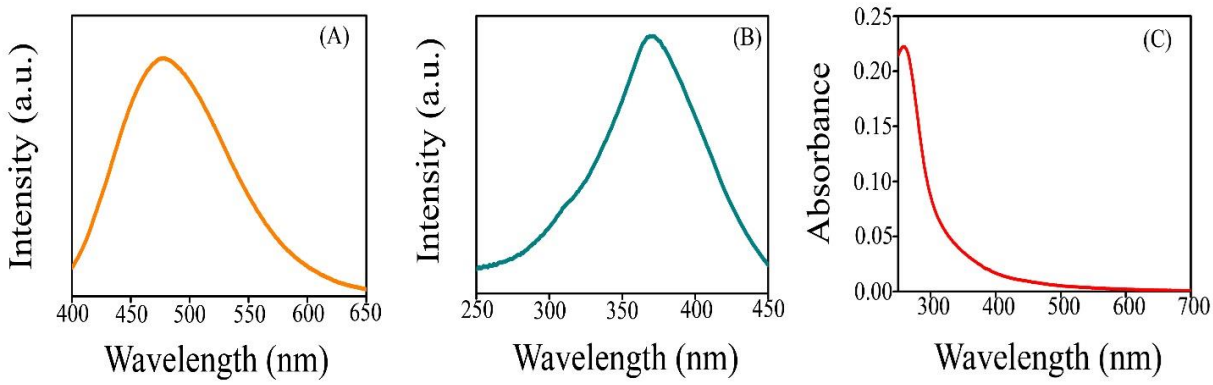

Fig. 5.1. (A) Emission spectrum of His Au NCs. Excitation wavelength was set at 370 nm (B) Excitation spectrum of His Au NCs. Emission wavelength was set at 475 nm (C) UV-visible absorbance spectrum of His Au NCs.

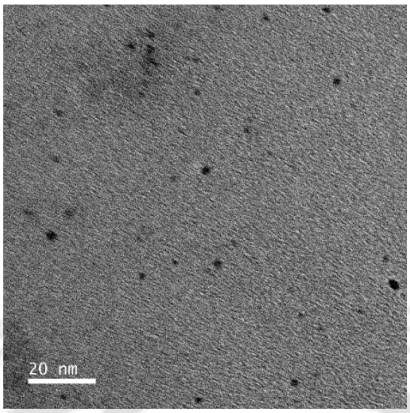

Fig. 5.2. TEM image of His Au NCs.

In order to pursue luminescence modulation of the as synthesized gold nanoclusters, varying amount of L-cysteine was added to the dispersion of His Au NCs. As evident from Fig. 5.3 A-B, successive addition of L-cysteine significantly altered the luminescence characteristics of His Au NCs in that both the peak intensity and peak position showed distinct changes with increasing amounts of L-cysteine in the dispersion. It may be noted that pristine His Au NCs exhibited emission maximum at 475 nm upon excitation at 370 nm. However, following addition of 10 µl of 100 mM L-cysteine the emission peak shifted to 480 nm with concurrent shift of the excitation peak maximum to 378 nm. Thereafter addition of another aliquot of 10 µl of 100 mM L-cysteine to the dispersion caused red shift in the emission peak maxima to 482 nm with concomitant shift in the excitation peak maxima to 382 nm. It is noteworthy that all these while, upon addition of the aforementioned aliquots of L-cysteine to His Au NCs, there was hardly any alteration in the maximum peak intensities in the emission as well as excitation spectra. When the total volume of 100 mM L-cysteine added to His Au NCs reached 30 µl, the emission peak maximum, now at 486 nm, showed significant quenching. Moreover, the corresponding excitation peak shifted to 397 nm with simultaneous decrease in intensity. Upon further addition of L-cysteine from a total volume of 40 µl to 80 µl to the His Au NC dispersion, the emission peak maxima was constant at 499 nm with slight quenching. The corresponding excitation peak underwent blue shift from 421 nm to 419 nm with slight decrease in intensity. Further addition of L-cysteine to His Au NCs from 90 µL to 440 µL led to continuous blue shift of the emission peak from 495 nm to 486 nm with slight

increase in intensity while the excitation peak blue shifted from 417 nm to 409 nm with nominal increase in intensity.

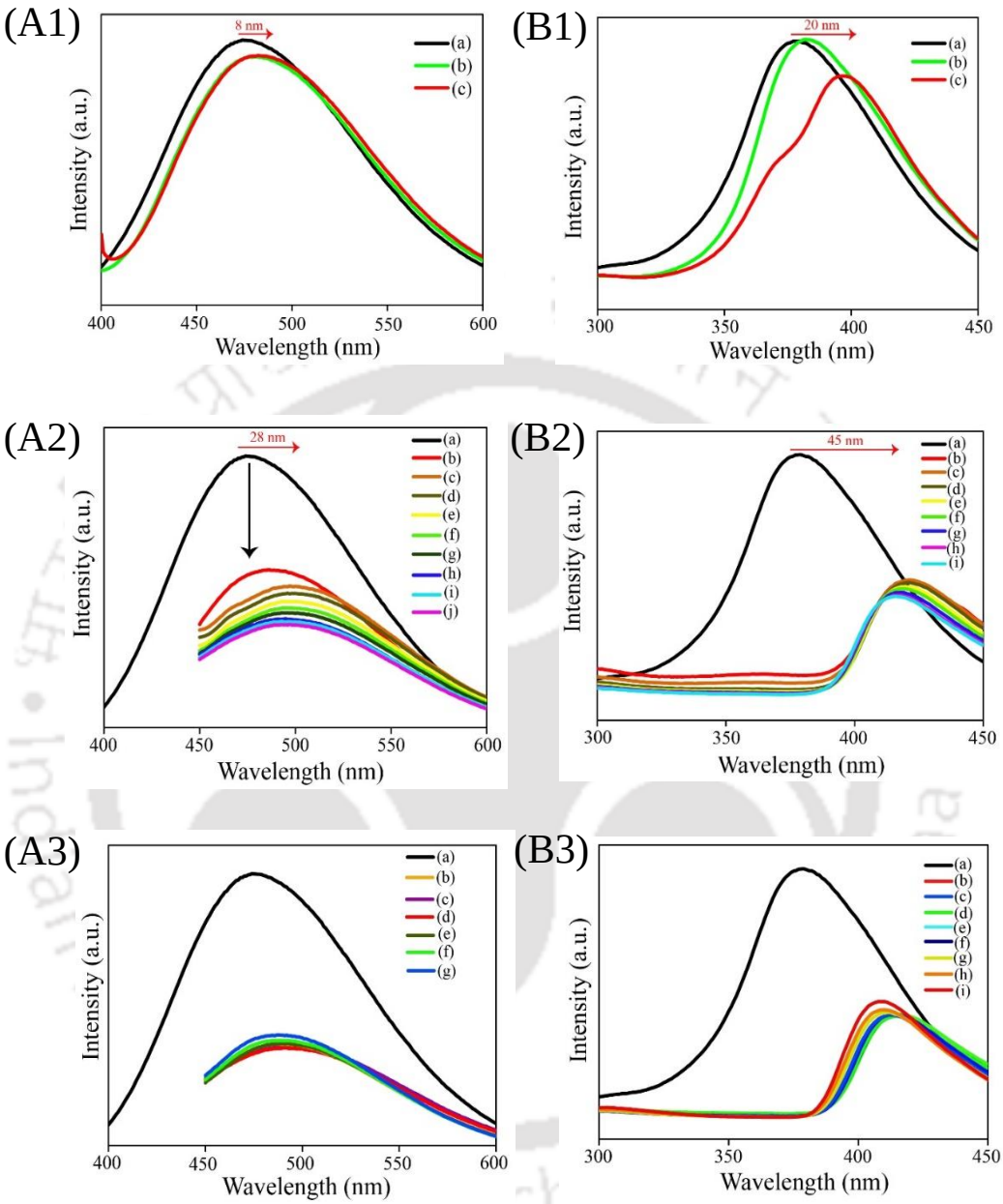

Fig. 5.3 (A1) Emission spectra of His Au NCs upon addition of (a) 0 µL, (b) 10 µL, (c) 20 µL of 100 mM L-cysteine and (B1) excitation spectra of His Au NCs upon addition of (a) 10 µL, (b) 20 µL, (c) 30 µL. (A2) Emission spectra of His Au NCs upon addition of (a) 0 µL, (b) 30 µL, (c) 40 µL, (d) 50 µL, (e) 60 µL, (f) 70 µL, (g) 80 µL, (h) 90 µL, (i) 100 µL, (j)110µL of 100 mM L-cysteine and (B2) excitation spectra of His Au NCs upon addition of (a) 10 µL, (b) 40 µL, (c) 50 µL, (d) 60 µL, (e) 70 µL, (f) 80 µL, (g) 90 µL, (h) 100 µL, (i) 110 µL of 100 Mm L-cysteine. (A3) Emission spectra of His Au NCs upon addition of (a) 0 µL, (b) 120 µL, (c) 130 µL, (d) 140 µL, (e) 190 µL, (f) 240 µL, (g) 340 µL of 100 mM L-cysteine and (B3)

excitation spectra of His Au NCs upon addition of (a)10 µL, (b) 120 µL, (c) 130 µL, (d) 140 µL, (e) 190 µL, (f) 240 µL, (g) 340 µL, (h) 440 µL, (i) 540 µL.

The changes in emission and excitation profiles of His Au NCs upon interaction with L cysteine is summarized in the following table:

Volume of 100 mM L-Cysteine	Emission peak maxima	Emission peak intensity	Excitation peak maxima	Excitation peak intensity
0	475	-	370	
10-20	480-482	constant	378-392	constant
30	486	rapid decrease	397	rapid decrease
40-80	499	slight decrease	421-419	slight decrease
90-440	495-486	slight increase	417-410	slight increase

Table 1. Trend in variation of luminescence of His Au NCs as function of added cysteine

In order to elucidate the reason behind the rich photo physical changes of Au NCs upon interaction with L Cysteine transmission electron microscopic (TEM) analysis were carried out. As evinced from Fig. 5.4 panel A, the TEM images of His Au NCs featured ultra-small nanoclusters of size ~ 2 nm devoid of crystallinity. However when 40 µL of L-cysteine was added to His Au NCs, the latter underwent aggregation into larger particles of sizes in the range of ~100 nm (Fig. 5.4 panel B). Intriguingly, upon interaction with this very concentration of L cysteine, the emission and excitation profiles of His Au NCs underwent significant bathochromic shifts as compared to pristine His Au NCs. Also, their peak intensities were phenomenally quenched upon addition of aforementioned amount of L-cysteine. Moreover, TEM analysis showed that the addition of L-cysteine upto a total volume of 440 µL led to disintegration of the macroscopic aggregates of His Au NCs formed upon interaction with 40 µL of L-cysteine (Fig.5.4 panel C). Interestingly, this concentration of added L-cysteine marked the partial restoration of the spectral characteristics of His Au NCs as that of its pristine form. Thus, the modulation of the spectral characteristics of His Au NCs upon interaction with L-cysteine was parallel with the TEM observations.

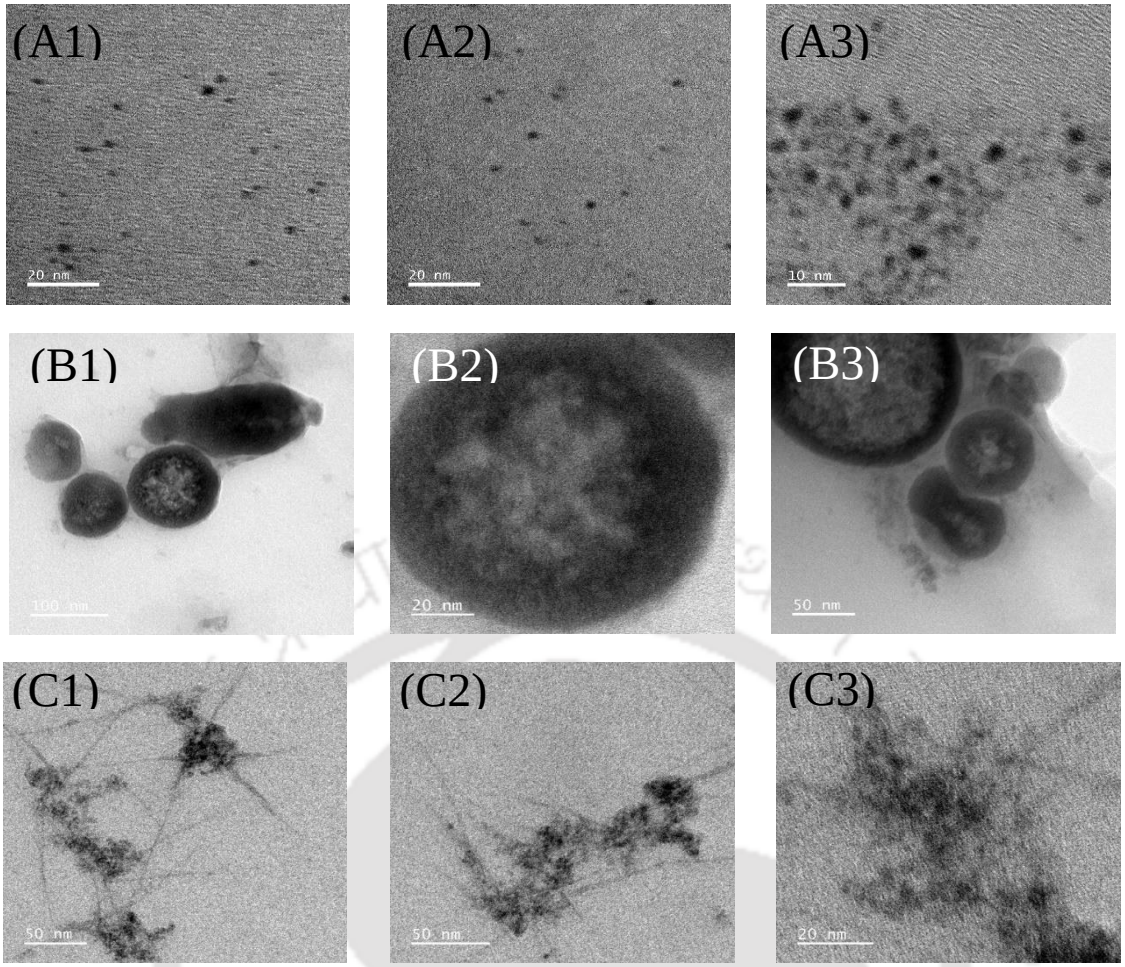

Fig. 5.4: TEM images of **(A1-A3)** As synthesized His Au NCs, **(B1-B3)** His Au NCs following addition of 40 µL of 100 mM L-cysteine and (C1-C3) His Au NCs following addition of 440 µL of 100 mM L-cysteine.

In the next step, an effort was made to understand the chemical interactions governing the luminescence modulation of His Au NCs upon interaction with L-cysteine. Firstly, the pH of all the dispersions of His Au NCs, upon successive addition of L cysteine, were checked. Notably, slight variation in pH were observed. However, such small variation in pH was unlikely to have affected such significant variation in luminescence of Au NCs. This possibly ruled out the role of pH in aggregation and disaggregation of His Au NCs (Table 2). Instead, this slight change in pH is commensurate with mechanism of protonation of imidazole rings of histidine moieties, as discussed in subsequent sections. Further, as evident from Table 2, the pH of a typical dispersion of His Au NCs is >6. At this condition, the side chain of histidine remains deprotonated. Therefore, to this dispersion, addition of cysteine may lead to protonation of side chains of histidine.

Solution	pH of the solution
His Au NCs	6.85
His Au NCs +10 µL of 100 mM cysteine	6.86
His Au NCs +20 µL of 100 mM cysteine	6.85
His Au NCs +30 µL of 100 mM cysteine	6.80
His Au NCs +40 µL of 100 mM cysteine	6.78
His Au NCs +50 µL of 100 mMm cysteine	6.76
His Au NCs +60 µL of 100 mM cysteine	6.80
His Au NCs +70 µL of 100 mM cysteine	6.79
His Au NCs +80 µL of 100 mM cysteine	6.79
His Au NCs +90 µL of 100 mM cysteine	6.78
His Au NCs +100 µL of 100 mM cysteine	6.82
His Au NCs +110 µL of 100 mM cysteine	6.75
His Au NCs +120 µL of 100 mM cysteine	6.76
His Au NCs +130 µL of 100 mM cysteine	6.76
His Au NCs +140 µL of 100 mM cysteine	6.76
His Au NCs +150 µL of 100 mM cysteine	6.77
His Au NCs +200 µL of 100 mM cysteine	6.8
His Au NCs +400 µL of 100 mM cysteine	6.79

Table 2: pH variation of dispersions of His Au NCs upon addition of varying amounts of cysteine.

Moreover, time resolved photoluminescence analyses were performed to understand the effect of L cysteine on the luminescence lifetimes of His Au NCs. Intriguingly, no discernible effect of cysteine was observed on the luminescence lifetime of His Au NCs (Table 3). This ruled out the possibility of excited state interactions between His Au NCs and cysteine. Thus, the interaction between His Au NCs and cysteine was likely to originate from ground state interactions.

Sample	T_1		T_2		T_3	
	Lifetime (ns)	**Contribution (%)**	**Lifetime (ns)**	**Contribution (%)**	**Lifetime (ns)**	**Contribution (%)**
His Au NCs	1.24	37.45	5.45	53.99	0.15	8.56
His Au NCs +40 µL of 100 mM cysteine	0.97	24.65	5.37	65.81	0.04	9.55
His Au NCs +440 µL of 100 mM cysteine	1.48	30.64	6.54	62.71	0.07	6.65

Table 3: Variation in luminescence lifetime of His Au NCs upon addition of cysteine.

In order to decipher the plausible mechanism of luminescence alteration of His Au NCs upon interaction with cysteine, X-ray photoelectron spectroscopy (XPS) was performed. XPS analysis was performed in two segments, volume of 100 mM cysteine added to His Au NCs - (i) 100 µl and (ii) 550 µl, to understand the effect of cysteine on the luminescence modulation of His Au NCs. As indicated by XPS analysis, the changes observed in the first segment could be attributed to reorientation and desorption of histidine from the surface of Au NCs owing to possible protonation of the histidine moieties by added cysteine. Fig. 5.5 (and Table 4) showed that the BE of N1s peak of His Au NCs appeared at 398.9 eV and 400.9 eV in corresponding to the signatures of imine nitrogen of imidazole ring (-N=C-) followed by amine nitrogen in imidazole ring (=C-NH-) and -NH2 group, respectively of the histidine ligands stabilizing the clusters. These values of BE of N 1s in histidine with their broad XPS peaks widths suggests

that the ligand is largely present in the neutral form in His Au NC. However, when 100 µl of cysteine was added to His Au NCs, the N 1s peak became structured with sharp peaks appearing at 401.6 eV and at 399.5 eV corresponding to $–NH_3^+$ and $-NH_2$ functional groups. The peak at 398.1 eV now appears as a small feature at 398.1 eV suggesting reduced presence of imine nitrogen of histidine. The above changes are consistent with the protonation of histidine moieties upon addition of cysteine leading to partial desorption of histidine from the surface of the clusters. This observation is supplemented with the appearance of S 2p peaks at 161.9 and 164.3 eV upon addition of 100 µl of cysteine to His Au NCs, which were attributed to formation of Au-S and presence of RSH from molecular cysteine respectively. The above observations could be explained on the basis of acidic nature of cysteine followed by ligand exchange. Cysteine might have protonated the amine and imidazole nitrogen of histidine leading to the above-mentioned changes in the BE of N 1s and corresponding changes in the XPS spectra of S 2p, where, owing to stronger gold thiol interaction (vis-à-vis weak gold nitrogen interactions), adsorption of cysteine on the surface of Au clusters might have occurred at the expense of histidine. This possibly led to the appearance of the aforementioned peak corresponding to Au-S BE at 161.9 eV. It is important to note here that the corresponding changes in the XPS peaks of Au 4f also corroborated adsorption of cysteine on to the surface Au NCs. As evinced by XPS analyses, the broad Au 4f peaks in His Au NCs become much sharper upon addition of 100 µL of cysteine which is consistent with the formation of strong Au-S bond following protonation, possible reorientation and desorption of histidine ligands from Au NCs. The signature peak of carboxylate peak at 288 eV in the C 1s XPS spectrum of His Au NCs was observed to shift to higher values at 288.8 eV upon addition of 100 µl cysteine to His Au NCs suggesting its protonation to COOH group. Concurrently, the broad peak of imidazole ring C, CH2 and CHCOO at 285.5 eV in His Au NCs was found to diminish. Instead, this feature is found to consist of three smaller peaks at 287.2 eV, ascribed to -C-NH2 of cysteine, at 286 eV, due to C-SH and a broad peak at 285.5 eV due histidine carbon (Table 4).

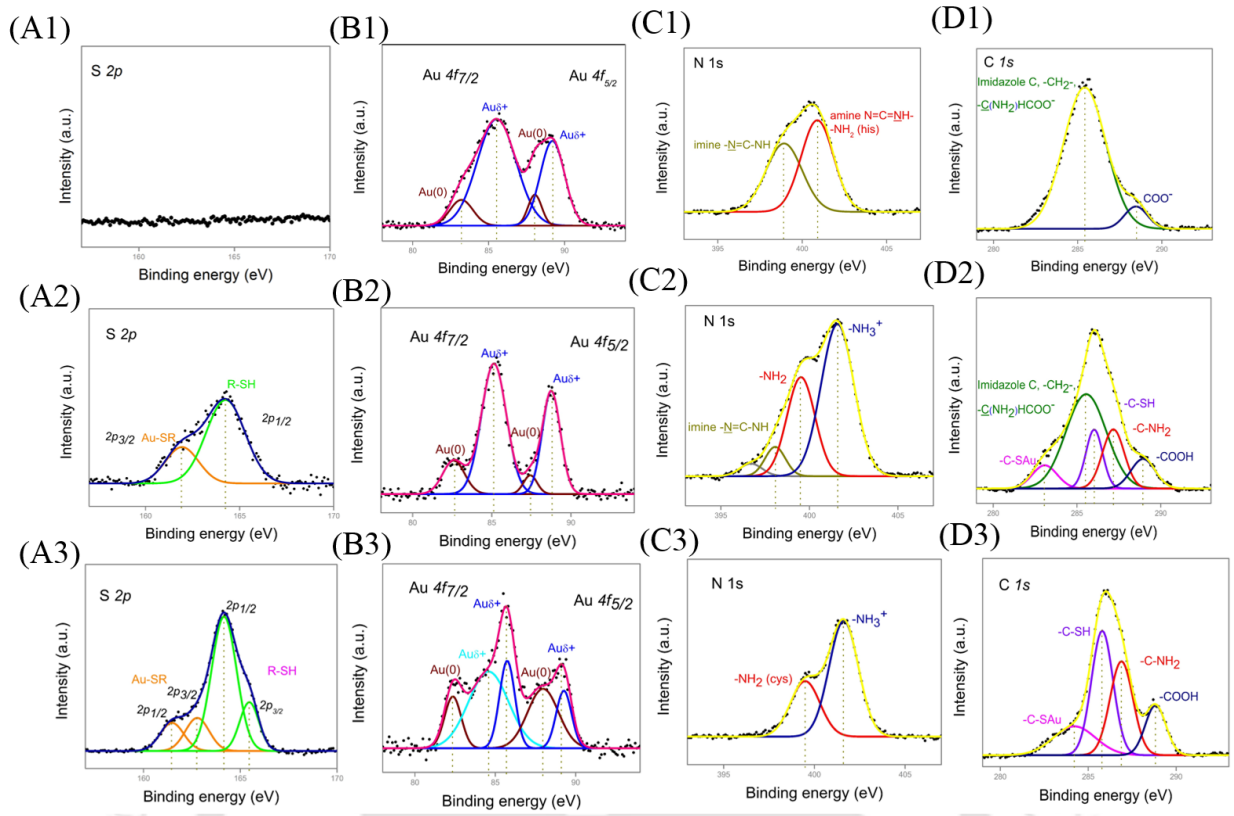

Fig. 5.5: XPS spectrum of S 2p of (A1) His Au NCs and of that following addition of (A2) 100 µL and (A3) 550 µL of 100 mM cysteine. XPS spectrum of Au of (B1) His Au NCs and of that following addition of (B2) 100 µL and (B3) 550 µL of 100 mM cysteine. XPS spectrum of N 1s of (C1) His Au NCs and of that following addition of (C2) 100 µL and (C3) 550 µL of 100 mM cysteine. XPS spectrum of C 1s of (D1) His Au NCs and of that following addition of (D2) 100 µL and (D3) 550 µL of 100 mM cysteine.

Element	BE@0 (width)	%	BE@100 (width)	%	BE@500 (width)	%	Peak assignment	Reference & notes
Au $4f_{5/2}$	88 (0.9)	6	87.4 (0.9)	4	88 (1.9)	23	Au(0)	**Nanoscale**, 2015,**7**, 16372-16380 **Nanoscale**, 2017,9, 15033-15043
	89.2 (1.6)	29	88.8 (1.1)	31	89.3 (1)	11	Au(δ+)	
Au $4f_{7/2}$	83.2 (1.5)	8	82.6 (1.4)	12	82.4 (1.0)	11	Au(0)	**Nanoscale**, 2018,10, 3792-3798 **J. Am. Chem**. Soc., 2005, 127, 5261–5270 **Nanoscale**, 2012, 4, 7727–7734
					84.6 (2.5)	38	Au(δ+)	
	85.5 (2.5)	57	85.1 (1.6)	53	85.6 (1.8)	17		Peak sharpens: Au-S bond formation δ+ assignment means oxidation state close to +1
Sulphur $2p_{3/2}$-$2p_{1/2}$=1.18eV, (2:1)	-	-	161.9 (1.8)	27	161.5 (1.2)	12	Au-SR	**Journal of Nanobiotechnology** volume 9, article number: 26 (2011) **Nanoscale**, 2014, 6, 8091-8099 **Langmuir** 2004, 20, 10223-10230 **Nanoscale**, 2012, 4, 7727–7734 **Colloids and Surfaces A: Physicochem. Eng. Aspects** 2000, 175, 121 – 128
					162.8 (1.2)	14	Au-SR	
			164.3 (2.1)	73	164.2 (1.3)	58	RS-H	
					165.5 (1)	16		$S_{3/2}$ and $S_{5/2}$ peaks: unresolved in fig3 due to poor signal to noise ratio. Incomplete resolution in fig 3F due to close overlapping shoulder peaks
Nitrogen 1s			396.7 (1.3)	3				**J. Phys. Chem. B**, 2005, 109, 884-891 **J. Phys. Chem. B** 2008, 112, 13655–13660

	398.9 (2.1)	45	398.1 (1.1)	7			imine (-N=C-NH)	**Langmuir** 2010, 26(11), 8606–8613 **Nanoscale**, 2012, 4, 7727–7734
			399.5 (1.6)	32	399.5 (1.6)	33	-NH_2 (cys)	**Langmuir** 2004, 20, 10223-10230
	400.9 (1.9)	55					amine(N=C-NH-) –NH_2 (his)	**J. Phys. Chem. C** 2014, 118, 10481−10487
			401.6 (1.8)	58	401.6 (1.6)	67	-NH_3^+	Deconvolution and assignment is complicated by zwitterionic and protonated forms of histidine & cysteine
Carbon 1s			283.1 (1.5)	8	284.2 (2.4)	17	C-SAu (cys)	**J. Phys. Chem. B**, 2005, 109, 884-891 **J. Phys. Chem. B** 2008, 112, 13655–13660 **Langmuir** 2004, 20, 10223-10230 **Applied Surface Science** 2018, 435, 870–879
	285.5 (2.5)	92	285.5 (2.4)	52			imidazole C, -CH_2- -$C(NH_2)HCOO^-$	
			286 (1)	13	285.8 (1.2)	38	C-SH (cys)	
	288 (1.4)	8	287.2 (1.3)	17	286.9 (1.3)	30	-C-NH_2 (cys) COO^-	
			288.9 (1.4)	10	288.8 (1.2)	15	COOH	

Table 4: Details of XPS analysis of His Au NCs and of that following addition of a cysteine

In the second segment, i.e. upon addition of 550 µl of cysteine to His Au NCs, further protonation and desorption of histidine from Au NCs might have occurred, resulting in increased adsorption of cysteine moieties on the surface of Au NCs. Accordingly the N 1s core spectra shows absence of imidazole ring nitrogen and instead shows the presence of sharp peaks due to $–NH_3^+$ (BE 401.6 eV) and $–NH_2$ groups (BE 399.5 eV) originating mainly from cysteine. Correspondingly, the Au-S peak was found to get significantly pronounced and resolved at 161.5 and 162.8 eV corresponding to the BE from 2p3/2 and 2p1/2 states of sulfur bound to gold atoms of the clusters. Moreover, possible further desorption of histidine was further supported from core spectra of C 1s where the broad peak due to imidazole ring carbon (285.5 eV) was drastically reduced while sharp peaks at 286.9 eV due to C-NH2 and at 285.8 eV due to C-SH were found to sharply increase with increasing amount of cysteine (550 µL). Interestingly, increased Au-SR formation is marked with a relative reduction in the intensity of Au(δ+) peak at 85.6 eV in the Au 4f7/2 XPS spectra upon addition of 550 µL of cysteine. Presumably, the thiol group of cysteine groups being much stronger electron donor than nitrogen of histidine, are able to more effectively reduce the oxidation state of Au(δ+) on the surface of the gold clusters at higher concentrations of cysteine. This leads to simultaneous reduction of the intensity of the 85.6 eV peak and the appearance of broad peak at a lower BE of 84.6 eV in the Au 4f7/2 XPS spectra. As this value of BE (84.6 eV) is higher than that of Au (0) 4f7/2 state (BE 82.4 eV), the former is assigned to gold atoms with lower oxidation state than those with BE 85.6 eV. Correspondingly, the 88 eV peak of Au 4f5/2 peak broadens due to possible unresolved contributions from this Au(δ+) state apart from Au(0) state. To sum up, upon addition of 100 µl of cysteine to His Au NCs, desorption of histidine from the surface of Au NCs took place due to possible protonation of the histidine moieties by cysteine. Thereafter, following addition of 550 µl of cysteine to His Au NCs, adsorption of cysteine on to the surface of Au NCs occurred owing to facile Au-thiol aurophilic interaction. The shift of the excitation wavelength of His Au NCs upon interaction with various systems may be explained on the basis of alteration in ligand to metal charge transfer. Owing to the higher electronic polarizability of S in contrast to N, ligand to metal charge transfer of Cys Au NCs is likely to be more facile than in case of N ligated His Au NCs. Owing to smaller energy gap between ground state and excited state in case of Cys stabilized Au NCs vis-à-vis His stabilized Au NCs, a bathochromic shift is likely to have occurred upon ligand exchange reaction of histidine by cysteine. The survey XPS spectrum has been given in the supporting information (Fig. 5.6). Also, the details of XPS analysis have been given in a tabulated form (Table 4). In

addition, the shift in binding energies of the functional groups of His Au NCs upon addition of cysteine to His Au NCs has been shown in Fig. 5.7.

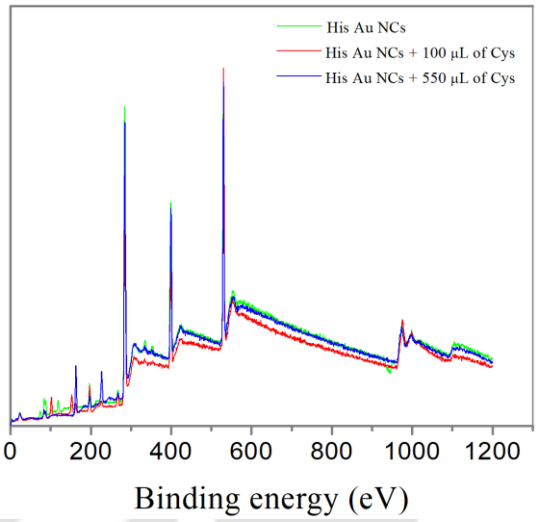

Fig. 5.6 Survey spectra of His Au NCs, His Au NCs + 100 µL cysteine and His Au NCs + 550 µL cysteine

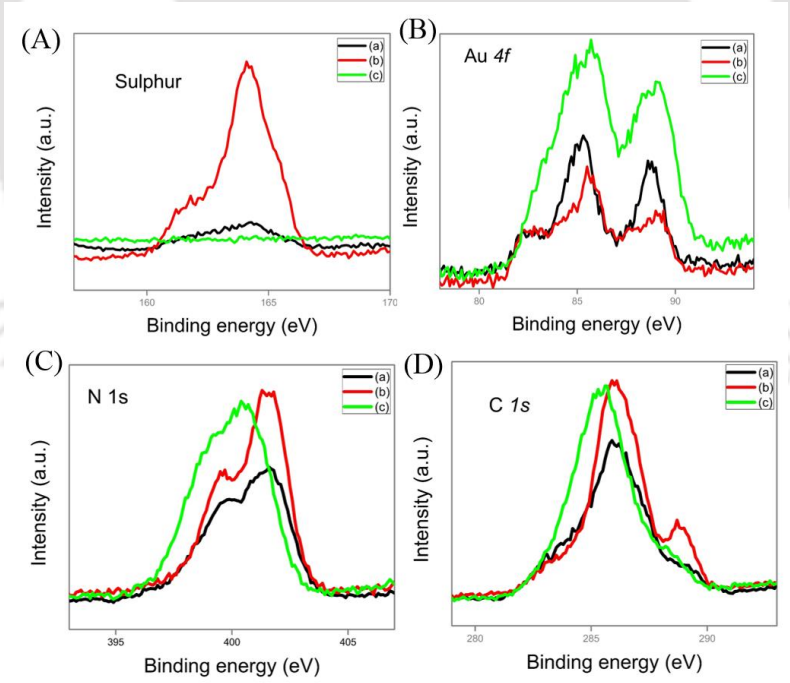

Fig. 5.7: XPS spectrum of (A) sulphur 2p, (B) Au 4f, (C) N 1s and (D) C 1s. (a) Black lines denote His Au NCs following addition of 100 µL cysteine, green lines denote only His Au NCs and red lines denote His Au NCs following addition of 500 µL cysteine.

Thus based on all the aforementioned observations, it is proposed that upon addition of cysteine to a dispersion of His Au NCs, the histidine (imidazole and NH_2 groups) moieties stabilizing the Au NCs underwent protonation by cysteine. This might have weakened the Au-N bonds, thereby allowing desorption of histidine molecules from Au NCs. This might have also led to aggregation of Au NCs owing to lesser stability in absence of stabilizer. Consequently, the luminescence of Au NCs might have red shifted owing to formation of larger particles as opposed to ultra-small clusters. It is worthy to be mentioned here that under this condition some amount of cysteine might also be getting adsorbed on the surface of the clusters. Upon further addition of cysteine, owing to strong aurophilic interaction between thiol and gold, cysteine molecules might have been adsorbed on to the bare aggregated Au NCs, thereby enabling disaggregation of formerly aggregated Au NCs into individual clusters. This might have led to partial restoration of emission wavelength of His Au NCs to the original value. Herein it is to be noted that the proposed mechanism of ligand exchange could not be further monitored through mass spectrometric analysis owing to possible oligomerization of histidine moieties, thereby leading to possibilities of misinterpretation of data. A schematic illustration depicting ligand exchange reaction mediated post synthetic modification of Au NCs for tailored luminescence is shown below:

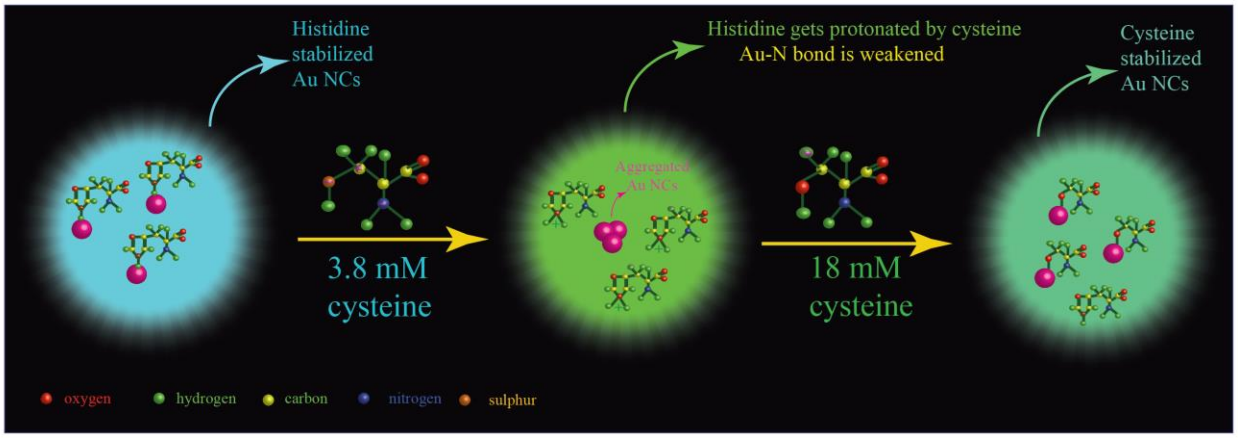

Conclusion

In summary, we have demonstrated a facile ligand exchange reaction between histidine stabilized gold clusters and cysteine, through which the luminescence of the clusters could be easily modulated. Such modulation of luminescence features of atomic clusters via post synthetic reaction is deemed important for broadening the application potential of metal clusters. Briefly, when 3.8 mM cysteine was added to a dispersion of His Au NCs, desorption of histidine ligands from the surface of His Au NCs occurred, resulting in aggregation of Au NCs to aggregates. Consequently, the luminescence spectrum of His Au NCs featured a bathochromic shift from 475 nm to 500 nm with concomitant decrease in luminescence intensity. However, following further addition of cysteine to a concentration of 18 mM, cysteine – owing to strong aurophilic interaction – was attached to Au NCs resulting in formation of atomic clusters stabilized largely by cysteine. Subsequently, the emission maximum of Au NCs was restored (nearly) to 486 nm i.e. similar to the emission of His Au NCs with partial recovery of luminescence intensity. Thus, we show that chemical reaction of atomic clusters may be used as a tool to modulate the luminescence of ultra-small nanoclusters to match the objective of desired applications. It has already been established in literature that ligand exchange reactions of magnetic nanoparticles transform water immiscible magnetic nanoparticles to water dispersible nanoparticles.[2] This widens the application potential of nanoscale particles, especially biological applications. In an allied vein, through this study, we show that desired luminescence properties of atomic clusters may be achieved via post synthetic chemical modification of ligand stabilized gold clusters. This may also be used as an easy handle to tune the luminescence of clusters to probe thiol molecules in biological medium.

References

1. Yang, X.; Shi, M.; Zhou, R.; Chen, X.; Chen. H. Blending of HAuCl4 and histidine in aqueous solution: a simple approach to the Au_{10} cluster. *Nanoscale*, **2011**, *3*, 2596.

2. M. Hatakeyama, H. Kishi, Y. Kita, K. Imai, K. Nishio, S. Karasawa, Y. Masaike, S. Sakamoto, A. Sandhu, A. Tanimoto, T. Gomi, E. Kohda, M. Abe and Hiroshi Handa. *J. Mater. Chem.*, **2011**, *21*, 5959-5966.

Chapter 6

Summary and Future Prospects

Summary

The present thesis work contains several aspects of metal nanocluster, synthesis and their application potential. In our current work, few particles level discrimination of bio-thiols has been achieved by dual emitting nanoprobe. Further zinc coordinated crystalline assembly of gold nanocluster and one step conversion of nanocluster to nanoparticle has been achieved for logic gate operation in mammalian cell. In addition, zinc mediated extensive aggregation of gold nanocluster has been achieved under visible light excitation. Using this we are able to probe molecules with different pka values. This is an important advancement in the nanoscale field for the development of sensors and bio imaging agents under visible light excitation. Moreover, chemical reaction assisted post synthetic modification of luminescence of metal nanocluster has been achieved via ligand exchange. Therefore chemical reaction of atomic cluster may be used as a tool to modulate the luminescence of ultra -small nanocluster to match the objective of desired application.

Future Prospects

The thesis work is envisioned to open up several aspect of nanoscale particles with desirable application potential. In current thesis, it has been shown that luminescent of AuNCs get significantly enhanced with interaction of zinc ion due to aggregation and absorb light in visible region. In future it is possible, by tuning reaction medium and modulating the ligands, to get cluster which absorb light in visible region which may be used for cellular imaging and probing molecules. Further chemical reaction of atomic cluster has been achieved by ligand exchange method. In future this may be used as a tool to modulate luminescence intensity and wavelength for desirable application.

List of Publications in Peer reviewed Journals

1. **Gayen, C.;** Basu, S.; Pan, U. N.; Paul, A. Few Particle-Level Chromaticity Index-Based Discrimination of Biothiols Using Chemically Interactive Dual-Emitting Nanoprobe. *ACS Omega* **2018**, *3*, 17220−17226.

2. **Gayen, C.;** Goswami, U.; Gogoi, K.; Basu, S.; Paul, A. Crystallization-Induced Emission Enhancement of Nanoclusters and One-Step Conversion of "Nanoclusters to Nanoparticles" as the Basis for Intracellular Logic Operations. *ChemPhysChem* **2019**, *20*, 953 –958.

3. **Gayen, C**.; Basu, S.; Goswami, U.; Paul, A. Visible Light Excitation-Induced Luminescence from Gold Nanoclusters Following Surface Ligand Complexation with Zn^{2+} for Daylight Sensing and Cellular Imaging. *Langmuir* **2019**, *35*, 9037−9043.

4. Basu, S.; **Gayen, C**. Tailoring the luminescence of atomic clusers via Ligand Exchange Reaction Mediated post synthetic modification. Phys. *Chem. Chem. Phys*. **2020**, *22*, 3959.

5. Basu, S.; Nawaj, W.; **Gayen, C**.; Paul, A. Photo induced chemical modification of surface ligands for aggregation and luminescence modulation of copper nanoclusters in presence of oxygen. *Phys. Chem. Chem. Phys* **2019,** *21*, 21776-21781.

6. Basu, S.; Hajra, A.; **Gayen, C**.; Paul, A. Zinc ion induced aggregation of gold clusters for visible light excitation based fluorimetric discrimination of geometrical isomers. *ChemPhysChem* 10.1002/cphc.201901044.

Permissions

JOHN WILEY AND SONS LICENSE TERMS AND CONDITIONS

Oct 10, 2019

This Agreement between IIT Guwahati -- Chirantan Gayen ("You") and John Wiley and Sons ("John Wiley and Sons") consists of your license details and the terms and conditions provided by John Wiley and Sons and Copyright Clearance Center.

License Number	4685651093182
License date	Oct 10, 2019
Licensed Content Publisher	John Wiley and Sons
Licensed Content Publication	ChemPhysChem
Licensed Content Title	Crystallization-Induced Emission Enhancement of Nanoclusters and One-Step Conversion of "Nanoclusters to Nanoparticles" as the Basis for Intracellular Logic Operations
Licensed Content Author	Anumita Paul, Srestha Basu, Kasturi Gogoi, et al
Licensed Content Date	Mar 14, 2019
Licensed Content Volume	20
Licensed Content Issue	7
Licensed Content Pages	6
Type of use	Dissertation/Thesis
Requestor type	Author of this Wiley article
Format	Print and electronic
Portion	Full article
Will you be translating?	No
Order reference number	-
Title of your thesis / dissertation	Interactive Molecules and Atomic Clusters: Reactions and Sensing Applications
Expected completion date	Oct 2019
Expected size (number of pages)	100
Requestor Location	IIT Guwahati Kameng Hostel B3-321 Amingaon Guwahati-781039 Guwahati, Kamrup 781039 India Attn: IIT Guwahati
Publisher Tax ID	EU826007151
Total	0.00 USD
Terms and Conditions	

TERMS AND CONDITIONS

This copyrighted material is owned by or exclusively licensed to John Wiley & Sons, Inc. or one of its group companies (each a"Wiley Company") or handled on behalf of a society with which a Wiley Company has exclusive publishing rights in relation to a particular work (collectively "WILEY"). By clicking "accept" in connection with completing this licensing transaction, you agree that the following terms and conditions apply to this transaction (along with the billing and payment terms and conditions established by the Copyright Clearance Center Inc., ("CCC's Billing and Payment terms and conditions"), at the time that

ACS Chemistry for Life®

Dear Chirantan,

Your permission requested is granted and there is no fee for this reuse.

In your planned reuse, you must cite the ACS article as the source, add this direct link: <https://pubs.acs.org/doi/10.1021/acsomega.8b02373>, and include a notice to readers that further permissions related to the material excerpted should be directed to the ACS.

Please do not hesitate to contact me if you need any further assistance.

Regards,
Jawwad Saeed
ACS Customer Services & Information
https://help.acs.org

Incident Information:

Incident #: 3066303
Date Created: 2019-10-11T10:36:44
Priority: 3
Customer: Chirantan Gayen
Title: Rights and Permission
Description: I am Chirantan Gayen. I am a author of "Few Particle-Level Chromaticity Index-Based Discrimination of Biothiols Using Chemically Interactive Dual-Emitting Nanoprobe" in ACS Omega (DOI-10.1021/acsomega.8b02373). I am using this article in thesis chapter. So i need Rights and Permission form you. Please do it needful.
Thank you.

Dear Dr. Gayen:

Thank you for contacting ACS Publications Support.

Your permission request is granted and there is no fee for this reuse. In your planned reuse, you must cite the ACS article as the source, add this direct link (https://pubs.acs.org/doi/10.1021/acs.chemrev.7b00776) and include a notice to readers that further permissions related to the material excerpted should be directed to the ACS.

I hope this information helped. Please let me know if I can be of further assistance.

Sincerely,

Ivan Zabala
ACS Customer Services & Information
https://help.acs.org
Incident Information:

Incident #: 3067643
Date Created: 2019-10-12T13:50:48
Priority: 3
Customer: Chirantan Gayen
Title: Rights and Permission
Description: I am Chirantan Gayen. I am using a figure of this paper "Metal Catalysts for Heterogeneous Catalysis: From Single Atoms to Nanoclusters and Nanoparticles" (DOI-10.1021/acs.chemrev.7b00776). So i need a permission from you. Please do it needful.
Thank you.

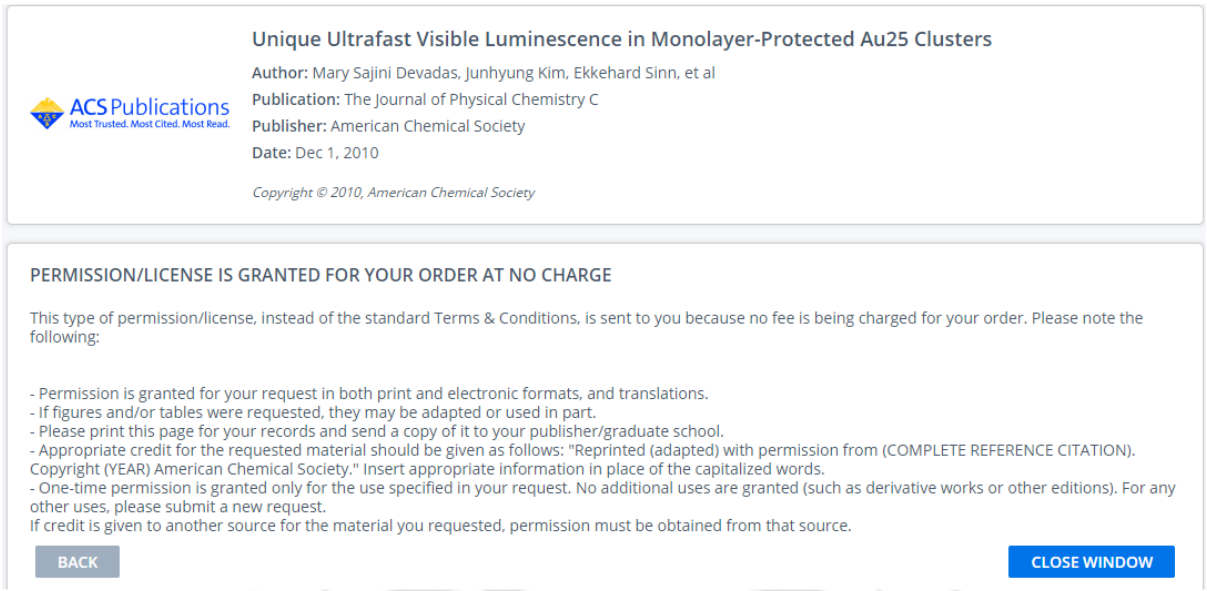

Unique Ultrafast Visible Luminescence in Monolayer-Protected Au25 Clusters

Author: Mary Sajini Devadas, Junhyung Kim, Ekkehard Sinn, et al

Publication: The Journal of Physical Chemistry C

Publisher: American Chemical Society

Date: Dec 1, 2010

Copyright © 2010, American Chemical Society

PERMISSION/LICENSE IS GRANTED FOR YOUR ORDER AT NO CHARGE

This type of permission/license, instead of the standard Terms & Conditions, is sent to you because no fee is being charged for your order. Please note the following:

- Permission is granted for your request in both print and electronic formats, and translations.
- If figures and/or tables were requested, they may be adapted or used in part.
- Please print this page for your records and send a copy of it to your publisher/graduate school.
- Appropriate credit for the requested material should be given as follows: "Reprinted (adapted) with permission from (COMPLETE REFERENCE CITATION). Copyright (YEAR) American Chemical Society." Insert appropriate information in place of the capitalized words.
- One-time permission is granted only for the use specified in your request. No additional uses are granted (such as derivative works or other editions). For any other uses, please submit a new request.

If credit is given to another source for the material you requested, permission must be obtained from that source.

BACK CLOSE WINDOW